BMR JOURNAL
of Australian Geology & Geophysics

VOLUME 5 NUMBER 4 DECEMBER 1980

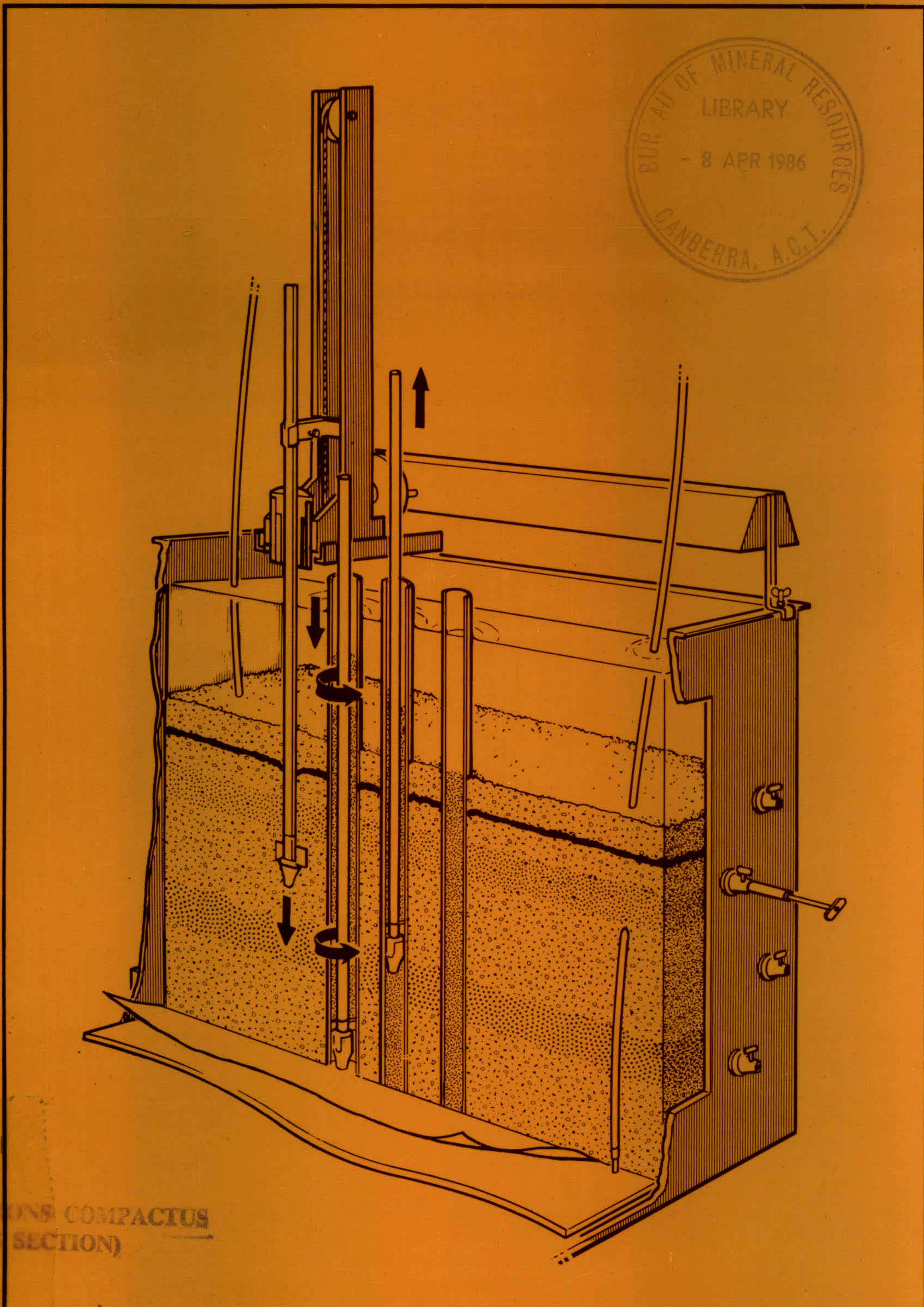

Front cover:

The sedimentation tank shown here in cutaway form is part of a laboratory experiment to study the effects of brine moving through sedimentary systems. The first results are reported in an article in this issue.

Cover design: Stuart Fereday.

The text figures in this issue were drawn by a cartographic team of J. Mifsud, R. Bates, I. Hartig, R. Anderson, and C. Fitzgerald.

ISSN 0313-9608

Printed by Graphic Services Pty Ltd, 516-518 Grand Junction Road, Northfield, S.A. 5085

BMR JOURNAL
of Australian Geology & Geophysics

Volume 5, No. 4
December 1980

AUSTRALIAN GOVERNMENT PUBLISHING SERVICE
CANBERRA 1980

BMR Journal of Australian Geology & Geophysics, 5, 1980, 243-256

The early geological history of the Proterozoic Mount Isa Inlier, northwestern Queensland: an alternative interpretation

D. H. Blake

Correlations within the Proterozoic succession are complicated by repetitions of similar rock types at different stratigraphic levels, especially acid and basic volcanics, quartz sandstones, and calcareous rocks, and also by disconformities, igneous intrusions of various ages, tight to isoclinal folding, intense faulting, regional metamorphic effects, and scarcity of reliable isotopic age data. Consequently, there is plenty of scope for alternative interpretations.

The interpretation proposed is that instead of equivalent sequences of cover rocks, known as the western and eastern successions, being separated by a narrow basement belt, as suggested previously for the Proterozoic Mount Isa Inlier, the oldest cover rocks in the west, those of the Haslingden Group, pre-date the eastern succession, and basic lavas (Eastern Creek Volcanics) within this group have no correlatives to the east. It is also suggested that volcanics previously regarded as part of the basement (Magna Lynn Metabasalt and Argylla Formation) are younger than most of the Haslingden Group, and that the extensive calcareous Corella Formation represents at least two quite separate units, one being younger than the Haslingden Group, and one being part of the underlying basement. These suggestions are consistent with U-Pb zircon dating carried out to date, as well as with the field evidence.

Introduction

The generally accepted view of the Proterozoic Mount Isa Inlier is that it consists of a central north-trending, largely igneous, basement belt flanked on either side by thick sequences of stratigraphically equivalent younger cover rocks known as the western and eastern successions. This interpretation, first proposed by Carter & others (1961), has been followed by most later workers (e.g. Plumb & Derrick, 1975; Derrick & others, 1977a). An alternative interpretation is proposed here: the oldest rocks of the western succession were deposited on the west side of a large high land mass, which included the central and eastern parts of the region, and, as the landmass became progressively eroded, sedimentation transgressed eastwards; therefore, there are no stratigraphic equivalents of the older units of the western succession in the east. Evidence is presented which shows that part of the Tewinga Group forming the basement igneous succession of Derrick & others (1976a) may be younger, not older, than the oldest rocks of the western succession (the Haslingden Group), and that much of the Corella Formation, the most widespread unit of the eastern succession, may be part of the pre-Haslingden Group basement.

The Mount Isa Inlier (Geological Survey of Queensland, 1975) (Fig. 1) is made up of Proterozoic igneous, metamorphic, and sedimentary rocks. The older rocks, those that are older than the Mount Isa Group (which hosts the Mount Isa Pb-Zn and Cu orebodies), crop out extensively in the southern part of the inlier, in the Mount Isa, Cloncurry, Duchess, and Urandangi 1:250 000 Sheet areas*.

A broad reconnaissance survey of the Mount Isa Inlier was carried out by geologists from the Bureau of Mineral Resources (BMR) and Geological Survey of Queensland (GSQ) during the 1950s. The results of this survey were reported in BMR Bulletin 51 (Carter & others, 1961). A more detailed survey of the Mount Isa Inlier has since been undertaken by BMR and GSQ: from 1969 to 1979 by Derrick and co-workers in the Cloncurry and Mount Isa Sheet areas and in Sheet areas to the north, and from 1975 to 1979 by Blake and co-workers in the Duchess and Urandangi Sheet areas to the south (Fig. 1).

The general geology of the Mount Isa Inlier is characterised by repetition of similar rock types, such as basic volcanics, acid volcanics, quartz sandstones, and calc-silicate rocks, at different stratigraphic levels; regional and local unconformities; abundant intrusive rocks of various ages; steeply dipping strata and tight to isoclinal folds with mainly northerly trends; innumerable faults, many along lithological boundaries and some along fold axes; regional metamorphism to greenschist and amphibolite grades; and economic deposits of copper, lead, zinc, silver, uranium, cobalt, and gold.

Major structural features mentioned in this paper are shown in Figures 1 and 2. One of these features is the Wonga Belt, which crosses the region from north to south. The Wonga Belt is a zone several kilometres wide containing strongly deformed, relatively high grade, metamorphic rocks; its western margin generally marks an abrupt change in metamorphic grade and structural complexity; its eastern margin south of the Fountain Range Fault is taken to be the north-trending Pilgrim Fault, but is uncertain further north.

Geochronology

Various methods of isotopic dating have been carried out on Precambrian rocks of the Mount Isa Inlier. Several Rb-Sr and K-Ar age determinations have been obtained, but are difficult to interpret because the rocks dated are acid volcanics and granites that have been affected by low-grade regional metamorphism, and consequently have had their primary Rb-Sr and K-Ar isotopic systems disturbed. However, this metamorphism does not appear to have affected U-Pb zircon dates, which are considered to be precise and stratigraphically meaningful. The zircon dates are typically 10 to 15 percent older than Rb-Sr total-rock dates, and more than 15 percent older than K-Ar dates. Because of the doubts about the Rb-Sr and K-Ar age determinations, the isotopic ages quoted in this paper, unless otherwise stated, are those obtained by the U-Pb zircon technique (Page, 1978, 1979, 1980, and in press).

*** Unless stated otherwise, 'Sheet area' refers to standard 1:250 000 Sheet area.**

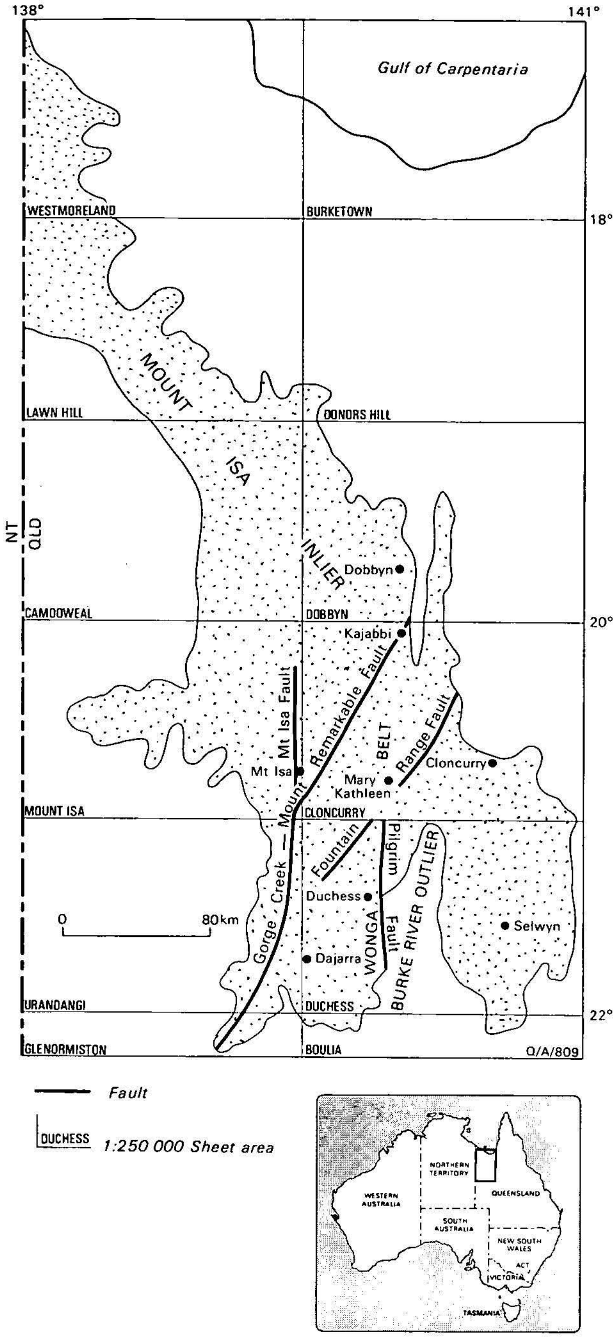

Figure 1. Locality map, showing major structural features.

Comments on Stratigraphy

The pre-Mount Isa Group stratigraphy of the Mount Isa Inlier in the Cloncurry and Duchess Sheet areas is summarised in Table 1, and the distribution of main rock unit groupings is shown in Figure 2. The correlation of rock units according to Derrick and co-workers is compared to that proposed by me in Figure 3. The main differences in the two correlation schemes are that I suggest that: 1, the upper part of the 'basement' Tewinga Group—the Magna Lynn Metabasalt and Argylla Formation—is younger than much or all of the Haslingden Group of the western succession, and hence is not part of the basement; 2, the Bottletree Formation underlying the Haslingden Group is older than, not a correlative of, the Argylla Formation; 3, the Eastern Creek Volcanics of the Haslingden Group are older than, not correlatives of, the Marraba Volcanics of the Malbon Group in the eastern succession; and 4, the Corella Formation of the eastern succession includes rocks older and younger than the Haslingden Group.

Tewinga Group

According to Derrick and co-workers (e.g., Derrick & others, 1977a), the Tewinga Group, together with the Kalkadoon and Ewen Granites, formed a central basement belt (mainly the Kalkadoon-Leichhardt Block, but also including the western part of the Wonga Belt) which separated at least the older units of the western succession from contemporaneous units of the eastern succession. As defined formally, the Tewinga Group comprises three formations: the Leichhardt Metamorphics at the base, consisting mainly of acid volcanics, the overlying Magna Lynn Metabasalt, mainly basaltic volcanics, and the Argylla Formation at the top, mainly acid volcanics. Acid volcanics commonly interfinger with basic volcanics at contacts between the Magna Lynn Metabasalt and overlying Argylla Formation, indicating that these two units are similar in age. However, a major time break is now known to separate at least part of the Leichhardt Metamorphics from the overlying Magna Lynn Metabasalt and Argylla Formation. Evidence for this is that:

1. the Leichhardt Metamorphics are intruded by innumerable basic dykes, many of which do not penetrate up into the Magna Lynn Metabasalt;
2. the Leichhardt Metamorphics, but not the overlying formations, are intruded by Kalkadoon Granite (isotopically dated at about 1860 m.y., Page, 1978) and Ewen Granite;
3. polymictic conglomerate indicative of subaerial erosion of crystalline basement rocks is present locally at the base of, or within, the Magna Lynn Metabasalt, but not lower in the sequence;
4. acid volcanics of the Leichhardt Metamorphics are dated at 1865 ± 3 m.y., whereas those of the Argylla Formation are dated at 1777 ± 7 m.y. (Page, 1978).

Lithologically, the two units of acid volcanics are difficult to tell apart, as both consist largely of ignimbrites and flow-banded lavas containing feldspar and quartz phenocrysts. Both also locally include some basic volcanics. The main differences appear to be that the acid volcanics of the Argylla Formation are generally pinker, more coarsely porphyritic, more commonly magnetic in hand specimen, and chemically richer in potassium, niobium and zirconium, and poorer in strontium (Wilson, 1979), than those of the Leichhardt Metamorphics; also, bedded sedimentary rocks and tuffs are more common in the Argylla Formation, especially towards the top of this unit. Because of the difficulty in distinguishing between them, some rocks mapped as Leichhardt Metamorphics may belong to the Argylla Formation, and *vice versa*. It is also possible that some acid volcanics underlying Magna Lynn Metabasalt, and therefore mapped as Leichhardt Metamorphics, may belong instead to the much younger Magna Lynn/Argylla sequence.

In the western part of the Duchess Sheet area, within and to the west of the Wonga Belt, massive to thin-banded quartzofeldspathic gneiss, augen gneiss, granitic to dioritic gneiss, migmatite, metaporphyry, amphibolite (including amygdaloidal metabasalt), meta-arkose, mica schist, quartzite, and minor banded calc-silicate rocks have been provisionally mapped as undivided Tewinga Group (Bultitude & others, 1978; Blake &

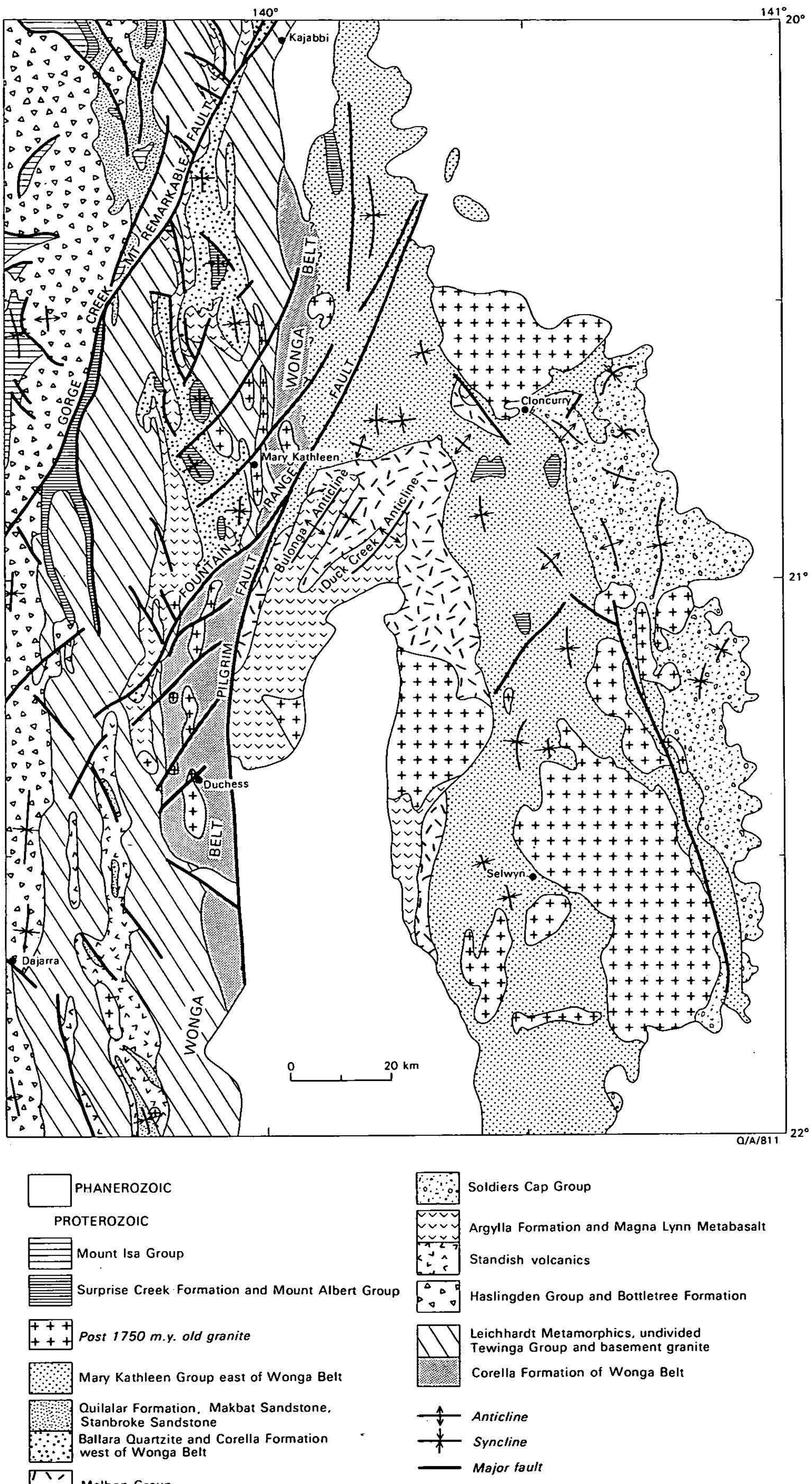

Figure 2. **Generalised geological map of Duchess and Cloncurry 1:250 000 Sheet areas showing distribution of Precambrian rock units.**

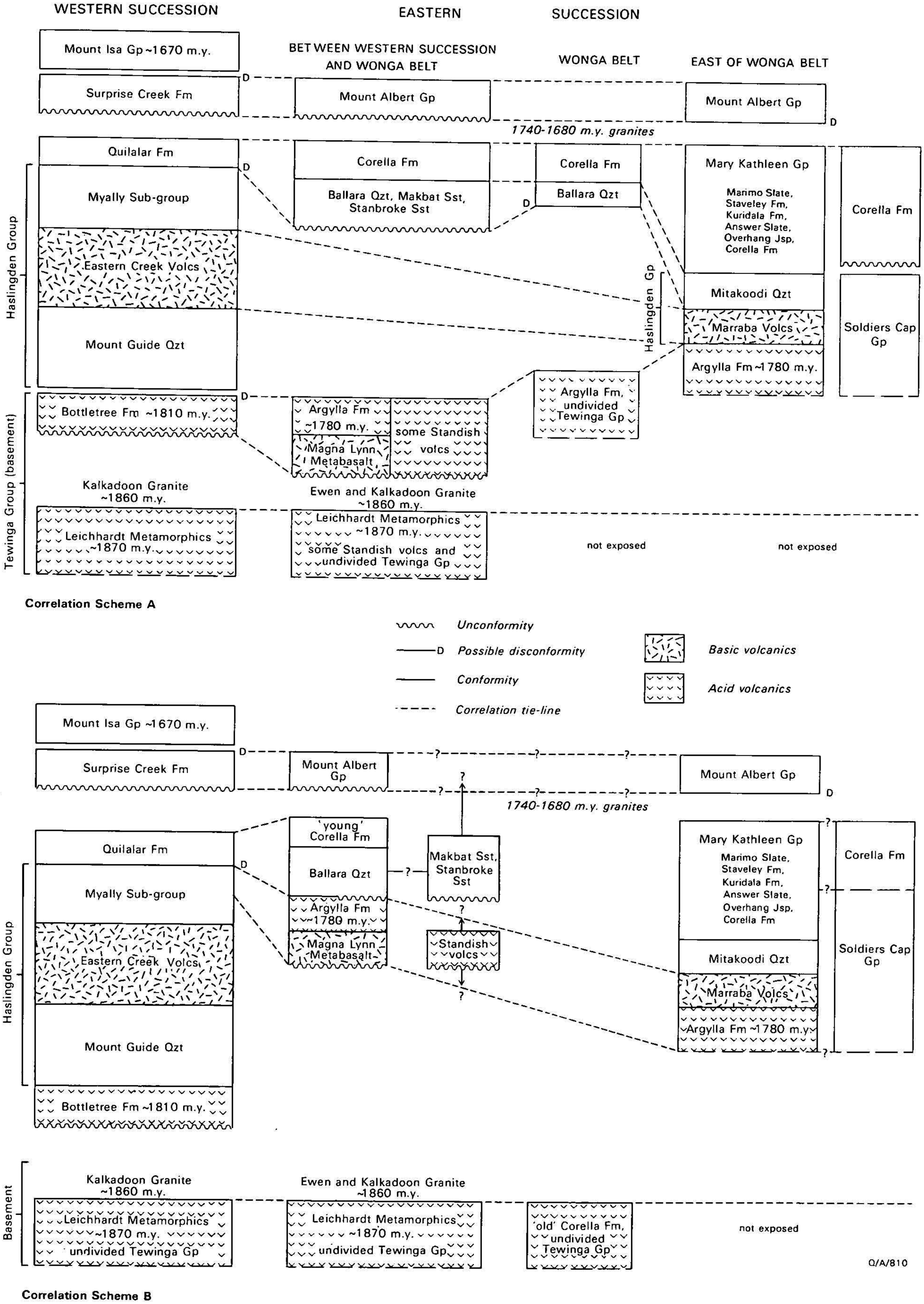

Figure 3. Stratigraphic correlation schemes for the Mount Isa Inlier in the Cloncurry and Duchess 1:250 000 Sheet areas. Scheme A, after Derrick and co-workers (Derrick & others, 1977a, 1980; Derrick, 1980 and personal communication, 1980); scheme B, proposed in this paper.

Unit and thickness (in metres)	*Main rock types*	*Relationships*	*Remarks*
MOUNT ISA GROUP[2] about 5000	Shale, siltstone, sandstone; thin tuff beds	Conformable or disconformable on Surprise Creek Formation; unconformable on Quilalar Formation, Haslingden Group	Host to major Ag, Pb, Zn, Cu deposits (e.g. Mt Isa, Hilton)
Surprise Creek Formation[2] 200-2000+	Sandstone, siltstone	Unconformable on Quilalar Formation, Kalkadoon Granite; disconformable? on Eastern Creek Volcanics	Host to small Cu deposits
MOUNT ALBERT GROUP[2] 1500-3700	Sandstone, siltstone, calcareous rocks	Unconformable on Corella Formation	Includes Deighton Quartzite and Roxmere Quartzite
Quilalar Formation[2] 500-1500	Sandstone, dolomite, siltstone	Conformable or disconformable on Haslingden Group; unconformable on Leichhardt Metamorphics, Kalkadoon Granite	
MARY KATHLEEN GROUP[2]	Slate, siltstone, sandstone, calcareous rocks	Conformable or disconformable on Overhang Jaspilite	East of Wonga Belt; host to small Cu deposits
Marimo Slate[1,2] about 2000			
Staveley Formation[1] 1000+	Calcareous to non-calcareous sedimentary rocks	Apparently conformable on Answer Slate and conformable to unconformable on Kuridala Formation	East of Wonga Belt; host to minor Cu and U deposits
Kuridala Formation[1] 1000+	Schistose sandstone, siltstone, shale; black slate	Uncertain; appears to pass laterally into Answer Slate and Soldiers Cap Group	East of Wonga Belt; host to Cu, Au, Co, Zn, Pb, U deposits
Answer Slate[1] possibly 1000+	Slate, phyllite, chert	Conformable on Mitakoodi Quartzite	East of Wonga Belt; host to Cu deposits
Overhang Jaspilite[2] up to 850	Calcareous siltstone, chert, jaspilite	Conformable on Mitakoodi Quartzite	East of Wonga Belt
Corella Formation[1,2] up to 1200 W of Wonga Belt, possibly 4000+ to E	Calc-silicate rocks, sandstone, siltstone	Conformable on Ballara Quartzite west of Wonga Belt	Probably includes rocks of more than one age; host to U and Cu deposits
Ballara Quartzite[1,2] max. about 1250	Sandstone	Conformable or unconformable on Argylla Formation	West of Wonga Belt
Stanbroke Sandstone[3] 300+	Sandstone, some calcareous rocks	Overlies Standish volcanics; inferred to be unconformable on basement rocks	
Makbat Sandstone[1] 300+	Sandstone	Overlies Standish volcanics	
MALBON GROUP[2]			
Mitakoodi Quartzite[1,2] max. about 1500	Sandstone	Conformable on Marraba Volcanics	Host to small Cu deposits
Marraba Volcanics[1,2] max. about 3000	Metabasalt, siltstone, limestone	Conformable on Argylla Formation	Host to small Cu deposits
SOLDIERS CAP GROUP[2] 6000+	Metamorphosed pelitic and arenaceous sediments, metabasalt, calc-silicate rocks	Uncertain	Host to small Cu, Pb, Zn deposits
Standish volcanics probably 1000+	Acid volcanics	Inferred to be unconformable on basement rocks	
HASLINGDEN GROUP[2]			
Myally Subgroup[2] about 4000	Sandstone, generally feldspathic	Conformable on Eastern Creek Volcanics	
Eastern Creek Volcanics[1,2] 3600-7200	Metabasalt, sandstone	Conformable on Mount Guide Quartzite; unconformable on basement granite	Host to Cu and U deposits
Mount Guide Quartzite[1,2] max. about 3000	Sandstone	Conformable on Bottletree Formation	
Yappo Member[3] max. about 3700	Conglomerate, sandstone	Conformable on and interfingers with Bottletree Formation; unconformable on basement granite and metamorphic rocks	
Bottletree Formation[3] 0-3000	Acid and basic metavolcanics; conglomerate, sandstone	Unconformable on basement granite and metamorphic rocks	
TEWINGA GROUP[2]			
Argylla Formation[1,2] 1000-3000+	Acid volcanics	Conformable on Magna Lynn Metabasalt	Host to Cu deposits
Magna Lynn Metabasalt[2] mainly less than 1000	Metabasalt	Unconformable on Leichhardt Metamorphics	Host to Cu deposits
Leichhardt Metamorphics[1,2] 1000+	Acid volcanics	Part of basement; base not exposed	Host to Cu deposits
Undivided Tewinga Group 1000+	Gneiss, schist, quartzite, migmatite, amphibolite	Part of basement; base not exposed	Host to Cu deposits

[1] unit defined by Carter & others (1961). [2] unit defined by Derrick & others (1976a, 1976b, 1976c, 1976d, 1977b, 1977c, 1980).
[3] unit defined by Blake, Bultitude & Donchak (in prep.).

Table 1. Summary of stratigraphy of the Mount Isa Inlier up to Mount Isa Group time, Cloncurry and Duchess 1:250 000 Sheet areas.
For correlations and relative ages see Figure 3.

others, 1978). These rocks represent a complex sequence of acid to basic volcanics, sediments which are mainly volcaniclastic, and probably some granitic to dioritic intrusives. They are intruded by Kalkadoon Granite, and some may be similar in age to the isotopically dated Leichhardt Metamorphics to the north. However, these undivided Tewinga Group rocks are thought more likely by me to represent either an older and more deeply eroded part of the Leichhardt sequence, or an older sequence altogether. Hence, the undivided Tewinga Group in the Duchess Sheet area may exclude equivalents of the Magna Lynn Metabasalt and Argylla Formation.

The crystalline basement of the Wonga Belt is taken by me to include, in addition to undivided Tewinga Group rocks, a sequence of mainly calc-silicate rocks mapped as Corella Formation immediately to the east (Fig. 2). Detailed studies have shown that metamorphism in parts of the Wonga Belt took place at pressures of 3 to 5 kb and temperatures of 600 to 650°C (Derrick, 1980), i.e., at depths of at least 10 km. Similar rocks of the undivided Tewinga Group west of the Wonga Belt were probably metamorphosed under comparable pressure and temperature ranges.

Haslingden Group and Bottletree Formation

According to Derrick & others (1976b), the Haslingden Group represents the oldest part of the western succession, and the basal formation, the Mount Guide Quartzite, rests unconformably on basement rocks. This formation consists of a partly conglomeratic lower unit and an upper unit of well-bedded sandstone. The conformably overlying Eastern Creek Volcanics consist of basaltic lavas, thought to be mainly subaerial, and interlayered arenaceous sediments. This basic volcanic unit is overlain conformably by the Myally Subgroup, a sequence of mainly feldspathic sandstones. Each of these units includes fanglomerate-type deposits derived from a landmass formed largely of igneous and metamorphic rocks to the east. The sediments of the Haslingden Group are thought to be shallow-water deposits, hence the total thickness of the Group, ranging in different parts of the region from about 6000 m to about 18 000 m, represents the amount of relative subsidence that must have taken place during deposition, and also indicates that the landmass to the east was probably mountainous for much of this time.

In the west of the Duchess Sheet area, south of the area mapped by Derrick & others, the basal part of the western succession is assigned to two locally interfingering and, hence, partly diachronous units, the Yappo Member of the Mount Guide Quartzite and the Bottletree Formation (≡ Rifle Creek beds of Bultitude & others, 1977). These two units are overlain conformably by the upper part of the Mount Guide Quartzite (≡ upper Mount Guide Quartzite of Derrick & others), and are separated by a major unconformity from the underlying basement, which consists of Kalkadoon Granite and schistose to gneissic and locally migmatitic rocks (undivided Tewinga Group). The Yappo Member (≡ lower Mount Guide Quartzite of Derrick & others) consists mainly of interbedded conglomeratic and arenaceous sedimentary rocks, but also includes some thin beds of pink to grey acid tuff. The Bottletree Formation contains similar rock types together with grey to maroon dacitic lava, basalt, and laminated basaltic tuff. Conglomerate in both units commonly contains abundant acid volcanic clasts, which are generally intensely flattened, even where other clasts are not deformed; these clasts may originally have been pumice, rather than solid rock, resulting from penecontemporaneous volcanism.

The Bottletree Formation extends northwards from the Duchess Sheet area into the southwest part of the Cloncurry Sheet area (Mary Kathleen 1:100 000 Sheet area), where it has been mapped as Argylla Formation by Derrick & others (1977a). These workers consider that this unit is separated from the overlying lower Mount Guide Quartzite (≡ Yappo Member) by a major disconformity. However, field evidence in the Duchess Sheet area indicates that the contact between the two units is concordant and probably conformable and gradational, and locally the two units appear to interfinger along strike. The correlation of the Bottletree Formation with Argylla Formation mapped to the east is based on lithologic similarities, although the two units are less alike than the Leichhardt Metamorphics and Argylla Formation. But U-Pb zircon dating appears not to support such a correlation, as provisional data obtained by R. W. Page (personal communication, 1980) indicate that the Bottletree Formation may be 20-30 m.y. older than the Argylla Formation to the northeast.

The field and geochronological evidence show that the Bottletree Formation is probably part of the Haslingden Group sequence, and may not be a correlative of the Argylla Formation. The boundary between the basement and overlying western succession is, therefore, taken to be the major unconformity beneath the Yappo Member and Bottletree Formation, not a postulated disconformity between the Bottletree Formation and overlying Mount Guide Quartzite.

Ballara Quartzite and Argylla Formation

The basal formation of the Mary Kathleen Group west of the Wonga Belt is the Ballara Quartzite (Derrick & others, 1977a, 1977b). It consists of a lenticular lower unit, up to 700 m thick, formed mainly of locally derived acid volcanic detritus, and an upper unit 500 to 1250 m thick, of mainly quartz sandstone, which probably had a different, more distant, source. The contact between the two units is abrupt rather than gradational.

The formation overlies the Argylla Formation and is overlain conformably by the Corella Formation. The nature of its contact with the Argylla Formation is in dispute. According to Derrick & others (1977a, 1977b) and Wilson & others (1977), the contact is an unconformity or disconformity representing the time interval during which the entire Haslingden Group was deposited to the west. However, the following field evidence can be interpreted as indicating that there is a negligible difference in age between the Ballara Quartzite and Argylla Formation, and that in places the two formations may interfinger.

- The contact between the Ballara Quartzite and Argylla Formation, as mapped in the Cloncurry Sheet area, has a local relief of several hundred metres. In some places the upper unit of Ballara Quartzite rests directly on acid lava or ignimbrite of the Argylla Formation; in other places it is separated from massive acid volcanics by up to 700 m of volcaniclastic sediments and some interbedded tuff, which can be mapped as either the lower unit of Ballara Quartzite or the upper part of the Argylla Formation. Irregular contacts with considerable local relief can, of course, be expected where acid volcanics, especially thick steep-sided bodies of lava, are overlapped by penecontemporaneous sediments, but perhaps are less likely where acid volcanics have been extensively eroded before being covered by shallow shelf sediments.

• The sediments of the lower unit of Ballara Quartzite are indistinguishable from volcaniclastic sediments interlayered with volcanic rocks in the upper part of the Argylla Formation.

• At several localities, beds of quartz sandstone similar to those in the upper unit of the Ballara Quartzite are interlayered with acid volcanics of the Argylla Formation and also, in some places, with underlying basalt lavas of the Magna Lynn Metabasalt.

• No discordance in bedding has been detected between the Ballara Quartzite and Argylla Formation.

A possible unconformity between Ballara Quartzite and underlying Wonga Belt rocks is exposed 18 km north of Mary Kathleen. The basement rocks here consist of acid metavolcanics, which have been assigned to the Argylla Formation by Derrick & others (1977a), but could equally well be much older and part of the Leichhardt Metamorphics sequence.

Derrick & others (1977a) consider that the Ballara Quartzite is represented within the Wonga Belt by discontinuous bands of quartzite, up to 40 m thick, at or near the contact between amphibolitic calc-silicate rocks mapped as Corella Formation and a sequence to the west consisting mainly of acid gneisses. An alternative interpretation is that the quartzite bands are part of the basement sequence and much older than the Ballara Quartzite to the west.

Corella Formation

As mapped by Carter & others (1961) and later workers, the Corella Formation crops out more extensively than any other formation of the Mount Isa Inlier. However, it may represent at least two separate units of widely different ages: a 'young' Corella sequence, regionally metamorphosed mainly to greenschist grade, and exposed west (and east?) of the Wonga Belt, and an 'old' Corella sequence within the Wonga Belt and made up largely of amphibolite grade rocks.

West of the Wonga Belt, where it reaches a maximum thickness of about 1200 m, the Corella Formation consists mostly of calcareous and pelitic metasediments, which are commonly scapolitic, and quartzose to calcareous sandstones, and is thought to represent a near-shore evaporitic carbonate shelf deposit (Derrick & others, 1977a, 1977b). It overlies the Ballara Quartzite conformably and is overlain unconformably by the Mount Albert Group. Possible Corella Formation 30 km east of Mount Isa, mapped as Charley Creek Formation by Carter & others (1961) and as Ballara Quartzite by Derrick & others (1977a), lies unconformably on Argylla Formation and Leichhardt Metamorphics.

Within the Wonga Belt, the sequence mapped as Corella Formation contains banded and brecciated calc-silicate rocks, quartzite and other meta-arenites, acid and basic metavolcanics, mica-schist, marble, and carbonaceous metasiltstone (Derrick & others, 1977a; Derrick, 1980; Bultitude & others, 1978; Blake & others, 1978). It differs from that of the Corella Formation to the west in being much thicker (possibly more than 4000 m thick), in containing a greater variety of rock types, including widespread volcanics, and in being generally more deformed as well as more metamorphosed. Also, these Corella rocks are commonly in concordant contact with acid gneisses to the west, rather than being separated from them by quartzite possibly equivalent to the Ballara Quartzite.

Because of the differences noted above, the previously assumed correlation of the Wonga Belt Corella Formation with the Corella Formation to the west is, in my view, in doubt, and I consider it more likely that the Wonga Belt Corella Formation is a separate and much older unit which belongs to the pre-Haslingden Group basement (Fig. 3B).

The 'old' Corella Formation is intruded by granite and rhyolite dykes isotopically dated at 1720-1740 m.y. (Page, 1978, 1979). These intrusions appear to be post-tectonic or late syntectonic, as they cut across trends in the country rocks and postdate at least part of the regional metamorphism. Hence, the 'old' Corella Formation must be older than 1740 m.y.; but how much older is uncertain. This minimum age for the 'old' Corella Formation is younger than the maximum age for the 'young' Corella rocks, given by the 1780 m.y. date for the underlying Argylla Formation. Hence the isotopic data presently available neither confirm nor negate the suggestion of an 'old' and a 'young' Corella Formation.

Standish volcanics, Makbat Sandstone, and Stanbroke Sandstone

These units are restricted to the Duchess Sheet area (Blake & others, 1978; Bultitude & others, 1978). The Standish volcanics consist predominantly of acid volcanic rocks, including ignimbrites and flow-banded lavas, which typically contain small feldspar and quartz phenocrysts set in a very fine-grained felsitic groundmass. In general these acid volcanics show few obvious effects of any regional metamorphism. Some basic volcanics are present locally. East of Dajarra the Standish volcanics overlie Kalkadoon-type granite, but their relationship to Kalkadoon Granite elsewhere remains somewhat equivocal. The unit is faulted against gneissic rocks mapped as Tewinga Group, and is intruded by pink medium to coarse-grained leucocratic granite (Wills Creek Granite).

The Makbat Sandstone, which crops out in the south of the area, and the Stanbroke Sandstone to the north are exposed in keels of synclines and 'half' synclines (one limb removed by faulting), overlying Standish volcanics probably unconformably. They are regarded as possible lateral equivalents, and may be correlatives of the Ballara Quartzite; alternatively, they could be correlatives of a younger unit, such as the Surprise Creek Formation.

Malbon Group and Soldiers Cap Group

These are generally regarded by other workers as the oldest groups of the eastern succession and broadly equivalent to each other and to the Haslingden Group of the western succession (e.g., Plumb & Derrick, 1975). The Malbon Group, as defined by Derrick & others (1976c), consists of two conformable formations, and ranges in thickness from about 1000 m to 3500 m. The older formation, the Marraba Volcanics, is conformable on the Argylla Formation. It consists of interlayered basaltic lavas and sediments, which are correlated by Carter & others (1961) and Derrick and co-workers, but not by me, with the Eastern Creek Volcanics of the Haslingden Group. The overlying Mitakoodi Quartzite, overlain conformably by units assigned to the Mary Kathleen Group, is considered by Derrick & others to be a possible equivalent of the Ballara Quartzite.

The Soldiers Cap Group crops out in the easternmost part of the Mount Isa Inlier. It consists mainly of arenaceous and pelitic metasediments and basaltic metavolcanics, and is at least 600 m thick; its base is not exposed. Basic volcanics in the upper part are correlated by Carter & others (1961) and Derrick and co-workers with the Marraba Volcanics and Eastern Creek Volcanics. The relationship of the Soldiers Cap Group to adjacent calc-silicate rocks mapped as Corella Formation is uncertain, but the two units do not appear to be separated by a major unconformity (Blake & Derrick, 1980), as was suggested previously (e.g., Carter & others, 1961; Glikson, 1972; Derrick & others, 1976d); both appear to have had similar deformational and metamorphic histories, both contain calc-silicate rocks, and contracts between them, where not marked by breccia, are concordant.

Unconformities

Two regional unconformities have been recognised in the western part of the region. The older one separates crystalline igneous and metamorphic rocks of the basement from overlying sedimentary and volcanic rocks of the Bottletree Formation, Haslingden Group and younger units. It is commonly marked by conglomerate containing clasts of the basement rocks, and represents a tectonic and metamorphic break. As such, it represents a classic major unconformity, and is a fundamental geological feature of the Mount Isa Inlier.

The other regional unconformity separates the Haslingden Group and Quilalar Formation from overlying rocks of the Surprise Creek Formation and Mount Isa Group. This unconformity is marked by local angular discordancies, and may be correlated with a similar unconformity between the 'young' Corella Formation and overlying Mount Albert Group west of the Wonga Belt. Unlike the older unconformity, it does not coincide with a change in metamorphic grade or degree of recrystallation. Between these two regional unconformities the sequence from the base of the Bottletree Formation to the top of the Quilalar Formation, and that from the base of the Magna Lynn Metabasalt to the top of the Corella Formation appear to be essentially conformable. Local angular discordancies can be expected within and on top of volcanic units such as the Argylla Formation, but the many bedded sequences within the volcanic units all appear to be concordant with beds in overlying sedimentary units.

No regional unconformities have been positively identified within the Wonga Belt or to the east. Eastwards from the Duck Creek Anticline area the sequence from the Argylla Formation, the oldest unit exposed, through the Malbon Group to the youngest units of the Mary Kathleen Group is apparently conformable, and no significant breaks in deposition have been demonstrated. Farther east, there no longer appears to be a major unconformity between the Soldiers Cap Group and Corella Formation.

Problems in stratigraphic correlations

Volcanic rocks

Basic and acid volcanic rocks are widespread in the region, and are of several different ages. Basin volcanics (basalt and andesite) are represented by lava flows, which are commonly amygdaloidal, and also by thin-bedded tuffs and rare pillow lavas. They are commonly interlayered with arenaceous to pelitic sedimentary rocks, and are thought to be mainly the products of subaerial or shallow-water volcanism. Acid volcanics are represented by pyroclastic rocks, especially ignimbrite deposits, together with flow-banded lavas, and are locally interlayered with tuffaceous sediments.

Volcanic rocks other than airfall tuffs tend to be confined within a few kilometres, or at most tens of kilometres, of their eruptive sites, filling depressions or forming volcanic cones of limited lateral extent. They may be very thick locally, but thin or absent in adjacent areas when topographic barriers are present. In regions such as Mount Isa, where similar volcanic rocks are known to occur at many different stratigraphic levels, correlations not based on outcrop continuity or demonstrable similarity in age should only be regarded as tentative.

Quartz sandstones

Quartz sandstones are widespread in the Mount Isa Inlier, where they are generally termed 'quartzites'. They form the bulk of such units as the Mount Guide Quartzite, Ballara Quartzite, and Mitakoodi Quartzite, and also occur in many other units. Distinguishing one quartz sandstone or quartzite from another is notoriously difficult, and there is the likelihood in the Mount Isa region of some quartzite bodies being assigned to the wrong stratigraphic unit.

Calcareous rocks

Similar correlation problems to those of volcanic rocks and quartz sandstones also apply to calcareous rocks in the Mount Isa region. Up to now, most of these rocks in the Cloncurry and Duchess Sheet areas have been assigned to the Corella Formation. However, as stated earlier, I think it likely that the Corella Formation of the Wonga Belt is similar in age to part of the Tewinga Group and, hence, is much older than the Corella Formation that overlies the Ballara Quartzite to the west. This suggestion is supported by the occurrence, 11 km south-southwest of Duchess, of interlayered calc-silicate rocks mapped as Corella Formation and augen gneiss similar to that mapped as undivided Tewinga Group to the west, underlying the Haslingden Group.

Igneous intrusions

Basic dykes occur throughout the region, and are of several ages. They consist of amphibolite, metadolerite and dolerite, tend to be concentrated in localised swarms, and mainly have northerly trends. Most are probably related to volcanism represented by the basic lavas present at various stratigraphic levels. They are particularly abundant in the Leichhardt Metamorphics, undivided Tewinga Group, Kalkadoon Granite, lower part of the Haslingden Group, within the Wonga Belt, and locally in the Argylla Formation and Standish volcanics. Few intrude the upper part of the Haslingden Group and overlying rocks in the west. Most dykes intruding the lower part of the Haslingden Group may be related to the Eastern Creek Volcanics, but some are much younger, as they postdate the Mount Isa Group (Glikson & others, 1976): these may be related to a younger sequence of basic lavas no longer exposed, or may not have had any extrusive equivalents. Thick basic sills intrude the Corella Formation west of the Wonga Belt, and are also present to the east, where they include some gabbro masses. Some basic bodies intruding granite form net-veined complexes of the Austurhorn type (Blake, 1966), as at Duchess (Bultitude & others, 1978).

Acid dykes, though much less common, are almost as widespread as basic dykes. Most may be related to acid volcanic units.

Numerous large granitic bodies are exposed, the oldest of which are probably those mapped as Kalkadoon Granite (Carter & others, 1961) and dated at about 1860 m.y. (Page, 1978). Phases of this granite intrude Leichhardt Metamorphics and undivided Tewinga Group and are overlain unconformably by the Bottletree Formation, Haslingden Group, Standish volcanics, and Quilalar Formation. The Kalkadoon Granite is massive to locally foliated, and shows mesozonal and catazonal, rather than epizonal, features, implying emplacement at considerable depth (Buddington, 1959); it appears to represent mainly syntectonic and immediately post-tectonic intrusions. Younger granites in the region form epizonal to mesozonal or catazonal intrusions. They include the Sybella Granite (Carter & others, 1961) in the west, phases of which intrude the Haslingden Group, various granites to the east (Carter & others, 1971; Derrick & others, 1977a, 1978) which post-date at least some rocks mapped as Corella Formation and have given isotopic dates of 1740 to 1670 m.y. (Page, 1978, 1979, 1980), and Wills Creek Granite (Blake & others, 1978), which intrudes Standish volcanics. Most, if not all the granites are composite bodies, and as mapped may include granites of various ages. For example, the Kalkadoon Granite may include some plutons which postdate the Haslingden Group, and the Sybella Granite may include plutons younger as well as older than the Mount Isa Group.

Structural complications

Tight to isoclinal folding and intense faulting characterise the southern part of the Mount Isa Inlier, and cause considerable problems in stratigraphic correlations. Most major folds have northerly trends, although some, such as the Duck Creek and Bulonga anticlines, trend northeast, and some, as near Cloncurry, trend east; axial planes are generally steep to vertical, and plunges are variable. Many of the faults also trend north; most of these may have developed during folding as slippage features along contacts between contrasting lithologies. Some faults coincide with the axial planes of tight folds, causing the development of 'half' synclines and anticlines in which one fold limb appears to be missing. The most prominent major faults in the region—the Mount Isa, Gorge Creek-Mount Remarkable, Fountain Range, and Pilgrim Faults (Fig. 1)—appear to postdate folding, as also do faults forming conjugate sets.

The presence of numerous faults with similar trends to folds in areas of steeply dipping strata makes the distinction of fault blocks from fold structures extremely difficult, except where bedded sedimentary rocks and identifiable stratigraphic successions are involved. Hence, in the southern part of the Mount Isa Inlier, synclines are readily mapped where units such as the Ballara Quartzite or Stanbroke Sandstone are exposed and show sedimentary facing structures, even where one side of the syncline has been removed by faulting; however, corresponding structures are not at all obvious where the only rocks exposed are massive acid volcanics, gneisses, and granites.

Although most of the faults identified in the region appear to be syntectonic and post-tectonic, some faulting no doubt took place during sedimentation and volcanism. Such penecontemporaneous faulting can account for abrupt changes in thickness of rock units (Smith, 1969; Glikson & others, 1976).

One consequence of the intense faulting is the occurrence of numerous shear zones. These range up to about 1000 m in width, and typically consist of chlorite and muscovite/sericite schist, quartzitic breccia, and, in crystalline terrain, mylonitic rocks. Even in the most intense shear zones, though, some recognisable remnants of the pre-existing rock are generally present.

Effects of regional metamorphism

The regional metamorphism of the Precambrian rocks ranges from lower greenschist to upper amphibolite grade. Major changes generally take place over horizontal distances of several kilometres in north to south directions, but, locally, over much shorter distances from east to west, across regional trends. As the metamorphic grade increases, relatively subtle differences in primary lithologies become masked, and relationships become obscured. This presents problems in stratigraphic correlations, which become acute where low grade rocks are faulted against higher grade rocks of similar overall composition—are the high grade rocks the more metamorphosed equivalents of the low grade rocks, or do they belong to a different and probably older unit? This question applies particularly to correlations between rock units of the Wonga Belt and those to the west, and also to the following discussion concerning possible correlatives of the Standish volcanics.

In the western part of the Duchess Sheet area felsitic acid porphyries mapped as Standish volcanics are faulted against gneissic acid rocks mapped as undivided Tewinga Group (Blake & others, 1978; Bultitude & others, 1978). Derrick and Wilson (in Blake & Derrick, 1979; Wilson, 1979) have suggested that the gneissic rocks are the more metamorphosed equivalents of the Standish porphyries, and that both are correlatives of the Leichhardt Metamorphics. That the Standish volcanics may be correlatives of the isotopically dated Leichhardt Metamorphics is not disputed: both units consist mainly of massive quartz-feldspar porphyry and contain only minor bedded clastic rocks. Alternatively, the Standish volcanics may be a much younger unit, the interpretation I favour. (However, since this was written, R. W. Page, personal communication, September 1980, has shown that the Standish volcanics and Leichhardt Metamorphics are similar in age—note added in proof.) The other suggestion of Derrick and Wilson, that the Standish volcanics and adjacent gneissic rocks are stratigraphic equivalents, seems unlikely on the following grounds.

1. The gneissic rocks show compositional and textural banding generally parallel to the foliation; the bands range from less than 1 m to about 100 m in thickness. In contrast, the Standish volcanics are typically massive, and rarely show any recognisable banding. The gneissic rocks appear to represent a heterogeneous sequence of mainly interlayered sediments and volcanics, not a sequence of massive acid porphyries comparable to those forming the bulk of the Standish volcanics.

2. If the gneissic rocks are indeed the more metamorphosed equivalents of adjacent Standish porphyries, faulting with vertical throws of many kilometres is implied, to bring linear belts of low greenschist grade Standish rocks alongside coarsely recrystallised,

amphibolite grade, gneissic equivalents. Such large faults would be a major crustal feature and should be evident north of the Fountain Range Fault; but this is not the case.

An alternative interpretation, and the one favoured by me, is that the Standish volcanics are much younger than the gneissic rocks, and are separated from them by a period of metamorphism and tectonism. I also consider it likely that the gneissic rocks are older than the isotopically dated Leichhardt Metamorphics.

An additional problem resulting from regional metamorphism is the distinction in gneissic terrains of metamorphosed acid volcanics and volcaniclastic sediments from metamorphosed granite and high-level intrusives, especially in the western part of the Duchess Sheet area and in the Wonga Belt. Original granites can usually be identified, but some acid gneisses, especially those with augen, could be interpreted equally well as either volcanics or high level intrusives. Acid gneiss interlayered with calc-silicate rocks mapped as Corella Formation 11 km south-southwest of Duchess (Bultitude & others, 1978) falls into this category. Good examples of acid gneiss clearly forming composite intrusive sheets are exposed in the Wonga Belt, 16 km north-northeast of Mary Kathleen: these have amphibolite margins, and are of the type formed by emplacement of acid and basic magma more or less at the same time (cf., Blake & others, 1965).

A geological history of the Mount Isa Inlier up to Mount Isa Group time

The geological history put forward here is summarised in Figure 4. It cannot be confirmed, but neither can it be disproved, by available geological evidence, and, hence, should be considered as one possible alternative to the model of Carter & others (1961) and Derrick and co-workers (e.g., Derrick & others, 1977a; Derrick, 1980). In spite of the recent BMR and GSQ investigations, there are still many uncertainties regarding the stratigraphy and geolical history of he region. Because of these uncertainties, there is plenty of scope for more than one interpretation, and present interpretations will need to be modified, revised, or discarded as additional information is obtained.

Pre-1870 m.y.

The oldest rocks exposed, now mainly gneisses and schists, are considered to represent mainly metamorphosed sediments and volcanics which were deposited during one or more periods of widespread volcanic activity in the region before about 1870 m.y. ago. They are taken to include the Leichhardt Metamorphics (isotopically dated at about 1870 m.y.), which may be the youngest preserved part of the sequence, Wonga Belt rocks, including the 'old' Corella Formation, and the undivided Tewinga Group of the Duchess Sheet area. Together, these rocks form the basement.

1870 m.y. to about 1810 m.y.

Most basement rocks were tightly to isoclinally folded and regionally metamorphosed, mainly to amphibolite grade, probably between about 1870 and 1850 m.y. ago. The tectonism was accompanied and immediately followed by the intrusion of Kalkadoon Granite at moderate to deep crustal levels, and the region was uplifted to form part of a large and probably mountainous landmass. A period of erosion commenced, and in time the landmass became sufficiently worn down for large areas of crystalline metamorphic rocks to be exposed and part of the Kalkadoon Granite batholith unroofed.

About 1810 m.y. to about 1780 m.y. (Fig. 4A)

After an erosional period of many millions of years, perhaps from about 1850 m.y. to about 1810 m.y. ago, sedimentation recommenced in the region, on the west side of the landmass. Coarse detritus was deposited in a subsiding basin on an irregular surface of crystalline basement rocks. This sedimentation was accompanied by basaltic to dacitic or rhyolitic volcanism. The resulting sediments and volcanics formed the Bottletree Formation and the Yappo Member of the Mount Guide Quartzite at the base of the Haslingden Group.

Subsidence continued in the basin throughout Haslingden Group time, more or less keeping pace with sedimentation. During this period the land area immediately to the east may have shown a corresponding uplift, as it continued to shed coarse detritus westwards to form alluvial fans close to the shoreline. A change in sedimentation took place after the deposition of the Bottletree Formation and Yappo Member, as these two units were succeeded conformably by relatively well-sorted sands, which now form the Mount Guide Quartzite.

The top of this formation marks the onset of the phase of basaltic volcanic activity which formed the Eastern Creek Volcanics. During this phase, a thick and widespread succession of basic lavas was laid down in the basin, together with interlayered sediments, which included sands similar to those of the underlying Mount Guide Quartzite. The lavas and interlayered sediments were succeeded conformably by Myally Subgroup sediments, mainly feldspathic and quartz-rich sands.

Most if not all of the Haslingden Group sediments appear to have been deposited in shallow water, and the thickness of the sequence, ranging up to about 18 000 m, is a measure of the amount of relative subsidence that took place in the depositional area.

Some of the huge volumes of quartz-rich sands in the Haslingden sequence may have come from the west and southwest, as suggested by Carter & others (1961), or alternatively, the landmass to the east may have been the main or only source. This landmass, inland from coastal ranges, may have had a mainly subdued relief for most of Haslingden Group time, with broad undulating upland areas supplying mature quartz-rich detritus to westward-flowing river systems.

About 1780 m.y. to about 1750 m.y. (Figs 4B, C)

By the end of Haslingden Group time, perhaps about 1770 m.y. ago, the landmass to the east had been worn down to form a mainly low-lying undulating area with some residual hills and ridges. A marine transgression at this time inundated the lower-lying areas, but left the highest ground as land. (This marine transgression can be likened to that which took place in the Mount Isa region in the Mesozoic, when all or most of the Mount Isa Inlier was covered by up to 100 m of fluvial and shallow marine sediments). However, before being inundated, the land area had been the site of widespread volcanic activity, and basic and acid lavas and ignimbrites filled depressions and formed local volcanic cones. These volcanics are represented by the Magna Lynn Metabasalt and Argylla Formation (dated at about 1780 m.y.)

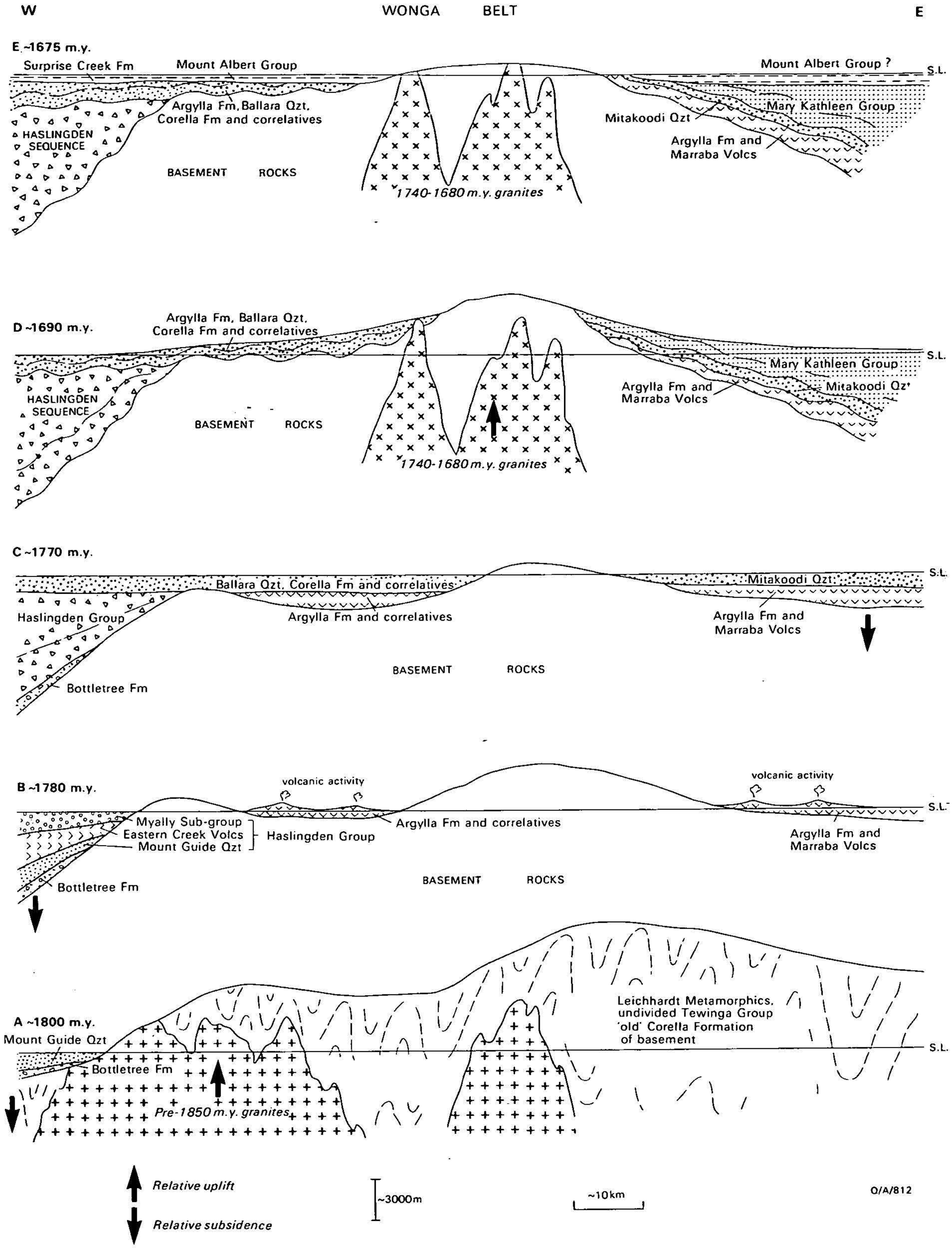

Figure 4. Stages in the development of the Mount Isa Inlier from about 1800 m.y. to about 1675 m.y. ago.

west of the Wonga Belt, and by the Argylla Formation, Marraba Volcanics, and possibly some of the volcanics of the Soldiers Cap Group to the east. The volcanism may be responsible for the high feldspar content (volcanic ash?) in sandstones of the Myally Subgroup.

In the west, the sand blanket of the marine transgression was deposited conformably on the Haslingden Group and unconformably on the basement rocks immediately to the east. Further east it was laid down conformably to unconformably on the Argylla Formation to form the upper unit of the Ballara Quartzite, and perhaps on Standish Volcanics to form the Makbat and Stanbroke Sandstones, and it onlapped eastwards onto basement rocks of the Wonga Belt, part of which remained above sea level. East of the Wonga Belt the same marine transgression may be represented by the Mitakoodi Quartzite.

The source of the quartz sand deposited during the marine transgression, like that of the Haslingden Group, is uncertain. Derrick & others (1977a) suggested that much of the Ballara Quartzite in the Cloncurry Sheet area may have been derived from a basement high to the west, between the present outcrops of Ballara Quartzite and Quilalar Formation, and this remains a possibility. The quartz-rich detritus could not have been derived from reworking of Haslingden Group sediments, as these were overlain conformably by the transgressive sand in layer-cake fashion, and so were not being eroded at this time. Similarly, volcanics of the Argylla Formation are an unlikely source: exposed contacts show these volcanics to be overlain by considerable thicknesses of quartz sandstone, and they do not appear to have formed significant land areas at this time; also, where they have been a source of detritus (as in the lower unit of Ballara Quartzite), the resulting sediments are highly feldspathic and relatively quartz-poor. A distant source cannot be ruled out: the quartz-rich sand may have been transported from outside the present confines of the Mount Isa Inlier. Another possibility is a more local source: the sand may represent residual regolithic material, developed by prolonged weathering of the crystalline basement rocks and reworked during the marine transgression.

Shallow-water sedimentation continued west of the Wonga Belt after the deposition of the Ballara Quartzite and its correlatives. Carbonate deposition became widespread; but sands, silts, and clays were also deposited. The calcareous sediments were commonly also evaporitic, and some were stromatolitic. They are represented by the upper part of the Quilalar Formation and the 'young' Corella Formation. East of the Wonga Belt, somewhat deeper water deposits may be represented by the possible turbidite-type sediments of the Answer Slate, Kuridala Formation and Soldiers Cap Group (Blake & others, 1979); these possible lateral equivalents show an overall increase in grainsize from the west to east, and hence may have had a source area to the east.

Some minor volcanic activity took place during and after the marine transgression, as is indicated by scattered occurrences of basic and acid volcanics in the sedimentary sequence. The latest igneous activity of this period may have been the intrusion of basic magma, mainly as sills, into the Corella Formation west of the Wonga Belt and into formations of the Mary Kathleen Group to the east.

The sequence from the base of the Magna Lynn Metabasalt to the top of the 'young' Corella Formation, and correlative sequences to the west and east, appear to be essentially conformable, and they span perhaps 30 million years, from about 1780 m.y. to perhaps about 1750 m.y. These sequences have a preserved thickness west of the Wonga Belt of up to 4000 m, and may be much thicker to the east.

About 1750 m.y. to about 1680 m.y. (Fig. 4D)

Between about 1750 m.y. and 1680 m.y. the region was subjected to another phase of tectonism, during which the 'young' Corella Formation and correlative and older rocks were gently folded and locally intruded, thermally metamorphosed, and in places metasomatised by granite. Much of the granite emplacement at this time appears to have taken place close to the Wonga Belt.

Local angular unconformities between the 'young' Corella Formation and correlatives and younger units in the west (Surprise Creek Formation, Mount Albert Group, Mount Isa Group) are attributed to gentle folding and associated uplift and erosion during this period. Regional metamorphic effects associated with the folding appear to have been minimal.

About 1680 m.y. to about 1670 m.y. (Fig. 4E)

Following the period of gentle folding, and some subsequent erosion, sediments of the Surprise Creek Formation and Mount Albert Group were deposited in the west. Those of the Surprise Creek Formation, were succeeded conformably or disconformably by sediments of the Mount Isa Group, which also overlapped on to older rocks. The Mount Isa Group contains numerous tuff beds, one of which has been dated at about 1670 m.y. (Page, in press).

Post Mount Isa Group time (about 1670 m.y. to about 1140 m.y.)

Some time after about 1670 m.y. the Mount Isa Group and older rocks were tightly folded and regionally metamorphosed to greenschist and amphibolite grades during one or more major tectonic events. The metamorphism may have occurred between 1670 and 1625 m.y. or between 1620 and 1490 m.y., or during both periods, as suggested by Page (1978) from Rb-Sr total-rock data. It certainly took place before the intrusion of the Lakeview Dolerite (Derrick & others, 1978), a unit of east to northeast-trending dykes which cut across regional trends and are neither deformed nor regionally metamorphosed. These dykes have been dated by Rb-Sr techniques at 1140 ± 12 m.y. (Page, 1976).

I attribute the main folding and metamorphism of the Haslingden sequence, Ballara Quartzite, and 'young' Corella Formation, and correlatives to this post-Mount Isa Group tectonism, not to the earlier 1750-1670 m.y. tectonic event.

Conclusions

Many uncertainties regarding relations of rock units and stratigraphic correlations still exist in the Mount Isa Inlier. Many aspects of the geological history remain in doubt, and interpretations put forward need to be questioned. As with most geological studies, much work remains to be done before the problems can be considered solved.

Some factors in the early geological history, up to Mount Isa Group time, seem to be reasonably well established. These include the following:

- Basement rocks were regionally metamorphosed and intruded by granite dated at about 1860 m.y. before being overlain unconformably in the west by sediments and volcanics of the Bottletree Formation and Haslingden Group.
- An interval of about 90 m.y. separates basement Leichhardt Metamorphics, dated at 1865 m.y., from overlying Magna Lynn Metabasalt and Argylla Formation.
- Acid and basic volcanics, quartz sandstone, and calcareous sediments are present at many stratigraphic levels.

- Acid and basic intrusions are widespread, and are of several different ages.

Some of the questions that remain are:

1. Do rocks mapped as Corella Formation belong to a single formation or to two or more units of significantly different ages, including a unit forming part of the basement sequence?
2. Are rocks assigned to the Leichhardt Metamorphics all of comparable age?
3. Is most or all of the Haslingden Group older or younger than the Argylla Formation to the east?
4. Are the basalts of the Eastern Creek Volcanics in the west similar or significantly different in age to those of the Marraba Volcanics to the east?
5. Are the Argylla Formation and overlying Ballara Quartzite closely comparable in age or are they separated by a major unconformity?
6. Were Wonga Belt rocks metamorphosed before, as well as after, the deposition of the Ballara Quartzite to the west?
7. How do units east of the Wonga Belt correlate with those to the west?
8. Finally, was there at any time a western succession of cover rocks separated from a stratigraphically equivalent eastern succession of cover rocks by a crystalline basement high?

Acknowledgements

This paper is partly the result of numerous discussions with colleagues, both in the field and in the office. In particular I am grateful to G. M. Derrick, R. J. Bultitude, K. R. Walker, E. K. Carter, and R. W. Page of BMR and P. J. T. Donchak and I. H. Wilson of GSQ, who have offered their own views, criticisms of mine, and advice not often heeded, on many occasions. The inevitable disagreements have been stimulating, and have not affected friendships. I wish to thank J. H. C. Bain and R. J. Tingey for reviewing versions of the manuscript.

References

BLAKE, D H., 1966—The net-veined complex of the Austurhorn intrusion, southeastern Iceland. *Journal of Geology*, **74**, 891-907.

BLAKE, D. H., & DERRICK, G. M., 1980—Mount Isa and Duchess projects: joint inspection of the Mount Isa/Duchess region July-August 1979. *In* Geological Branch Summary of Activities 1979. *Bureau of Mineral Resources, Australia, Report* **222**.

BLAKE, D. H., ELWELL, R. W. D., GIBSON, I. L., SKELHORN, R. R., & WALKER, G. P. L., 1965—Some relationships resulting from the intimate association of acid and basic magmas. *Quarterly Journal of the Geological Society, London*, **121**, 31-49.

BLAKE, D. H., DONCHAK, P. J. T., & BULTITUDE, R. J., 1978—Precambrian geology of the Dajarra 1:100 000 Sheet area, northwestern Queensland—preliminary data. *Bureau of Mineral Resources, Australia, Record* **1978/46** (unpublished).

BLAKE, D. H., JAQUES, A. L., & DONCHAK, P. J. T., 1979—Precambrian geology of the Selwyn region, northwestern Queensland—preliminary data. *Bureau of Mineral Resources, Australia, Record* **1979/86** (unpublished).

BLAKE, D. H., BULTITUDE, R. J., & DONCHAK, P. J. T., in preparation—Definitions of newly named and revised Precambrian stratigraphic and intrusive rock units in the Duchess and Urandangi 1:250 000 Sheet areas, Mount Isa Inlier, northwestern Queensland. *Bureau of Mineral Resources, Australia, Report.*

BUDDINGTON, A. F., 1959—Granite emplacement with special reference to North America. *Geological Society of America Bulletin* **70**, 671-747.

BULTITUDE, R. J., BLAKE, D. H., & DONCHAK, P. J. T., 1978—Precambrian geology of the Duchess 1:100 000 Sheet area, northwestern Queensland—preliminary data. *Bureau of Mineral Resources, Australia, Record* **1978/112** (unpublished).

BULTITUDE, R. J., GARDNER, C. M., & NOON, T. A., 1977—A recently discovered unconformity near the base of the Proterozoic Cloncurry Complex south of Mount Isa, northwestern Queensland. *BMR Journal of Australian Geology & Geophysics*, **2**, 311-4.

CARTER, E. K., BROOKS, J. H., & WALKER, K. R., 1961—The Precambrian mineral belt of north-western Queensland. *Bureau of Mineral Resources, Australia, Bulletin* **51**.

DERRICK, G. M., 1980—Marraba, Queensland. *Bureau of Mineral Resources, Australia, 1:100 000 Geological Map Commentary.*

DERRICK, G. M., WILSON, I. H., & HILL, R. M., 1976a—Revision of stratigraphic nomenclature in the Precambrian of northwestern Queensland. I: Tewinga Group. *Queensland Government Mining Journal*, **77**, 97-102.

DERRICK, G. M. WILSON, I. H., & HILL, R. M., 1976b—Revision of stratigraphic nomenclature in the Precambrian of northwestern Queensland. II: Haslingden Group. *Queensland Government Mining Journal*, **77**, 300-6.

DERRICK, G. M., WILSON, I. H., & HILL, R. M., 1976c—Revision of stratigraphic nomenclature in the Precambrian of northwestern Queensland. IV: Malbon Group. *Queensland Government Mining Journal*, **77**, 514-7.

DERRICK, G. M., WILSON, I. H., & HILL, R. M., 1976d—Revision of stratigraphic nomenclature in the Precambrian of northwestern Queensland. V: Soldiers Cap Group. *Queensland Government Mining Journal* **77**, 600-4.

DERRICK, G. M., WILSON, I. H., HILL, R. M., GLIKSON, A. Y., & MITCHELL, J. G., 1977a—Geology of the Mary Kathleen 1:100 000 Sheet area, northwest Queensland. *Bureau of Mineral Resources, Australia, Bulletin* **193**.

DERRICK, G. M., WILSON, I. H., & HILL, R. M., 1977b—Revision of stratigraphic nomenclature in the Precambrian of northwestern Queensland VI: Mary Kathleen Group. *Queensland Government Mining Journal*, **78**, 15-23.

DERRICK, G. M., WILSON, I. H., & HILL, R. M., 1977c—Revision of stratigraphic nomenclature in the Precambrian of northwestern Queensland. VII. Mount Albert Group. *Queensland Government Mining Journal*, **78**, 113-6.

DERRICK, G. M., WILSON, I. H., & HILL, R. M., 1978—Revision of stratigraphic nomenclature in the Precambrian of northwestern Queensland. VIII: Igneous rocks. *Queensland Government Mining Journal*, **79**, 151-6.

DERRICK, G. M., WILSON, I. H., & SWEET, I. P., 1980—Quilalar and Surprise Creek Formations—new Proterozoic units from the Mount Isa Inlier: their regional sedimentology and application to regional correlations. *BMR Journal of Australian Geology & Geophysics*, **5**, 215-23.

GEOLOGICAL SURVEY OF QUEENSLAND, 1975—Queensland geology, scale 1:2 500 000. *Department of Mines, Brisbane.*

GLIKSON, A. Y., 1972—Structural setting and origin of Proterozoic calc-silicate megabreccias, Cloncurry region, northwestern Queensland. *Journal of the Geological Society of Australia*, **19**, 53-63.

GLIKSON, A. Y., DERRICK, G. M., WILSON, I. H., & HILL, R. M., 1976—Tectonic evolution and crustal setting of the middle Proterozoic Leichhardt River fault trough, Mount Isa region, northwestern Queensland. *BMR Journal of Australian Geology & Geophysics*, **1**, 115-29.

PAGE, R. W., 1976—Mount Isa/Cloncurry Project, Queensland. *In* Geological Branch Summary of Activities 1975. *Bureau of Mineral Resources, Australia, Report* **194**, 106.

PAGE, R. W., 1978—Response of U-Pb zircon and Rb-Sr total rock and mineral systems to low-grade regional metamorphism in Proterozoic igneous rocks, Mount Isa, Australia. *Journal of the Geological Society of Australia*, **25**, 141-64.

PAGE, R. W., 1979—Mount Isa Project. *In* Geological Branch Summary of Activities 1978. *Bureau of Mineral Resources, Australia, Report* **212**, 181-2.

PAGE, R. W., 1980—Mount Isa Project. *In* Geological Branch Summary of Activities 1979. *Bureau of Mineral Resources, Australia, Report* **222**, 226.

PAGE, R. W., in press.—Depositional ages of the stratiform base metal deposits at Mount Isa and McArthur River, Australia, based on U-Pb zircon dating of concordant tuff horizons. *Economic Geology.*

PLUMB, K. A., & DERRICK, G. M., 1975—Geology of the Proterozoic rocks of the Kimberley to Mount Isa region. *In* KNIGHT, C. L. (editor)—Economic geology of Australia and Papua New Guinea: 1. Metals. *Australasian Institute of Mining and Metallurgy Monograph* **5**, 217-52.

SMITH, W. D., 1969—Penecontemporaneous faulting and its likely significance in relation to Mount Isa ore deposition. *Geological Society of Australia Special Publication*, **2**, 225-35.

WILSON, I. H., 1978—Volcanism on a Proterozoic continental margin in northwestern Queensland. *Precambrian Research*, **7**, 205-35.

WILSON, I. H., 1979—BMR-GSQ field review of the geology of the Mount Isa region, 1979. *Geological Survey of Queensland Record* **1979/44** (unpublished).

WILSON, I. H., DERRICK, G. M., HILL, R. M., DUFF, B. A., NOON, T. A., & ELLIS, D. J., 1977—Geology of the Prospector 1:100 000 Sheet area (6857), Queensland. *Bureau of Mineral Resources, Australia, Record* **1977/4** (unpublished).

BMR Journal of Australian Geology & Geophysics, 5, 1980, 257-263

Some aspects of interstitial water movements in simulated sedimentary systems

B. Bubela[1]

Biological and abiological factors influencing interstitial water movements in sediments were studied in a simulated system. The porosity and permeability of the system decreased significantly during the 10 months of the experiment. The major governing processes were the production of an algal mat at the water-sediment interface, formation of biomass in interstitial spaces, diagenetic changes of buried algal material, and the formation of iron sulphide, evaporites, and gas locks in the sediments. The relevance of heteropermeability to the flow of underground fluids, as related to ore genesis, movement of non-miscible liquids, and environmental studies, and that of gas locks to cementation is discussed.

Introduction

Many of the world's lead, copper and zinc ore bodies are found in rocks initially deposited in sedimentary environments containing carbonates (Renfro, 1974). Water movement is frequently responsible for many of the characteristics encountered in such environments. Transport of metals, pH and Eh of the interstitial waters, and saturation of such waters in respect of a variety of ions are some of the factors which may be influenced by the hydrology of the sediments. An understanding of at least some of those affecting water movements in sedimentary environments is necessary for the evaluation of processes leading to ore genesis in sediments. Therefore, an experimental system was devised (Bubela & others, 1978) for the simulation and the study of selected processes related to such water movements. The system was designed and operated to study diagenetic changes, caused by biological and abiological activities, in the pores of the sediments.

To enable the correlation of observations from the experiment with a natural environment, a number of sediment samples were collected from an intertidal area in the northern part of Spencer Gulf, South Australia. This area resembles in some aspects environments described by Renfro (1974) and Kinsman (1969) as suitable for investigation of mechanisms involved in ore genesis. This paper presents the results pertinent to the movement of the interstitial waters in such environments.

Apparatus

The apparatus consists of a set of interconnected tanks, of a total capacity of approximately 5000 litres, equipped with a programmable memory bank controlling temperature, illuminating cycles, water circulation through a variety of pathways (Bubela & others, 1978), and a coring rig for collecting cores of poorly consolidated sediments (Bubela & Ferguson, 1973).

Methods

To simulate a simple sedimentary system, where biological and abiological changes could be expected to take place in experimentally acceptable time limits, the central tank was filled as follows: the charge consisted of quartz sand overlaid with crushed high-magnesium calcite, which was covered by fragmented algal mat. The top layer of the sediments was made of crushed aragonite. Living algal mat from Spencer Gulf was seeded on the sediments' top surface. A layer of ferric oxide baked on quartz sand was added as a trap for H_2S on the top of the buried algal mat. Natural sea water was used as the aquatic phase. It covered the sediments up to a depth of 15 cm. Chemical and physical composition of the tank content is presented in Tables 1 and 2, and Figure 1.

The sea water was originally circulated upwards through the sediments at a rate of 2 cm (~20 litres) per day for about 6 weeks. After that, the permeability of the system decreased considerably, owing to chemical and biological changes, and the fluid became stationary. The temperature of the supernatant waters was kept at 25°C, the sediment temperature at 18°C, and the illumination on a cycle of 12 hours off and 12 hours on. After 10 months the water level in the tank was lowered 20 cm below the sediment surface and the surface temperature was raised to 35°C for 4 weeks.

To establish that there was vertical water-movement caused by capillary forces during the evaporative cycle, a saturated solution of sodium fluorescein in concentrated seawater of 10% salinity was injected (at two locations) into the sediments. Cores were collected from these locations after 4 weeks and were examined under ultraviolet light for the fluorescein distribution. Previous experiments indicated that no significant amounts of fluorescein were absorbed from highly saline solutions onto sediment particles as used in the tank.

Water content, bulk density and porosity* of the tank's components were determined in standard ways.

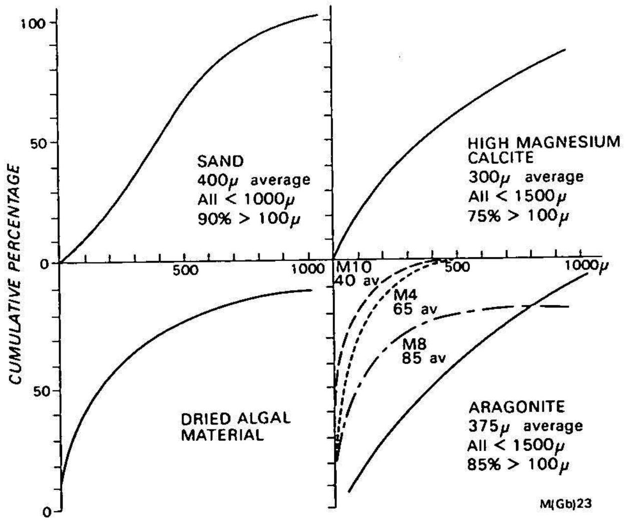

Figure 1. Particle size distribution of sediments used in the tank. M4, M8, and M10 are samples collected.

1. Baas Becking Geobiological Laboratory, P.O. Box 378, Canberra City, ACT 2601, Australia.

	Algal mat	Aragonite	Organic matter	Magnesium calcite (15.4% mol Mg Carbonate)	Sand	Spencer Gulf		Total core less mat
Thickness (*cm*)		18.5^{a} 16.0^{e}	1.5^{a} ~ 2	19^{a} 16.5^{e}	17^{a} 14.5^{e}			
Bulk density (*g/ml*)		1.53^{b} 1.78^{d} 1.86^{e} 1.50^{f}		1.35^{b} 1.47^{d} 1.65^{e}	1.60^{b} 1.68^{d} 1.63			
Density (g/cm^{-3})		2.66^{a} 2.71^{l}		2.16 2.71^{l}	2.59^{a} 2.59^{l}			
Void ratio ϕ (*fraction of bulk volume*)		$.44^{b}$ $.38^{c}$ $.30^{d}$ $.30^{e}$		$.53^{b}$ $.52^{c}$ $.45^{d}$	$.38^{b}$ $.38^{c}$ $.35^{d}$ $.37^{e}$	$.62^{h}$ $.41^{i}$ $.42^{j}$	$.58^{h}$ $.39^{i}$	
Permeability (*millidarcies*) V = Vertical H = Horizontal	V$<0.1^{j,c}$ V$<0.1^{d}$	V 1800^{b} V $1500^{i,c}$ V $3660^{i,c}$ V 1270^{d} H 3100^{d} V $5354^{d,f}$ V $169^{d,g}$ V 80^{e} H 2710^{e}	V $495^{b,k}$ V $15^{c,k}$ V $6^{d,k}$ V $\sim 1.25^{e,k}$	V 4500^{b} V 4000^{c} H 10000^{c} V 3800^{d} H 9460^{d} V 3640^{e} H 9130^{e}	V 5500^{b} V 5500^{c} H 22600 V 5300^{d} H 21800^{d} V 5280^{e} H 17920^{e}	V $.24^{i}$ H 3400^{i}	$.28^{i}$	V 330^{b} V 10^{c} H 641910^{c} V 4^{d} H 607690^{d} V 1^{e} H 458240^{e}
Organic carbon (*ppm dry weight*)		160^{a} 8300 top 1300^{d} below surface 16000 or ^{e}	24700^{a} 43400^{d} 32000^{e}	7900^{a} 4800^{d} 4400^{e}	700^{a} 30^{d} 36^{e}			

a: original e: 9 months i: 10 cm deep
b: 1 month f: dried j: 25 cm deep
c: 2 months g: rewetted k: calculated
d: 5 months h: surface l: Hodgman, C. D., 1960

Table 1. Physical properties of sediments.

	Density ($g\ cm^{-3}$)	Viscosity (*cP*)	Surface tension (mNm^{-1})	Dissolved solids (*m%*)
Distilled water (standard)	0.998	0.936	73.5	0
Seawater[a]	1.025	1.056	73.6	3.80
Surface water	1.061^{d}	nd^{d}	80.1^{d}	8.6^{d}
	1.094^{e}	1.138^{e}	88.1^{e}	13.0^{e}
	1.1165^{f}	1.262^{f}	86.8^{f}	15.6^{f}
NaCl 13% w/w	1.095	1.085	75.25	13.0
Water from outer tank	1.022^{d}	nd	74.4^{d}	3.2^{d}
Water from under the reaction tank	1.020^{f}	1.058^{f}	73.9^{f}	3.00^{f}
	1.029	1.068	nd	4.3
Interstitial water from:				
Aragonite	1.066^{d}	nd	nd	9.3^{d}
	1.1084^{f}	1.285^{f}	82.8^{f}	14.0
	1.046^{d}	nd	nd	6.5^{d}
Organic layer	1.030^{d}	nd	nd	4.3^{d}
		1.172^{f}	$\sim 200^{f}$	
Magnesium calcite	1.026^{d}	nd	78.1^{d}	3.8^{d}
(15.5 mol % Mg carbonate)	1.053^{e}	1.113^{f}	78^{f}	7.0^{e}
Sand	1.025^{d}	nd^{c}	77.5^{d}	3.6^{d}
	1.031	1.070	76^{f}	5.0^{e}
Dry mat and seawater	1.020	1.050	75	3
Dry organic layer and water	1.022	1.033	79	3

a = original d = 5 months
b = 1 month e = 8 months
c = 2 months f = 9 months
nd = not determined due to lack of material.

Table 2. Physical properties of the aquatic component of the simulating system at 23°C.

For the determination of specific gravity of liquids an AP PAAR DMA Calculating Digital Densitometer (Anton Paar—Germany) was used. Surface tensions were measured on a Spinning Drop Interfacial Tensiometer M300 (University of Texas) by the method of Cayias & others (1975). Permeability of the sediments was determined with a modified Hassler cell as described by Pirson (1958). Grain size was determined by wet (methanol) and dry sieve analyses on a sieve shaker. Organic carbon was estimated with thermoconductors as CO_2 on a LECO Induction Furnace W12 Carbon Determinator (Laboratory Equipment Corp, Michigan, USA).

The permeability of the organic layer was calculated using equation

$$k_{TV} = \frac{1}{l_1/k_1 + l_2/k_2 + \ldots + l_n/k_n}$$

(1) (Engelhardt, 1977)

where k_{TV} is the total vertical permeability, $k_1 \ldots k_n$ are individual permeabilities and $l_1 \ldots l_n$ are thicknesses of individual layers.

The total horizontal permeability (k_{TH}) of the tank sediments was calculated using equation

$$k_{TH} = l_1k_1 + l_2k_2 + \ldots + l_nk_n$$

(2) (Engelhardt, 1977)

$l_1 \ldots l_n$, and $k_1 \ldots k_n$ being the thicknesses and individual horizontal permeabilities of the layers.

The change of direction of the fluid through strata due to variation of permeability was calculated from equation

$k_1 : k_2 = \tan\alpha_1 : \tan\alpha_2$ (3) (Engelhardt, 1977)

where k_1, k_2 are vertical permeabilities of the strata and α_1, α_2 are the inclination angles from the perpendicular of the fluid pathways.

Results

Algal mat

Within the first 3 months, when the salinity of the aquatic phase was 4.5%, a continuous algal mat developed on the water-sediment interface (Fig. 2). The thickness of the mat increased from 1 mm after three months to about 6 mm after 10 months. The dominant filamentous blue-green alga was tentatively identified as *Schizothrix* sp. (possibly *Microcoleus* sp.) and the subdominant as *Phormidium* sp. Readily identifiable bacteria were *Beggiatoa* sp. and purple sulphur bacteria. Diatoms and the unicellular blue-green alga *Aphanocapsa* sp. were also present.

During its growth, the algal mat became firmly attached to the sediments (Fig. 3) and, because of its low permeability (0.1 md), it presented an effective barrier both to liquids and gases. The mat created an effective boundary between an oxidative environment, the surface waters of redox potential of +200 mV, and the strongly reducing underlying sediments of a redox potential of −340 mV. The sediments were black, containing free and hot phosphoric acid-labile sulphide. The low permeability of the mat to gases was evident when biologically produced gases in the sediments caused the mat to detach from the sediment surface and gas-containing blisters were formed at the end of the 4th month. The gases were a mixture of CO_2, H_2S, and methane. As the mat was of low permeability and the biogenic gas could not escape, interstitial water was partially removed by the gas from the upper sediments and undersaturated conditions with respect to water content became predominant.

The algal mat remained visually unchanged up to the 8th month, when the salinity of the supernatant waters reached 13%. At this stage, the mat started to die off and bacterial bloom developed, persisting for about 3 days. When the salinity reached approximately 15%, the algal mat recovered, and its continuity over the surface of the sediments was reestablished.

While the mat limited a free movement of fluids, it permitted passage of at least some metal ions. At pH 7.7, 20°C, and concentration gradient 500 μ moles over 1 mm mat thickness, Cu passed at 75 μ moles per cm^2 per day. However, metal bound to an organo-complex (ethylendiamine-tetraacetic acid) did not pass through the mat in 72 hours.

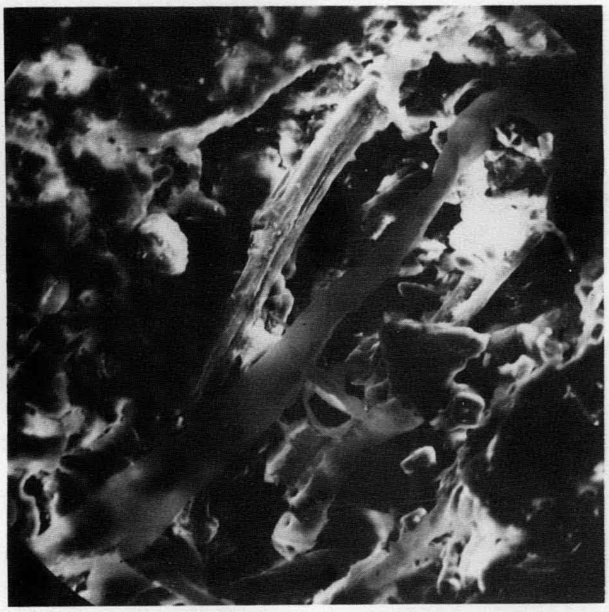

Figure 2. Scanning electron microscope picture of the algal mat at the water-sediment interface. x 150.

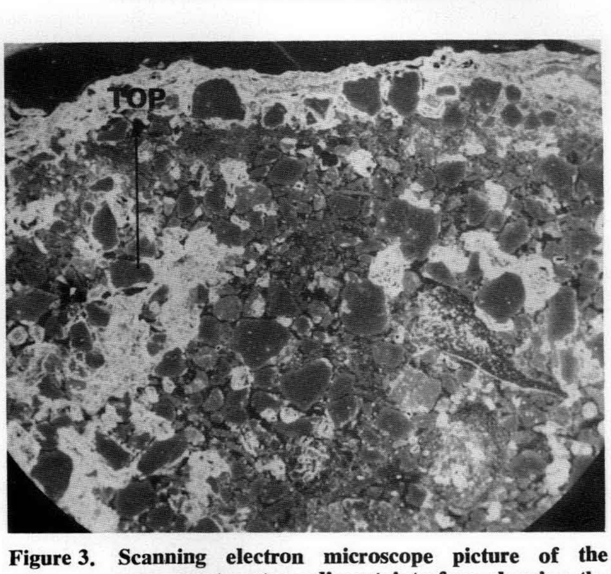

Figure 3. Scanning electron microscope picture of the uppermost water-sediment interface showing the sealing effect of the algal mat. x 40.

---

* porosity $= \frac{V_p}{V_t}$ where V_p = pore volume and V_t = total volume

Porosity

The interparticle spaces in the sediments decreased with time, the highest decrease occurring in the aragonite, the lowest in the quartz sand. The porosities of the tank's sediments were much lower (0.3-0.4) than the porosities of samples collected from Spencer Gulf (0.5-0.6) (Table 1). The intraparticle porosity of the tank's sediments was highest in the calcite and lowest in the quartz sand (Table 1).

Permeability

The permeability of the algal mat has been described. The permeabilities to brines of the samples from the tank and samples collected from Spencer Gulf are presented in Table 1; measurements ranged from ~640 d to 1 md. The permeability of the individual strata in the tank decreased in time both vertically and horizontally.

The permeability of an air-dried sample of the aragonite sediment increased about 4 times. When the sample was rewetted by imbibition, air locks decreased its permeability to 12% of its original value (Table 1).

The two locations where fluorescein was injected differed in their algal covers. One was practically free of the algal mat, while the other had a cover approximately 6-8 mm thick. The mat-free area showed vertical fluorescein movement of about 12 cm (up to the surface), while in the other case no significant movement was detected in 4 weeks.

New mineral phases

Chemical analysis and visual observations demonstrated an increase in microfine iron sulphide by biological sulphate reduction through the sediments. This sulphide originated from the sulphate in the seawater used in the experiment. After 8 months, the aragonite contained 15 μg, the magnesium calcite 50 μg, and the sand ~1 μg of sulphide per 1 g of the dry sediment. The organic layer contained 280 μg sulphide per 1 g of dry weight. The sulphide could not be identified by its X-ray diffraction (XRD) pattern.

During the evaporative cycle, patches about 2-3 mm thick, some brown, some white, appeared on the top of the algal mat. The white material was identified by XRD as a mixture of gypsum and halite, while the brown material consisted of halite, gypsum, and protodolomite, and, at the last stage, dolomite.

Salinity

The aquatic phase in the tank had originally a SG 1.024 at 20°C, corresponding to ~3.8% NaCl. During the 8 months, the salinity on the top of the sediments increased gradually to SG 1.094/20°C~12.5% NaCl. Despite this considerable increase, the density and salinity at the bottom of the sediments were 1.029 and 4.3% respectively. No significant changes in the salinity of the interstitial waters occurred in the upper layers of the sediments when the water level was lowered 20 cm below the surface of the sediments and the surface temperature was elevated to 35°C.

Organic carbon

The concentration of organic carbon increased in all the sediments but the sand. The maximum increase occurred in the buried organic layer and in the aragonite layer just below the surface (Table 1). The quartz sand analysis indicated that 95% of the organic carbon originally present was lost in 9 months.

Discussion

Material

The experiment simulated some of the processes occurring in an intertidal environment, where biological activity and resulting diagenetic changes in the organic and mineral components of the sediments significantly affect mechanisms involved in metal accumulation, transport, and deposition (Renfro, 1974). The reasons for using the material incorporated into the tank were as follows:

Algal mat is the principal source of organic matter in the intertidal zone, both at the water sediment interface and buried in the sediment, where it is used as a source of organic carbon during microbiological activity. Therefore, it was used in both locations in the tank.

Carbonates are frequently associated with metal deposits in sedimentary environments, often as dolomite (Renfro, 1974). Dolomitisation processes involving metastable carbonates in the temperature range of 20-25°C and atmospheric pressure in simulated systems have been demonstrated (Bubela, 1975, Davies, 1977). Therefore, metastable carbonates were included in the tank.

Porosity and permeability

The decrease in porosity of the sediments was to a large extent due to their diversity in particle size distribution and the water movements through the tank.

During sedimentation of particles of less than 100 μm diameter, frictional forces hinder sedimentation, and sediments of high porosity result (Hamilton & Menard, 1976). While the tank sediments had a mean average particle size ~400 μm and porosity in the range 0.3-0.4, samples collected in the Spencer Gulf, having a mean particle diameter less than 100 μm, had porosity in the range 0.5-0.6.

It has been shown that high ionic strength of the aquatic phase of the environment affects the static charges on settling clay particles, and high porosity sediments result (Rosenquist, 1962, Meade, 1964). The evaporation rate in Spencer Gulf is approximately 2050 mm per year. Therefore, the high porosity of the Spencer Gulf samples (Table 1) may have been at least partially caused by the high salinity of their environment.

The high intraporosity of the calcite and aragonite was due to their biogenic origin, being encrusting coralline algae and branched coral, respectively.

The changes in permeability of the sediments with time were due to a number of factors.

The decrease in porosity affected the permeability directly. Organic material accumulated by biological activity in the narrow interstitial spaces. The organic content of the sediments, with the exception of the quartz sand, increased with time (Table 1). The maximum decrease of permeability occurred in the sediments with the highest organic carbon increase, the aragonite and organic layers; while in sand, the permeability changed only marginally in 9 months.

The increase of organic carbon in the sediments had its origin in the photosynthetic processes associated with the algal population at the water-sediment interface. The organic compounds produced there served as nutrients for the heterotrophic microorganisms in the sediments, thus supporting the production of biomass in the sediments. The substrates were transported through sediments by water movement or by diffusion.

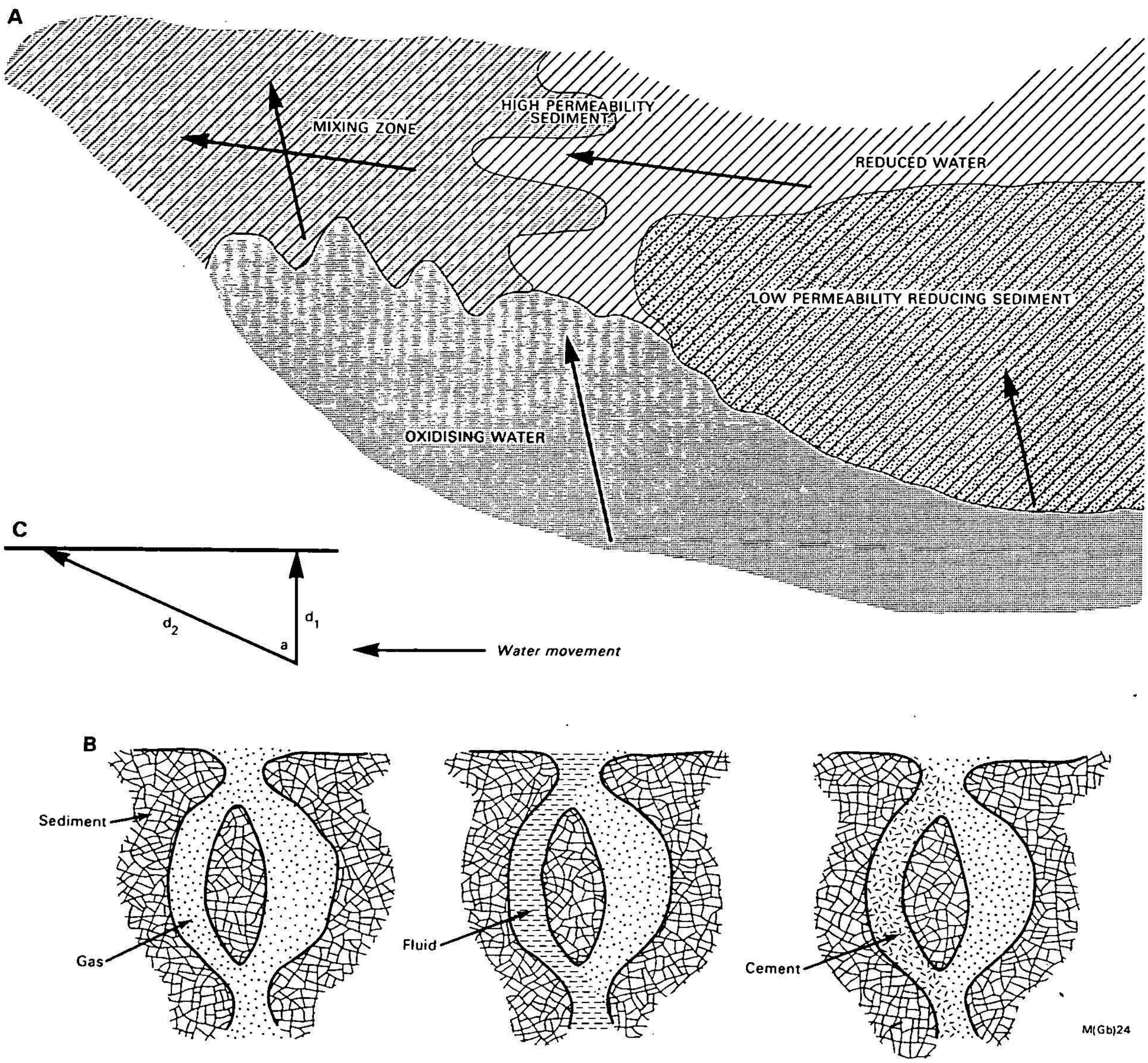

Figure 4.

A. Waters originating in an oxidizing zone pass through a low permeability reducing zone, acquiring certain characteristics. Owing to the directional changes on their re-entry into the high permeability zone, the waters are mixed and their characteristics altered. **B.** A pore space consisting of two capillaries of significantly different diameters, sharing common inlet and outlet, is gas-filled, owing to drying out and/or biological activity. During imbibition, capillary forces fill the narrow capillary preferentially with fluid, while the other capillary becomes gas-locked. The narrow capillary may become blocked by cementation at some later stage, while the broad one is preserved. **C.** Diagrammatic presentation of an increase of fluid pathway caused by heteropermeability. d_1 = original distance to be travelled; d_2 = distance travelled on deflection; a = angle of deflection.

The recovery of the algal mat after its decay at the 13% salinity level could have been due to the adaptation of the existing algal population to new environmental conditions or because a different algal population, more halophilic or at least halodurant, was established. The bacterial bloom during the algal decay may be explained by a sudden influx of nutritional material, originally a constituent of the living algae, into the supernatant water. As soon as the algal mat recovered, the supply of the nutrients decreased and the bacterial bloom ceased.

The iron sulphide formed in the interstitial spaces contributed to the decrease in the porosity of the sediments. The amounts produced were significantly high, in combination with the biologically formed organic mass, to cause a slight cementation of the sediments and reduce their permeability.

The decrease in the directly measured permeabilities of the individual strata could not explain the much lower overall permeability throughout the sediments in the tank. The only strata where permeability could not be measured directly, because of its consistency, was the organic layer. Using equation (1), the permeability of the organic layer was calculated and shown to have decreased by 99% over 8 months.

A total horizontal permeability of the tank sediments was calculated from equation (2). The horizontal permeabilities, individual as well as total, were several magnitudes higher than the corresponding vertical permeabilities, as is quite common in natural sediments, owing to grain orientation, imbrication, etc.

In nature, the pore water movement is not always perpendicular to or parallel to the sedimentary layering. In the case of heteropermeable sediments, a deviation from the 0° and 90° inclinations can increase the length of the pathway of the fluids considerably. If we use as an example the two neighbouring layers in the tank, the high magnesium calcite (k_{Mg} = 3800 md) and the organic layer (k_0 = 4 md), and assume that the fluids pass through the organic layer at an inclination of 10° from the perpendicular, it is possible, using equation (3), to calculate that the fluids will then pass through the magnesium calcite at an inclination of ~89° from the perpendicular. Considering the original perpendicular pathway in the tank of 20 cm, the pathway could increase to more than 11 metres, an increase of ~6000% (Fig. 4C). Therefore, fluids passing through a heteropermeable environment of significantly different permeabilities may travel distances far in excess of the shortest possible pathway, and in directions influenced by the relative permeabilities of the environment.

Directional changes of underground flow may have significant influence on ore-forming processes in sedimentary environments. Critical values of pH and Eh were stipulated in such processes by Butler (1969) and Kinsman (1969). It has been postulated by Renfro (1974) that in certain sabkha-like environments, during ore-genetic processes, waters will pass upwards from their oxygenated source beds through the overlying, hydrogen sulphide-charged algal mat in order to reach the zone of an evaporative discharge. In nature, low-permeability organic deposits may be found as isolated lenses in higher permeability sediments, such as in the situation represented in Fig. 4A. In this situation, oxygenated waters would acquire certain characteristics (pH, Eh, salinity, organic carbon, metal concentration, etc.), required for metal deposition, by passing through the low permeability layer.

Significant directional changes and consequential increases of pathways of the underground waters are effected by the heteropermeability of the sediments. These waters may lose their acquired characteristics by molecular diffusion and physical mixing with the surrounding waters. Therefore, the conditions facilitating or hindering the deposition of metals or polluting components may be significantly changed.

The accumulation of evaporites on the algal mat surface at the early stage of the evaporative cycle made the mat even more impermeable, and crust formation reduced the evaporation rate, thus inhibiting the movement of interstitial waters to the surface. In the absence of the algal mat, the sealing effect of only the evaporites was not complete, as demonstrated by the movement of the fluorescein solution.

On drying at room temperature, the permeability of the sediment may increase quite considerably (Table 1). When the sediment was dried and then rewetted by imbibing prior to the permeability test, the permeability of the sample decreased by about 90%. The explanation is evident from measurements of the apparent densities of the wet, dried and rewetted samples (Table 1): only 46% of the air-filled spaces became water-logged when the sample was immersed in water. This was due to the interlocking capillary system, where, because of the range of pore size and the differences in the interfacial tensions of air and water, some passages became preferentially water-logged and produced a number of airlocks (Fig. 4B).

The significance of this process becomes apparent when one considers porous surfaces exposed to drying and then rewetting under low hydraulic pressures, as in intertidal zones and sabkha areas. A barrier to the flow of interstitial waters and an interference with the diagenetic processes in the sediments may be formed.

Another effect of this mechanism is feasible. A localised undersaturation of the pores during processes of cementation may be instrumental in restoring some of the permeability to the sediment at a later stage. The preservation of pore space is due to air-locks in the sediments. No cementation will take place where there is no interstitial water (Fig. 4B). The permeability may be restored when airlocks are removed by high hydraulic pressure, resulting in rapid forced flow through the capillaries, and by solution of the trapped gases in the interstitial waters.

If the gases are trapped in the sediments for a considerable time, they may eventually dissolve in the formation fluid and cementation may proceed. Should later additional cementation take place, the precipitated material may differ from the cement deposited originally and the qualitative heterogeneity of the cemented sediments will increase.

Conclusions

The simulated system indicated a number of factors influencing the hydrology of sedimentary environments.

The porosity and, subsequently, the permeability of sediments may be affected by:

- settling of the sediments;
- biological activity, resulting in interstitial spaces becoming blocked by microbiologically produced organic matter;
- consolidated buried organic matter producing highly impermeable strata;
- algal mat of low permeability isolating the sediment-water interface;
- production of new minerals and cementation.

Changes in permeability and porosity of the components of sediments may affect:

- movement of free and complexed metals;
- distance and directional components of travel of fluids in the sediments;
- conditions for the deposition of solutes from interstitial waters;
- microenvironmental conditions (pH, Eh, availability of substrates, etc.) governing microbiological activity.

The effect of the mat on the hydrology of given sediments may be quite significant, depending on its size. Renfro (1974) reported algal mats in the Persian Gulf ten miles wide and continuing uninterrupted along the coastline for several hundred miles. Therefore, the influence of mats on the surface or near surface hydrology of an environment has to be taken into consideration.

Surface and near-surface water movements are frequently used to explain metal accumulation, transport, and deposition in evaporative, saline environments, an example being the sabkhas in the Arabian Gulf (Butler, 1969). In such environments the combined affects of the algal mat, the evaporites, and the gas locks may create a strong barrier to the free movement of the interstitial waters. Therefore, some caution has to be exercised when models of such environments are being devised to explain the major components of the mechanisms operating there.

Taking into consideration all of the above observations, it is realised that a number of factors of apparently localised significance may play an important role in ore-genetic processes, in the movements of non-miscible liquids through sediments, in diagenetic processes of biological and abiological origin, and in general evaluation of processes taking place in many environments. The results obtained with the simulated system are compatible with the values obtained with the samples from Spencer Gulf. Even if at this stage the connection between the experimental work and the field work is rather tenuous, it indicates that the conditions in our simulated sedimentary system do represent a situation encounterable in nature.

Acknowledgements

The author is grateful to Dr J. Bauld for the identification of the microorganisms, and to P. Duff of the Bureau of Mineral Resources, and C. Robison and C. Manning for their skilful technical assistance. The Baas Becking Laboratory is supported by the Australian Mining Industry Research Association, Bureau of Mineral Resources, Geology and Geophysics, and the Commonwealth Scientific and Industrial Research Organization.

References

BUBELA, B. & FERGUSON, J., 1973—Apparatus for studies of artificial sediments. *Journal of Sedimentary Petrology*, **43**, 1167-70.

BUBELA, B., FERGUSON, J., & DAVIES, P. J., 1975—Biological and abiological processes in simulated sedimentary systems. *Journal of the Geological Society of Australia*, **22** (2), 135-45.

BUBELA, B., JOHNS, I. A., & FERGUSON, J., 1978—A system for simulation of evaporative sedimentary environments. *BMR Journal of Australian Geology & Geophysics*, **3** (2), 166-70.

BUTLER, G. P., 1969—Modern deposition and geochemistry of coexisting brines. *Journal of Sedimentary Petrology*, **39**, 79-89.

CAYIAS, J. L., SCHECHTER, R. S., & WADE, H., 1975—The measurement of low interfacial tension via the spinning drop technique. *In*: *ACS Symposium Series*, **8**, Adsorption of Interfaces, 234-47.

CLARK, N. J., 1960—Elements of petroleum reservoirs. *Henry L. Dorothy Series, Society of Petroleum Engineers, Dallas, Texas*, 195-219.

DAVIES, P. J., BUBELA, B., & FERGUSON, J., 1977—Simulation of carbonate diagenetic processes. *Chemical Geology*, **19**, 187-214.

ENGELHARDT, W., 1977—The origin of sediments and sedimentary rocks. *Wiley, New York*, 189-209.

HAMILTON, E. L., & MENARD, H. W., 1956—Density and porosity of sea-floor surface sediments off San Diego, California. *American Association of Petroleum Geologists Bulletin*, **40**, 754-61.

HODGMAN, C. D., 1949—Handbook of Chemistry and Physics, *Chemical Rubber Publishing Co., Cleveland, Ohio*, 31st edn, 1274-91.

KINSMAN, D. J. J., 1969—Modes of formation, sedimentary association, and diagnostic features of shallow-water and supratidal evaporites. *American Association of Petroleum Geologists Bulletin*, **53**, 830-40.

LURIA, S. E., 1960—*In* GUNSALAS, I. C., & STAINER, R. Y. (editors)—The Bacteria, *New York, Academic Press*. v. 1, chap. 1.

MEADE, R. H., 1964—Removal of water and rearrangement of particles during the compaction of clayey sediments. *United States Geological Survey Professional Paper*, **497-B**, 1-23.

PIRSON, S. J., 1958—Oil Reservoir Engineering, *McGraw-Hill, New York*. 2nd edn, 62-7.

RENFRO, A. R., 1974—Genesis of evaporite-associated stratiform metalliferous deposits—a sabkha process. *Economic Geology*, **69**, 33-45.

ROSENQUIST, I. T., 1962—The influence of physico-chemical factors upon the mechanical properties of clays. *Proceedings of the 9th National Conference on Clays and Clay Minerals. Pergamon Press, Oxford*, 12-27.

BMR Journal of Australian Geology & Geophysics, 5, 1980, 265-270

Rb-Sr geochronology of the Jervois Range area in the eastern part of the Arunta Block, NT

L. P. Black

New Rb-Sr isotopic data are presented for the Jervois Range area in the eastern part of the Arunta Block. The post-metamorphic Jinka and Jervois Granites yield an age of about 1750 m.y. An alaskitic granite is dated at about 1460 m.y. Pegmatite formation occurred about 1660 m.y. ago. Mineral ages are generally younger than total-rock ages, but no values significantly less than that of the alaskitic granite were found. This means that the Alice Springs Orogeny, which extensively reset large areas of the Arunta Block to the west, did not affect the Jervois area. In this and other geochronological comparisons, the Jervois area seems more akin to the rocks of the Tennant Creek Block, 400 km to the northwest, than to those of the Arunta Block.

Introduction

This article documents new isotopic ages from a geochronologically poorly understood area around the Jervois Range, in the eastern part of the Arunta Block, NT (Fig. 1). Much of the geology is as yet unpublished, including a detailed study by Dobos (1978). A generalised map of the Jervois Range area after Smith & others (1964), with sample localities, is presented in Figure 2. The following summary is primarily derived from the publications of Dobos (1975) and Warren (1978).

BMR workers (e.g. Shaw & Warren, 1975; Shaw & Stewart, 1976; Stewart & Warren, 1977; Shaw & others, 1979) have judged the Arunta Block to contain three major depositional units with distinctive lithologies and probable stratigraphic significance. The oldest of these (designated Division I) consists of volcanics and immature sediments which have generally been regionally metamorphosed to granulite facies. Division II rocks contain a larger proportion of derived sediments; Division III is represented by mature pelite and quartzite.

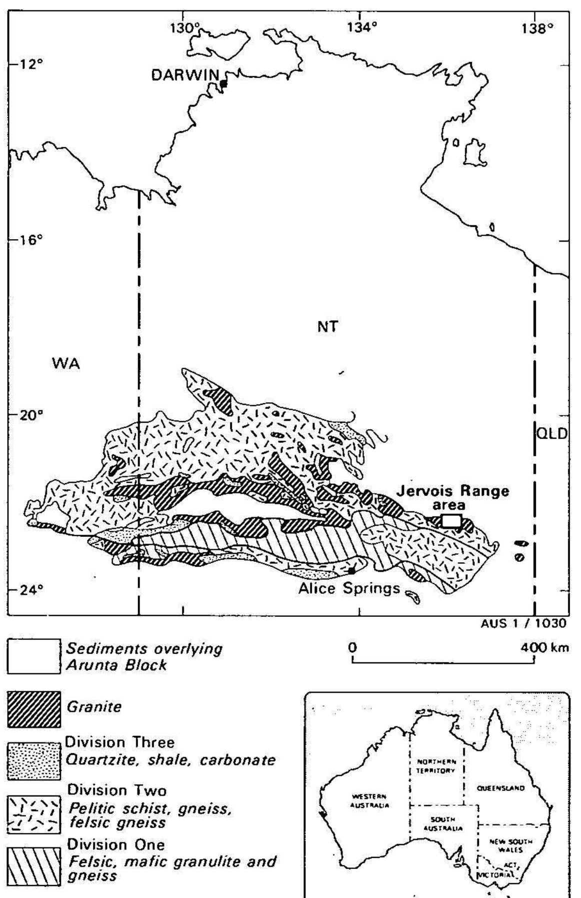

Figure 1. Generalised geology of the Arunta Block (after Shaw & others, 1979) with location of the Jervois Range area.

Only Division II rocks are thought to be represented in the Jervois Range area, where they are informally known as the Bonya sequence. Rock types include two-mica schist and gneiss, orthoamphibolite, magnetite quartzite, and lesser amounts of calc-silicate gneiss and marble. Characteristic minerals in originally pelitic rocks (though not necessarily in the same assemblage) are chlorite, muscovite, biotite, andalusite, sillimanite, quartz, magnetite, cordierite, almandine, and staurolite. These indicate lower amphibolite metamorphic conditions which locally range to upper amphibolite grade. The metamorphics are intruded by post-tectonic granites, the dominant members of which are called the Jinka and Jervois Granites, and pegmatites. In the area, the Arunta Block is unconformably overlain by late Proterozoic to Devonian platform sediments, including those of the Georgina Basin.

The origin of mineralisation in the district is somewhat speculative. Hydrothermal epigenetic and volcanogenic origins have been advanced. Tungsten and minor copper mineralisation in the Bonya Scheelite District are preferentially located in calc-silicate horizons adjacent to later cross-cutting pegmatites, which might possibly only have remobilised the ore minerals. Copper, lead, zinc, bismuth, and tungsten mineralisation near Jervois camp occurs in 'stratabound' and lensoid deposits.

Analytical techniques

Gelignite was used for the collection of samples at each site. Analytical procedures, which incorporated a mixed Rb^{85}-Sr^{84} spike, were based on the procedures outlined in Page & others (1976) and Williams & others (1976). Regression of the analyses is based on the work of McIntyre & others (1966). The value 1.42×10^{-11} y^{-1} (Steiger & Jäger, 1977) has been used for the decay constant of Rb^{87}. All uncertainty limits are expressed at the 95% confidence level. Isotopic data are presented in Table 1.

Geochronology

Granites

Previous studies on the Jinka Granite in the Jervois Range area have yielded conflicting isotopic ages. From

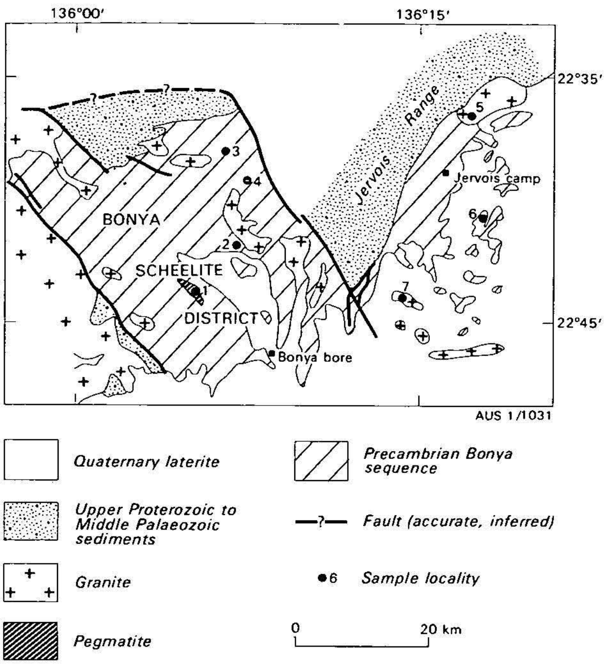

Figure 2. Geology of the Jervois Range area, after Smith & others (1964).
Full sample numbers are 1—72090538; 2—72090539, 40 3—72090541; 4—72090542; 5—72090543; 6—72090545; 7—72090546, 75090547, 48, 49, 50, 51.

concordant total-rock, microcline, biotite, and muscovite data, Riley (*in* Compston & Arriens, 1968) derived an age of 1690 m.y. for the Jinka Granite, older than the value of about 1460 m.y. obtained by Hurley & others (1961) by the K-Ar method on the same rocks. A further determination, by Wilson & others (1960) on muscovite, after applying a 3 percent correction for known systematic bias in Rb determination, yielded a still older age of about 1785 m.y. Because it was based on more analyses, Compston & Arriens (1968) preferred the 1690 m.y. age to the 1785 m.y. value.

Sampling a single blast site (e.g. see Marjoribanks & Black, 1974) was not a successful dating technique for these granites, because individual sites possess insufficient spread in Rb/Sr to precisely define total-rock isochrons. The isochrons have been derived either by grouping samples from separate outcrops, often kilometres apart, or by combining mineral and total-rock data. Petrographically distinct but related samples (72090541—foliated hornblende biotite granodiorite and 72090542—biotite granodiorite) from two sites in the Jinka Granite north-northwest of Bonya Bore (localities 3 and 4, Fig. 2) yield an age of 1812 ± 85 m.y. (initial ratio = 0.700 ± 0.003) from a model 2 isochron (see McIntyre & others (1966) for a discussion of regression models) with MSWD of 34. Samples from six sites in the related (S. Dobos, pers. comm., 1978) Jervois Granite (actually a biotite granodiorite) about 10 km south of Jervois Camp (locality 7, Fig. 2) produce a similar age (1808 ± 80 m.y.) and initial ratio (0.698 ± .006) from a model 2 isochron with MSWD of 3.3. Simultaneous regression of all 28 data points (Fig. 3) produces a relatively precise age (1775 ± 27 m.y., initial ratio = 0.701 ± .001) which is considered to approximate the crystallisation age of these granites. The scatter of analytical points about the isochron (MSWD = 16) probably results from slight differences in the ages of the separate masses or from subsequent migration of Sr and/or Rb. The low indicated initial $^{87}Sr/^{86}Sr$ of the granites is consistent with petrographic and chemical data (Dobos, 1975) in suggesting that these are I-type granites (Chappell & White, 1974). Indeed, the initial ratio is so low that it precludes any but the briefest crustal history for the granite precursor. The uppermost part of the initial ratio range (i.e. about 0.702) would appear to be the most realistic value for a granite of this age. This would require that the lowermost part of the age limits (i.e. about 1750 m.y.) should most closely approximate the time of granite crystallisation.

Minerals from these rocks yield significantly younger ages than the total-rock systems. A biotite-plagioclase pair for 72090541 yields an age (1485 m.y.) which is indistinguishable from that derived from a model 1 isochron for plagioclase, total-rock, K-feldspar, and biotite fractions (1479 ± 23 m.y., initial ratio = 0.731 ± .001) from 72090542. Similar ages from other minerals in the area, and from mineral and total-rock samples to the west (Black, unpublished analyses) indicate a widespread event in the Arunta Block at this time. A slightly older biotite age of 1547 m.y. for 72090546 probably reflects partial isotopic resetting during this event.

A pink foliated alaskitic granite 5 km north of Jervois camp (locality 5, Fig. 2) was probably emplaced during this latter event. A limited spread in Rb/Sr at the sampling site does not allow the derivation of a more precise total-rock age than 1559 ± 133 m.y., even though the analytical points fit the regression within the limits of experimental error. Addition of plagioclase and K-feldspar analyses improves the spread in Rb/Sr without introducing any component of non-analytical dispersion to the isochron. The age and initial ratio are now precisely determined at 1459 ± 10 m.y. and 0.788 ± .003 (Fig. 4). The perfect nature of the isochron defined by both mineral and multiple total-rock components most probably originated during the crystallisation of the granite. Black & others (1979) have shown that the resetting of total-rock isochrons during structural-metamorphic events is unlikely to produce perfect isochrons. The high initial ratio for the alaskitic granite indicates that it has a clearly different source, considerably higher in Rb/Sr, and most probably from a higher crustal level, than that for the Jinka and Jervois Granites.

A biotite-microgranite dyke 6 km south-southeast of Jervois camp (72090545, locality 6, Fig. 2) has similar mica ages (biotite—1503 m.y.; muscovite—1669 m.y.) to those of other rocks in the area.

Pegmatites

Two pegmatites in the Jervois Range area (localities 1 and 2, Fig. 2) were emplaced during a third event, of intermediate age. 72090538 is a medium to coarse-grained tourmaline and muscovite bearing pegmatite near Samakand prospect. Regression of all eight total-rock points yields an 'isochron' with high MSWD (60) which is curved at high values of Rb/Sr. This curvature presumably results from the large grain size of this pegmatite and the difficulties of sampling it representatively. From Figure 5 it can be seen that constituent microcline plots on an approximate extension of this curved trend and has clearly been at least partly reset, probably during the youngest documented event in the area (about 1480 m.y.). Any sample composed dominantly of microcline will obviously trend away

Sample No.	Rb (μg/g)	Sr (μg/g)	Sr^{87}/Sr^{86}	Rb^{87}/Sr^{86}	Age (m.y.)
72090538	Pegmatite at Samakand prospect				
A T.R.	1798	29.76	6.7306	277.3	
B T.R.	113.8	12.02	1.4544	29.35	
C T.R.	124.5	32.60	1.0260	11.37	
D T.R.	749.0	16.75	4.9875	183.2	
E T.R.	462.2	13.59	3.7968	127.9	
H T.R.	234.6	11.04	2.4939	72.09	
I T.R.	1153	24.66	4.9885	191.6	
K T.R.	534.7	19.83	2.9547	94.96	
muscovite	3802	26.63	444.6	18 315	1686
K-feldspar	8256	132.5	7.1041	292.6	
72090540	Pegmatite at Jericho mine				
A T.R.	253.0	22.58	1.5458	35.01	
B T.R.	318.0	26.69	1.5959	37.40	
C T.R.	441.2	31.73	1.7568	44.27	
D T.R.	334.4	13.10	2.7627	88.54	
E T.R.	441.4	8.656	6.0979	224.9	
F T.R.	534.3	78.24	1.2018	20.67	
G T.R.	318.4	22.39	1.7947	45.42	
H T.R.	439.2	25.97	2.0140	55.07	
I T.R.	431.8	36.45	1.5914	37.16	
J T.R.	708.3	39.55	2.0906	58.70	
muscovite	1614	15.88	22.860	929.0	1659
K-feldspar	1396	30.48	4.8394	187.4	
72090539	Mica schist at Jericho mine				
A T.R.	268.0	43.75	1.1402	18.44	
B T.R.	271.4	45.32	1.1331	18.01	
C T.R.	260.6	63.04	.99918	12.28	
D T.R.	257.2	63.17	.99179	12.08	
E T.R.	263.8	50.74	1.0697	15.54	
F T.R.	267.3	43.78	1.1407	18.37	
muscovite	301.3	41.97	1.2360	21.80	1634
biotite	621.5	12.54	5.1143	204.8	1492
plagioclase	93.90	247.2	.75052	1.101	
72090541	Jinka Granite				
A T.R.	165.1	85.34	.84929	5.664	
C T.R.	183.8	89.34	.85783	6.027	
F T.R.	185.7	90.11	.85851	6.037	
I T.R.	192.0	89.05	.86496	6.321	
K T.R.	193.6	87.97	.86954	6.521	
K-feldspar	425.0	101.2	.99258	12.46	
biotite	1075	11.94	12.914	570.5	1485
plagioclase	103.2	138.4	.77678	2.168	
72090542					
B T.R.	158.6	253.7	.74402	1.811	
D T.R.	184.4	262.7	.75085	2.035	
E T.R.	138.0	271.7	.73935	1.471	
F T.R.	191.2	260.6	.75384	2.128	
G T.R.	140.0	277.1	.73921	1.463	
H T.R.	135.0	274.6	.73780	1.4235	
biotite	611.5	12.74	4.9869	196.6	1516
plagioclase	32.07	302.8	.71266	.3059	
72090543	Alaskitic granite				
A T.R.	258.1	24.57	1.4719	32.59	
B T.R.	279.0	27.10	1.4476	31.87	
C T.R.	262.9	26.76	1.4171	30.33	
D T.R.	274.3	26.54	1.4535	32.02	
E T.R.	270.2	25.66	1.4712	32.68	
F T.R.	249.6	24.89	1.4410	31.03	
G T.R.	273.9	25.50	1.4849	33.37	
H T.R.	278.4	27.17	1.4493	31.73	
I T.R.	277.9	24.65	1.5262	35.16	
J T.R.	283.5	25.53	1.5136	34.58	
K-feldspar	727.6	16.98	4.3220	167.5	
plagioclase	24.31	7.035	1.0033	10.27	
72090545					
muscovite	788.1	19.33	4.6101	162.7	1669
biotite	893.7	18.30	5.0402	200.8	1503
72090546	Jervois Granite				
A T.R.	255.9	141.2	.83540	5.299	
E T.R.	198.1	111.4	.83279	5.200	
I T.R.	189.8	112.4	.82624	4.934	
J T.R.	200.7	105.2	.84075	5.581	
75090547					
A T.R.	186.2	107.4	.82842	5.062	
D T.R.	185.0	112.2	.82412	4.814	
75090548					
A T.R.	207.4	108.8	.84184	5.578	
C T.R.	211.9	106.7	.84749	5.813	
75090549					
A T.R.	209.8	109.9	.84132	5.585	
D T.R.	201.0	108.5	.83806	5.418	
75090550					
A T.R.	202.9	98.54	.85631	6.033	
C T.R.	201.7	99.36	.85279	5.944	
E T.R.	204.2	98.11	.85917	6.100	
75090551					
A T.R.	202.9	120.8	.82366	4.905	
B T.R.	189.1	125.8	.81201	4.384	
C T.R.	187.6	123.5	.81289	4.430	
D T.R.	188.2	126.6	.81101	4.336	
72090546					
biotite	899.5	10.86	11.799	498.9	1547

Table 1. Rb-Sr analyses from the Jervois Range area.

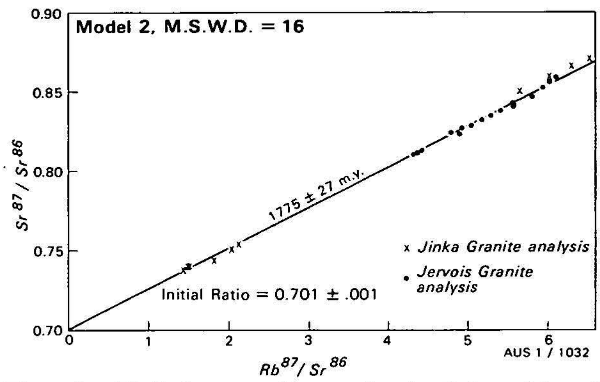

Figure 3. Rb-Sr isochron diagram for the Jinka and Jervois Granites.

from the initial total-rock line towards this reset composition. The most microcline-rich rock sample (A) plots closest to the feldspar point, and is furthest of all total-rock points below the isochron derived below, as would be expected. The analytical points with lowest Rb/Sr values would be expected to yield the line most closely approximating the correct age. Deletion of the three most enriched samples produces a model 2 isochron with reasonable MSWD (11); indicated age and initial ratio are 1648 ± 57 m.y. and 0.757 ± .018. Highly enriched muscovite from the pegmatite yields a similar age (Table 1.).

This Samakand pegmatite age is further supported by that from the nearby fine to medium-grained and mineralogically similar pegmatite (72990540) at the Jericho mine (Fig. 6). All ten total-rock samples from this pegmatite closely define a model 2 isochron with low MSWD (3.7). Age and initial ratio are 1642 ± 26 m.y. and 0.714 ± .015. A muscovite separate yields a similar age of 1659 m.y. whereas microcline, as was the case with 72090538, plots below the isochron, presumably for the same reason. The high but different initial ratios presumably indicate that the pegmatites (separated by 10 km) were derived from different high crustal rocks.

Additional support for the age of the pegmatites is provided by a quartz-muscovite-biotite schist. This schist would be expected to have been isotopically reset by the heat and volatiles emanating from the Jericho pegmatite with which it is in immediate contact. Its age (see (Fig. 7), at 1625 ± 50 m.y., is indeed indistinguishable from that of the pegmatite. In addition, the initial ratios of schist and pegmatite, although

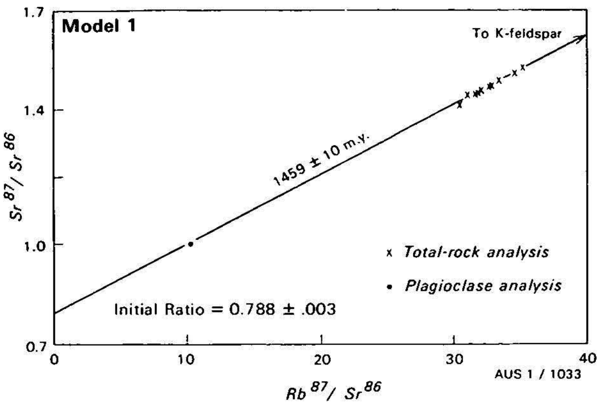

Figure 4. Rb-Sr isochron diagram for alaskitic granite.

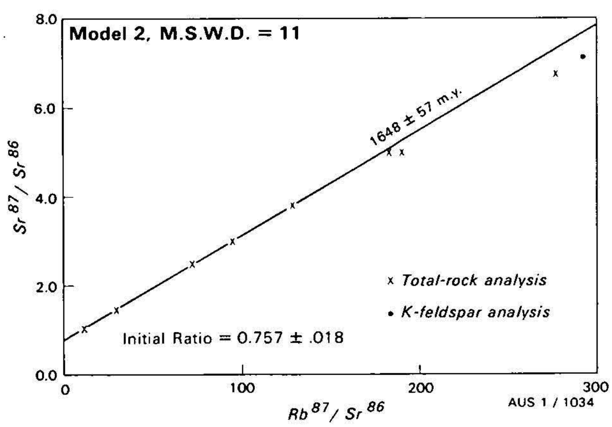

Figure 5. Rb-Sr isochron diagram for pegmatite from the Samakand prospect.
The three most enriched total-rock analyses and the K-feldspar analysis are deleted from this regression (see text).

imprecisely determined, are also indistinguishable, as would be expected. Muscovite from the schist, although poorly enriched in Rb/Sr, yields a similar age (1634 m.y.), but biotite (1493 m.y.) appears to have been reset by the pervasive retrogressive event at about 1480 m.y.

Comparisons with the remainder of the Arunta Block

Several geochronological correlations can be made between the Jervois Range area and the rocks of the Arunta Block to the west, where isotopic work is still in progress. The oldest isotopically recorded event in the Jervois Range is the intrusion of the Jinka and Jervois Granites at about 1750 m.y. This becomes a minimum age estimate for the main metamorphism in the country rocks, which must predate these post-tectonic granites. The earliest detected metamorphism in the Arunta Block itself has been dated by Rb-Sr total-rock studies (Black, 1975; Iyer & others, 1976; L. P. Black, unpublished analyses). From the evidence presently available, an estimate of 1770-1810 m.y. would seem most appropriate for this event. As this value fits the geochronological constraints imposed by the Jinka and Jervois Granites data (i.e., older than 1750 m.y.) it seems logical to conclude that the main metamorphism in the Jervois Range area was synchronous with the earliest high-grade (up to granulite facies) metamorphism recorded to the west.

Similarly, the pegmatite-forming event at about 1660 m.y. in the Jervois Range correlates closely in age with an amphibolite facies metamorphism (Black, 1975; Armstrong & Stewart, 1975) to the west. A leucocratic, garnet and muscovite-bearing granite near Mount Ida, which has been dated at 1710 ± 40 m.y. (Black, unpublished data), may be part of the same event or perhaps a little older.

So far, there is little evidence in the Jervois Range area of the approximately 1570 m.y. event which produced amphibolite-facies metamorphism in the Chewings Range (Marjoribanks & Black, 1974), granitic gneiss in the Strangways Range, and pegmatites in several areas (Black, unpublished analyses).

The youngest event detected in the Jervois Range area at about 1470 m.y. compares with a generally retrogressive metamorphism which is widespread in the Reynolds Range, about 300 km west of the Jervois area. Unpublished work by Black also indicates that there was some granite emplacement at this time in the west.

Subsequently, the crust in the Jervois Range area appears to have stabilised, whereas intrusion, deformation and metamorphism continued elsewhere in the Arunta Block. In particular, both the extensive granite-forming and migmatite-forming event at about 1050 m.y. (Marjoribanks & Black, 1974) and the Alice Springs Orogeny, which caused widespread retrogression throughout large areas of the Arunta Block between 300 and 400 m.y. ago (Stewart, 1971; Armstrong & Stewart, 1975; Black, 1975; Black & Gulson, 1978), had no effect on the rocks of the Jervois Range. This would suggest that there is a major structural break between the two areas. This break probably corresponds to the Delny-Mount Sainthill Fault system, which Warren (1978) has documented as a slightly north-of-west-trending feature, extending at least 130 km across the Arunta Block to the south and west of the Jervois Range area.

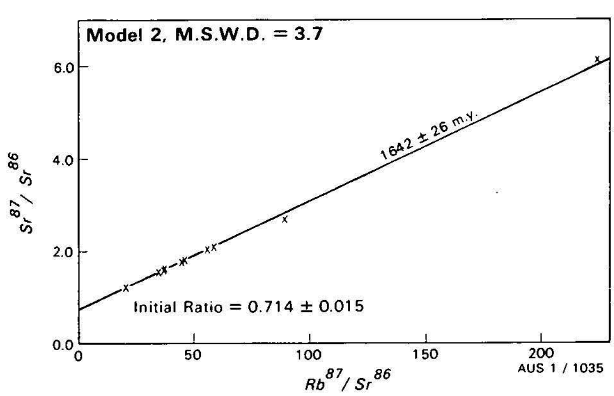

Figure 6. Rb-Sr isochron diagram for pegmatite from the Jericho mine.

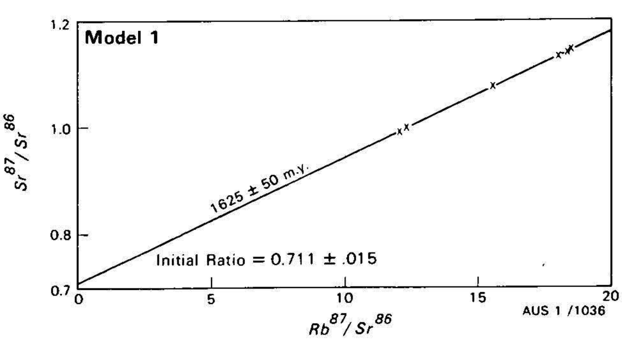

Figure 7. Rb-Sr isochron diagram for schist from the Jericho mine.

Comparisons with the Tennant Creek Block to the north

At our present state of knowledge, the Jervois Range area is more akin to the Tennant Creek Block (dated by Black, 1977) in its total geochronological history than to the rest of the Arunta Block. The oldest age from the Tennant Creek area is 1920 ± 60 m.y. for amphibolite-facies metamorphism. Although this is somewhat older than any Jervois ages, there remains a strong possibility that these rocks actually represent basement which is older than the Warramunga Group.

The oldest ages from indisputable Warramunga Group rocks are provided by Rb/Sr dating of muscovite separates from mineralised samples. The resultant age of 1810 m.y., which is in general agreement with the age deduced for the main metamorphism at Jervois, is also thought to date the main structural-metamorphic event in the Tennant Creek Block. A Rb-Sr mica age from the Tennant Creek Granite is also close to this value.

Ages of 1766 ± 80 m.y. and 1733 ± 40 m.y. for shale and volcanics within the Warramunga Group probably date a subsequent structural-metamorphic event in the Tennant Creek area. Biotite from the North Seismic Adamellite (1738 m.y.) and a total-rock isochron for porphyry (1752 ± 30 m.y.) also yield ages which are indistinguishable from the age of the Jinka and Jervois Granites (~1750 m.y.).

Total-rock isochrons for lamprophyre, the Warrego Granite, and two localities of the Red Bluff Granite, yield ages of 1664 ± 16 m.y., 1662 ± 20 m.y., 1648 ± 50 m.y., and 1640 ± 36 m.y., in close agreement with the age of about 1660 m.y. derived for the Jervois Range pegmatites.

The last well-documented event in the Tennant Creek area is provided by a Rb-Sr total-rock age of 1450 ± 36 m.y. for the Cabbage Gum Granite. This matches the value of about 1470 m.y. derived above for alaskite and micas within the Jervois area. The Gosse River East Granite yields the only age younger than this in the Tennant Creek Block. This date, however, must be considered with some suspicion, for it is not precisely determined (1330 ± 100 m.y.) and is unsupported by other data.

Overall, there is a remarkable similarity of ages between the Jervois Range and Tennant Creek areas. The similarity suggests that these are stratigraphically comparable areas which have remained at a relatively high, essentially geologically stable, crustal level since about 1470 m.y. This conclusion supports the contention of Warren (1978) who equates the Bonya supracrustal sequence in the Jervois area with 'Division II' rocks of the Arunta Block, which have in turn been lithologically correlated with the Warramunga Group of the Tennant Creek Block (Shaw & Stewart, 1976).

Acknowledgements

I wish to thank Petrocarb Exploration N.L., Central Pacific Minerals, and S. Dobos for their help in the field. Technical assistance in the laboratory was provided by T. K. Zapasnik, J. L. Duggan, and M. W. Mahon. The manuscript was critically discussed with R. D. Shaw, A. J. Stewart, J. Ferguson, and K. R. Walker. I would particularly like to thank R. G. Warren for her help throughout this study.

References

Armstrong, R. L., & Stewart, A. J., 1975—Rubidium-strontium dates and extraneous argon in the Arltunga Nappe Complex, Northern Territory. *Journal of the Geological Society of Australia*, **22**, 103-15.

Black, L. P., 1975—Present status of geochronological research in the Arunta Block, N.T.—*Geological Society of Australia Incorporated, Abstracts of First Australian Geological Convention—Proterozoic Geology—Adelaide, 1975*, 37.

Black, L. P., 1977—A Rb-Sr geochronological study in the Proterozoic Tennant Creek Block, central Australia. *BMR Journal of Australian Geology & Geophysics*, **2**, 111-22.

Black, L. P., Bell, T. H., Rubenach, M. J., & Withnall, I. W., 1979—Geochronology of discrete structural-metamorphic events in a multiply deformed Precambrian terrain. *Tectonophysics*, **54**, 103-37.

Black, L. P., & Gulson, B. L., 1978—The age of the Mud Tank Carbonatite, Strangways Range, Northern Territory. *BMR Journal of Australian Geology & Geophysics*, **3**, 227-32.

Chappell, B. W., & White, A. J. R., 1974—Two contrasting granite types. *Pacific Geology*, **8**, 173-4.

Compston, W., & Arriens, P. A., 1968—The Pre-cambrian geochronology of Australia. *Canadian Journal of Earth Sciences*, **5**, 561-83.

Dobos, S. K., 1975—Metamorphism in the northeast Arunta Block, N.T.—*Geological Society of Australia Incorporated, Abstracts of First Australian Geological Convention—Proterozoic Geology—Adelaide, 1975*, 38.

Dobos, S. K., 1978—Phase relations, element distributions, and geochemistry of metamorphic rocks from the eastern Arunta Block, N.T. *Ph.D. thesis, Macquarie University* (unpublished).

Hurley, P. M., Fisher, N. H., Pinson, W. H., & Fairbairn, H. W., 1961—Geochronology of Proterozoic granites in the Northern Territory, Australia. Part I: K-Ar and Rb-Sr age determinations. *Geological Society of America Bulletin*, **72**, 653-62.

Iyer, S. S., Woodford, P. J., & Wilson, A. F., 1976—Rb-Sr isotopic studies of a polymetamorphic granulite terrane, Strangways Range, central Australia. *Lithos*, **9**, 211-24.

McIntyre, G. A., Brooks, C., Compston, W., & Turek, A., 1966—The statistical assessment of Rb-Sr isochrons. *Journal of Geophysical Research*, **71**, 5459-68.

Marjoribanks, R. W., & Black, L. P., 1974—Geology and geochronology of the Arunta Complex, north of Ormiston Gorge, Central Australia. *Journal of the Geological Society of Australia*, **21**, 291-300.

Page, R. W., Blake, D. H., & Mahon, M. W., 1976—Geochronology and related aspects of acid volcanics, associated granites, and other Proterozoic rocks in The Granites-Tanami region, northwestern Australia. *BMR Journal of Australian Geology & Geophysics*, **1**, 1-13.

Shaw, R. D., Langworthy, A. P., Offe, L. A., Stewart, A. J., Allen, A. R., Senior, B. R., & Clarke, D., 1979—Geological report on 1:100 000 scale mapping of the southeastern Arunta Block, Alice Springs 1:250 000 Sheet area, Northern Territory. *Bureau of Mineral Resources, Australia, Record* **1979/47**, unpublished.

Shaw, R. D., & Stewart, A. J., 1976—Arunta Block—regional geology. *In* Knight, L. C. (editor), Economic Geology of Australia and Papua New Guinea: 1. Metals. *Australasian Institute of Mining and Metallurgy, Monograph* **5**, 437-42.

Shaw, R. D., & Warren, R. G., 1975—Alcoota, N.T.—1:250 000 Geological Series. *Bureau of Mineral Resources, Australia, Explanatory Notes* **SF/53-10**.

Smith, K. G., Smith, J. W., Woolley, D. R. G., Pulley, J. M., Vine, R. R., Gough, K., & Milligan, E. N., 1964—Huckitta, N. T.—1:250 000 Geological Series. *Bureau of Mineral Resources, Australia Explanatory Notes*, **SF/53-11**.

STEIGER, R. H., & JÄGER, E., 1977—Subcommission on geochronology: Convention on the use of decay constants in geo-and cosmo-chronology. *Earth and Planetary Science Letters*, **36**, 359-62.

STEWART, A. J., 1971—Potassium-argon dates from the Arltunga Nappe Complex, Northern Territory. *Journal of the Geological Society of Australia*, **17**, 205-11.

STEWART, A. J., & WARREN, R. G., 1977—The mineral potential of the Arunta Block. *BMR Journal of Australian Geology & Geophysics*, **2**, 21-34.

WARREN, R. G., 1978—Delny-Mount Sainthill Fault System, eastern Arunta Block, Central Australia. *BMR Journal of Australian Geology & Geophysics*, **3**, 76-9.

WILLIAMS, I. S., COMPSTON, W., CHAPPELL, B. W., & SHIRAHASE, T., 1976—Rubidium-strontium age determinations on micas from a geologically controlled, composite batholith. *Journal of the Geological Society of Australia*, **22**, 497-506.

WILSON, A. F., COMPSTON, W., JEFFERY, P. M., & RILEY, G. H., 1960—Radioactive ages from the Precambrian rocks in Australia. *Journal of the Geological Society of Australia*, **6**, 179-95.

BMR Journal of Australian Geology & Geophysics, 5, 1980, 271-278

Hydrogeology of a raised coral atoll — Niue Island, South Pacific Ocean

G. Jacobson & P. J. Hill

Niue Island, in the south Pacific Ocean, is a raised coral atoll with an area of 259 km². The original atoll rim is preserved as a peripheral ridge about 60 m above sea level, and the original lagoon floor now forms an internal basin about 35 m above sea level. Drilling has proved limestone of Miocene age to a depth of more than 200 m. Gravity and magnetic surveys indicate that the limestone probably overlies volcanic bedrock at a depth of about 300 m below sea level. The classical Ghyben-Herzberg freshwater lens does not exist on Niue Island. Results of electrical resistivity depth probes indicate that in the centre of Niue the freshwater layer is 40-80 m thick and beneath the former atoll rim it is 50-170 m thick. It decreases to 0 within 500 m of the coast, where salt water mixing occurs along fissures in the limestone. The irregular configuration of the freshwater layer is ascribed to permeability differences in the limestone. Considering the recharge conditions on Niue, the safe yield of a freshwater layer 50 m thick would be about 4000 m³ of groundwater per year per hectare. Aquifer tests on two specially constructed bores indicate specific capacity (yield-to-drawdown ratio) of about 12 l/s per metre of drawdown, and a safe long-term pumping rate of about 8 l/s.

Introduction

Niue Island, which supports a population of 3500, occupies a land area of 259 km² in the south Pacific Ocean at 19°S, 169°50′W (Fig. 1). The economy consists of subsistence agriculture, a small amount of commercial export agriculture, and a government sector. The reliability of the island's water supply has been questioned in recent years in view of proposals to further develop commercial agriculture, especially passionfruit and lime plantations, which would require irrigation.

The present water supply is derived from rainwater tanks, one dug well, and 45 bores spread around the rim of the island. The bores are 70 mm diameter, uncased, and are equipped with low-yielding electric or diesel pumps, or windmills; they have been constructed at various times since 1964 (Schofield, 1968).

An evaluation of the island's groundwater resources was carried out from March to May 1979 by a BMR team. The field investigation included inspections of caves and springs; a census of hydrological data of existing water bores; gravity and magnetic surveys to determine the depth, and shape of, the island's basement; electrical resistivity surveys to determine the thickness of the freshwater layer; drilling and construction of two water production bores and two observation bores; aquifer testing; measurements of tidal response in bores; and water sampling for electrical conductivity measurement and chemical analysis.

Geology

The geology of Niue Island and the occurrence of a freshwater lens within it, have been described by the New Zealand Geological Survey (Schofield, 1959). Soils mapping has been done by the New Zealand Soils Bureau (Wright & van Westerndorp, 1965).

Niue Island is a raised coral atoll with limestone and coral sand exposed on it. The original atoll topography is preserved (Fig. 2): the flat bottomed lagoon floor, Schofield's Mutalau Lagoon, is now an internal basin at an elevation of about 35 m; the narrow atoll rim, Schofield's Mutalau Reef, is now a peripheral ridge around the island at an elevation of about 60 m; and the former lagoon passage is now a dry valley to the south of Alofi, at an elevation of about 42 m. There is a narrow terrace, the Alofi Terrace, at an elevation of 25 m along most of the coast line; steep cliffs descend from the terrace to the sea. Younger coral terraces, 2-4 m above sea level, fringe parts of the east and south coast, and a fringing coral reef about 100 m wide encircles the island at sea level. Concentric lineaments are apparent on aerial photographs of the southwest of the island, and are probably strandlines of the former lagoon.

Recent mineral exploration drilling by Avian Mining Pty Ltd has proved limestone to a depth of more than 200 m in central Niue. The limestone varies in texture from hard and dense to soft and chalky or sugary; the sequence also includes beds of unconsolidated sand and hard, recrystallised dolomite. The limestone is jointed and cavernous to great depths. Palaeontological determinations on drill core samples by G. C. H. Chapronière (BMR) indicate that most of the limestone sequence to a depth of 170 m below sea level is Middle

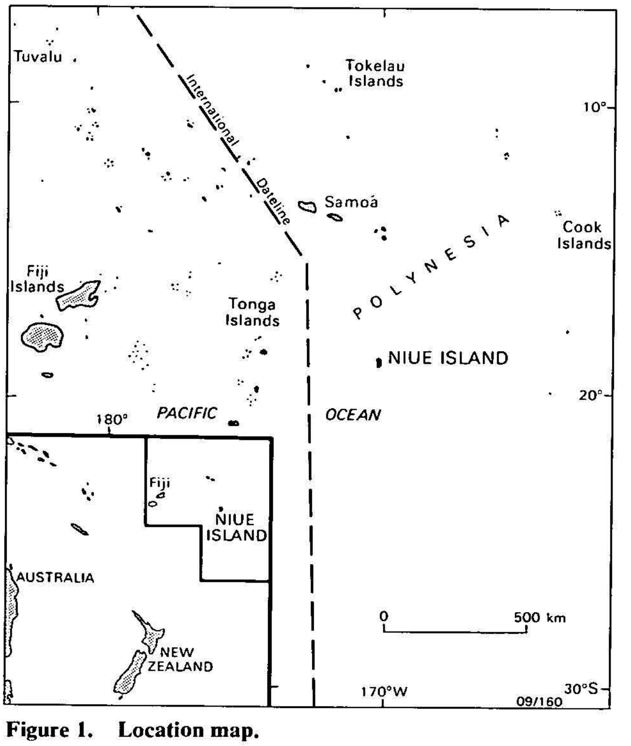

Figure 1. Location map.

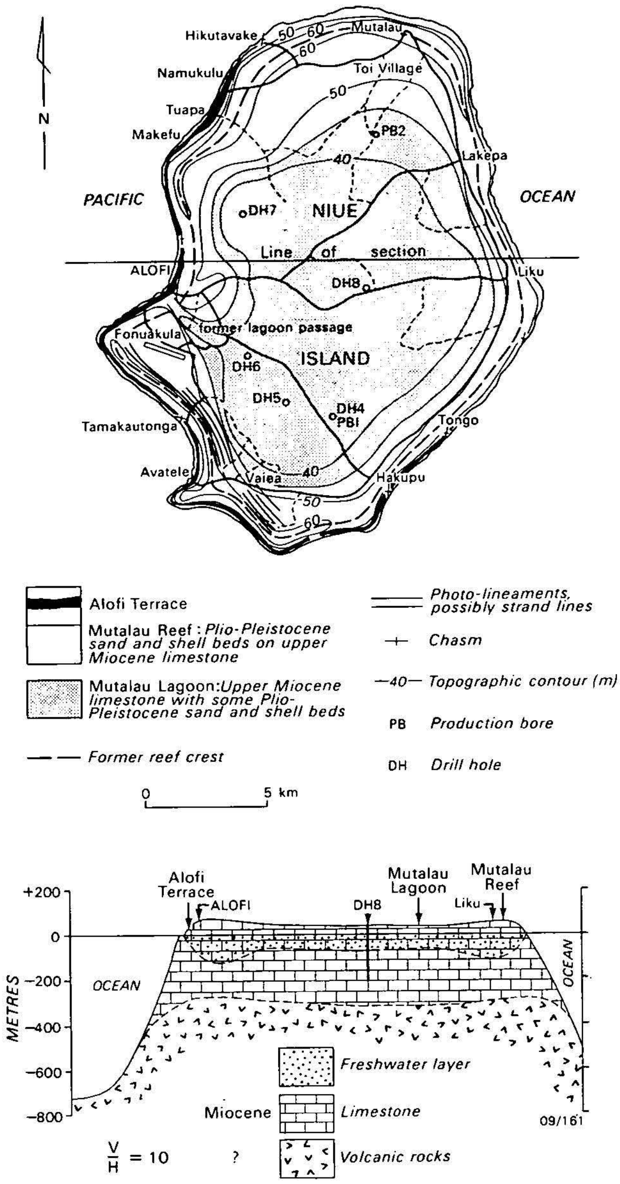

Figure 2. Geology.

to Late Miocene (Jacobson & Hill, 1980). Fossils from surface localities in the interior of Niue have previously been dated as Plio-Pleistocene (Schofield, 1959); they were probably taken from a thin veneer of younger sediments in parts of the former lagoon.

The island is underlain by a seamount that rises 4000 m from the floor of the Pacific Ocean (Brodie, 1966), and magnetic surveys have indicated a caldera-like volcanic substructure (Schofield, 1959). Gravity and magnetic survey results of the present investigation indicate that Niue has a dense, reversely magnetised, volcanic core centred in the south of the island, and that the volcanic rock is at an average depth of about 300 m below sea level (Hill, in prep.).

Soil occupies only 52 percent of the surface of Niue, and is generally thin. Much of the soil is radioactive, and the origin of the radioactivity has been variously ascribed to volcanic ash fallout (Wright & van Westerndorp, 1965), radioactive elements trapped from sea water in the former lagoon (Fieldes & others, 1960), and hydrothermal emanation from the volcanic substructure (Schofield, 1967).

The caves in the limestone are of three types (Fig. 3). Along the coast, marine erosion has exposed many caves close to, or just above, present sea level. These caves exhibit the rounded shapes and intricate solution features which indicate phreatic, below water table, origin, although they are above the present water table.

The second type are the steep-walled chasms which are sub-parallel to the coast on the inner side of the Alofi terrace (Schofield, 1959). They form interconnected systems up to 500 m long and 25 m deep, and contain brackish pools, which are an expression of the basal groundwater aquifer. These pools have been used by the Niueans as a water source in times of drought.

A third type of cave has developed in the interior basin of Niue, where many small dolines give access to flat-roofed caves consisting of branching passages a few metres below ground level. These caves commonly contain soil washed in through fissures, and small freshwater pools are found in places on either a rock or a soil floor. Many of these vadose zone caves were traditionally used by the Niueans for burial.

The water balance

There is no surface runoff on Niue and the water balance is:

rainfall = evapotranspiration + groundwater recharge

The annual rainfall recorded at Alofi has ranged from 1065 mm to 3185 mm, with a mean of 2041 mm. Figure 4 shows the variations from the long term mean. The worst recorded drought was 1940-44, when the annual rainfall was 23.6 percent below the mean for a 5-year period. In two other droughts, 1925-6 and 1976-7, the annual rainfall was more than 32 percent below the mean for a 2-year period.

The rainfall is seasonal with a wet season from December to April. The mean monthly rainfall ranges from 84 mm in June to 307 mm in March (Fig. 5).

No pan evaporation measurements are available for Niue, so evapotranspiration has been calculated by the climatological method of Thornthwaite (1948). Using Niue temperature data, and allowing for latitude, potential evapotranspiration has been estimated as 1417 mm annually. Monthly potential evapotranspiration ranges from 83 mm in July to 153 mm in January (Fig. 5).

The water balance shows a water surplus for 11 months of the year, with a rainfall greater than potential evapotranspiration, and a water deficit for one month. The water deficit of 9 mm in June is assumed to be made up by soil moisture recharge in July, so that the soil moisture budget balances, and actual evaporation equals potential evapotranspiration.

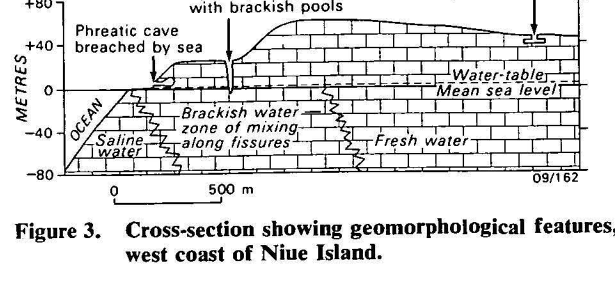

Figure 3. Cross-section showing geomorphological features, west coast of Niue Island.

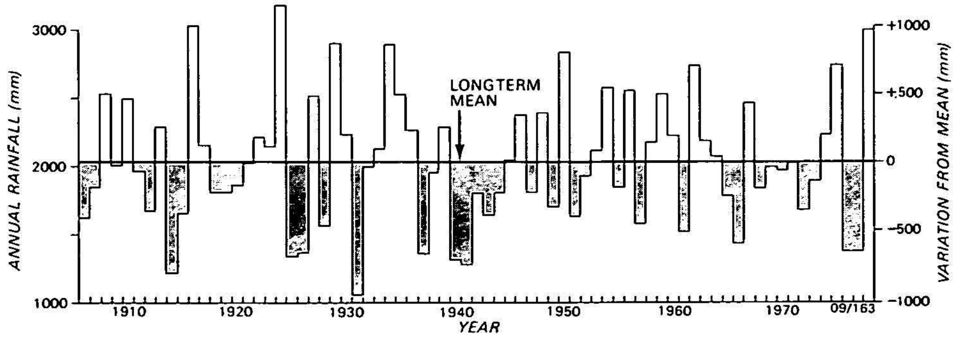

Figure 4. Rainfall variation from mean, 1906-78.

Groundwater recharge has been calculated on a monthly basis by subtracting evapotranspiration from rainfall. Recharge is estimated as 624 mm annually, with 85 percent of this in the period December to April.

Recharge to the basal groundwater body takes place through the vadose zone, which consists of porous and fissured limestone, 30-60 m deep. The porosity of the limestone is variable: tests on drill core indicate that it averages 22 percent, but ranges from 3 to 44 percent. Permeability tests on drill core indicate an average horizontal permeability of about 0.6 m/day, and an average vertical permeability of about 0.2 m/day. Very rapid infiltration can be observed everywhere on Niue: after prolonged heavy rainfall the ground is dry in a few minutes. It is likely that groundwater recharge in the vadose zone takes place mainly along vertical fissures and solution channels. Beneath the water table, groundwater movement is probably by a combination of intergranular and fissure flow.

The freshwater layer

The basal freshwater aquifer extends throughout the island and is unconfined, its top surface being the water table. The thickness of the freshwater layer has been mapped by resistivity depth probing, which is applicable because of the contrast in electrical resistivity between the unsaturated and freshwater-saturated limestone, and the underlying saltwater-saturated rock.

The geoelectric section

Resistivity depth probes were made at 25 sites distributed throughout the island, using Wenner and Schlumberger electrode arrays. Typical field curves show an increase in apparent resistivity with increased electrode spacing to a maximum at an electrode spacing of about 100 m; further increase in electrode spacing leads to a decrease in apparent resistivity.

In order to interpret the geoelectric section, it was assumed that the water table is 1 m above mean sea-level in the interior of the island, and that the freshwater layer is underlain by a zone of diffusion, about 30 m thick, in which the water is half as saline as seawater, i.e., has a resistivity of 0.4 ohm-m. With the additional assumptions of horizontal stratification and isotropic layers, interpretations of the sounding curves were obtained by computer, using a resistivity inversion program. The interpretations show a geoelectric section with a freshwater layer of resistivity 1100-7500 ohm-m separated by the transition zone from the seawater-saturated rock, which has a resistivity of about 3 ohm-m.

The groundwater conductivity was logged in one bore and compared with the resistivity measured at the same location (Fig. 6). In this bore, the transition zone of saltwater mixing was about 40 m thick. The base of the freshwater layer as determined by resistivity coincided with a bore-water conductivity of about 2500 μS/cm.

Aquifer configuration and groundwater flow

For a typical freshwater lens on a small oceanic island the depth of the saltwater interface is given by the Ghyben-Herzberg equation,

$$h_s = \frac{\rho_f}{\rho_s - \rho_f} h_f$$

where h_s is the depth of the saltwater interface below sea level, h_f is the height of the water above sea level, ρ_s is the saltwater density, and ρ_f is the freshwater density (Herzberg, 1901). Density measurements on Niue waters show that the saltwater is 1.0233 and the freshwater 0.9977 g/cm^3.

Levelling of the water table with respect to the mean sea level datum of Niue was undertaken in 13 accessible bores. Water-table contours (Fig. 7) show that the top surface of the aquifer is at a maximum 1.83 m above mean sea level datum in the centre of the island, although there is some indication of local reversals of this trend. Applying the Ghyben-Herzberg equation

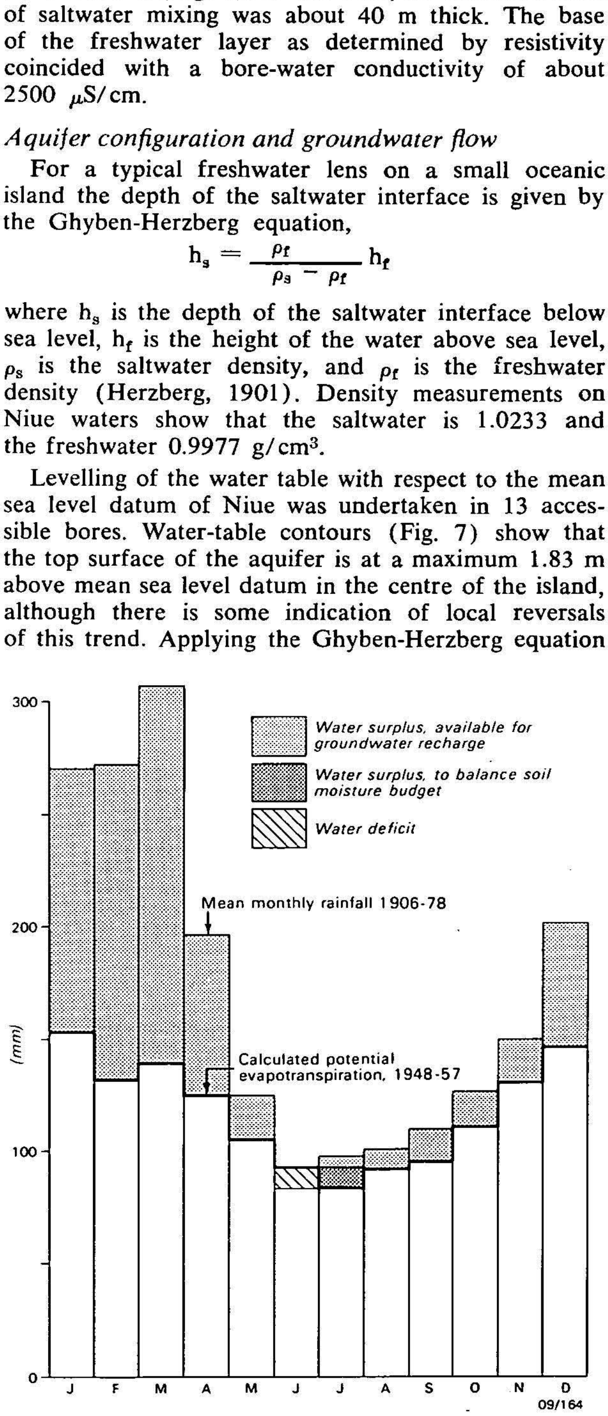

Figure 5. Monthly rainfall and evapotranspiration.

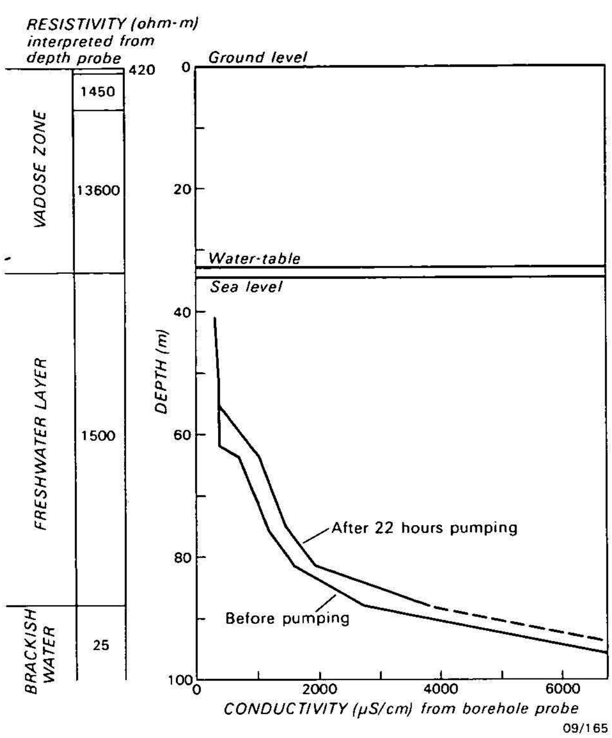

Figure 6. Groundwater conductivity profile measured in a bore hole, compared with results of resistivity depth probe.

to the measured water-table elevations, the maximum freshwater lens thickness should be 71.28 m in the centre of the island, decreasing steadily to 0 at the coast. However, the thickness of the freshwater layer inferred from resistivity data (Fig. 8) ranges from 40-80 m in the centre of Niue, to 50-170 m beneath the former atoll rim, and 0 at the coast. Thus the freshwater layer is approximately doughnut shaped, which is different from its characteristic lens shape on small oceanic islands of homogenous or isotropic permeability distribution.

The Ghyben-Herzberg theory was developed for homogenous sand aquifers, but the Niue aquifer is fissured and porous limestone with varying directional permeability. An asymmetric freshwater layer has been determined beneath the island of Bermuda (Vacher, 1978), which is composed of two types of limestone with differing permeabilities. There, the freshwater layer is thicker within the younger, less permeable, limestone. On Niue the irregular shape of the freshwater layer is probably also due to a variation of permeability within the limestone, with less permeable material underlying the rim of the island. This could be the case if the former lagoonal sediments are porous calcarenites while the former atoll rim is underlain by recrystallised or cemented reef limestone with lower permeability. In fact, there is some evidence that the rock beneath the rim of the island is extensively dolomitised (Schofield & Nelson, 1978).

The groundwater is recharged by infiltrating rain water over the entire island. If lateral flow of groundwater towards the coast is restricted by the lower permeability of the rock nearer the coast, then equili-

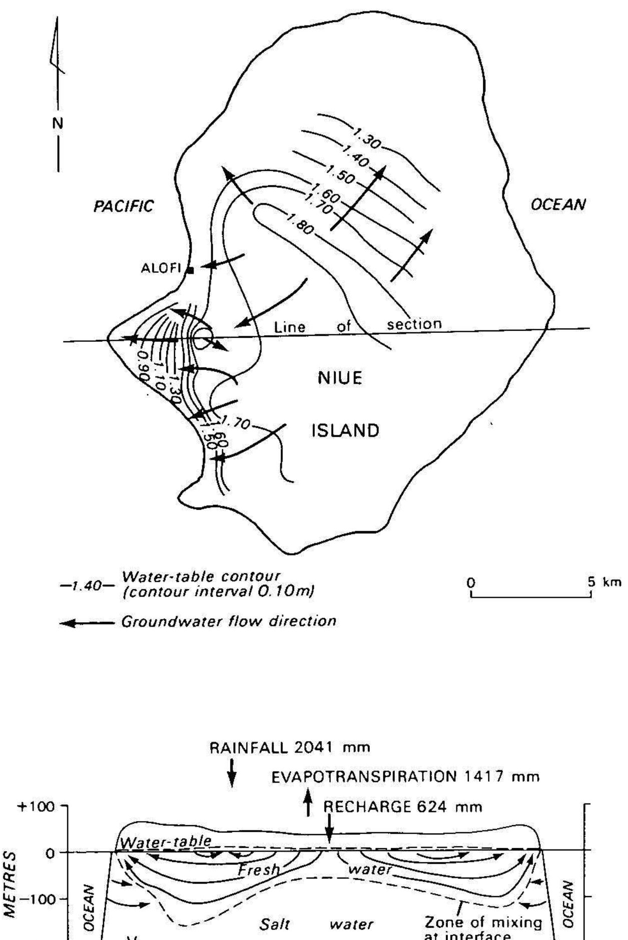

Figure 7. Water table contours and groundwater flow.

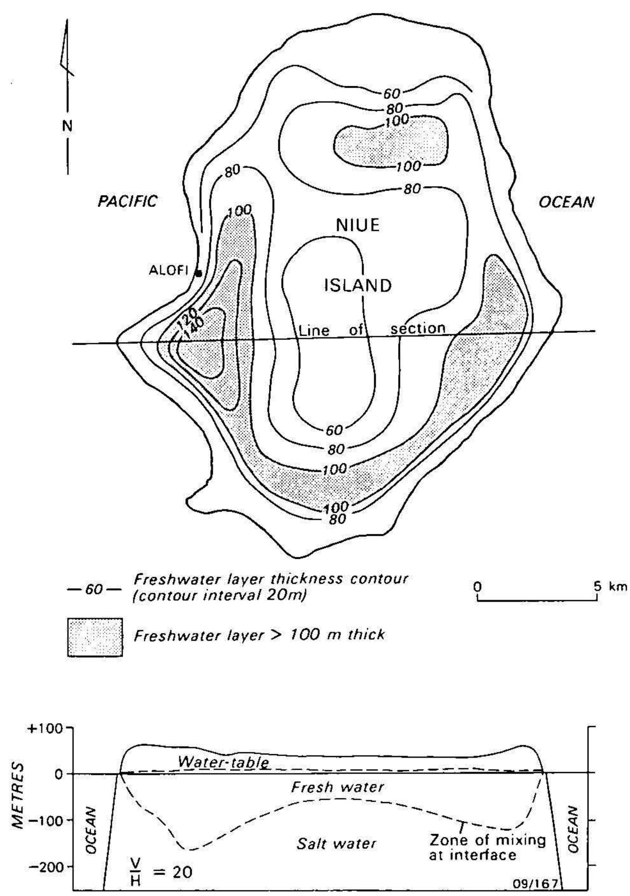

Figure 8. Thickness of the freshwater layer inferred from resistivity data.

brium conditions require a deeper section of rock for the lateral transmission of groundwater. The freshwater layer is therefore thicker in the less permeable rocks.

Freshwater storage

Aquifer porosity can be inferred from field resistivity data, using laboratory measurements of resistivity and porosity on drill core samples, and an empirical formula (Archie, 1942).

Aquifer porosity inferred in this way (Fig. 9) is greatest—more than 25 percent—in the central and southern interior of Niue. Freshwater storage in terms of effective water thickness (Fig. 10) is greatest—more than 25 m—beneath parts of the rim of the island. A mean value of 17.6 m was obtained for the effective water thickness; multiplying this by the area of island (259 km^2), leads to the conclusion that the freshwater layer contains about 4.6 km^3 of water.

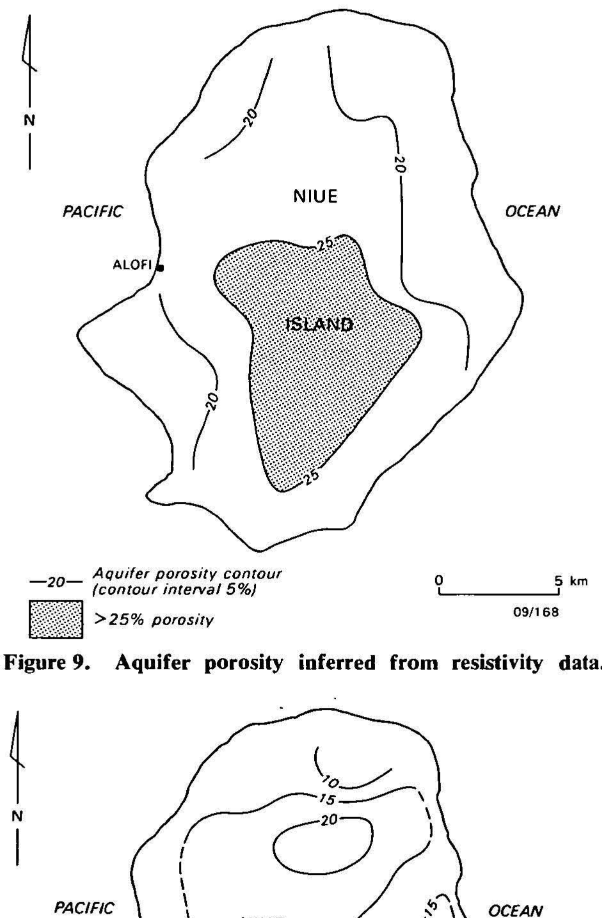

Figure 9. Aquifer porosity inferred from resistivity data.

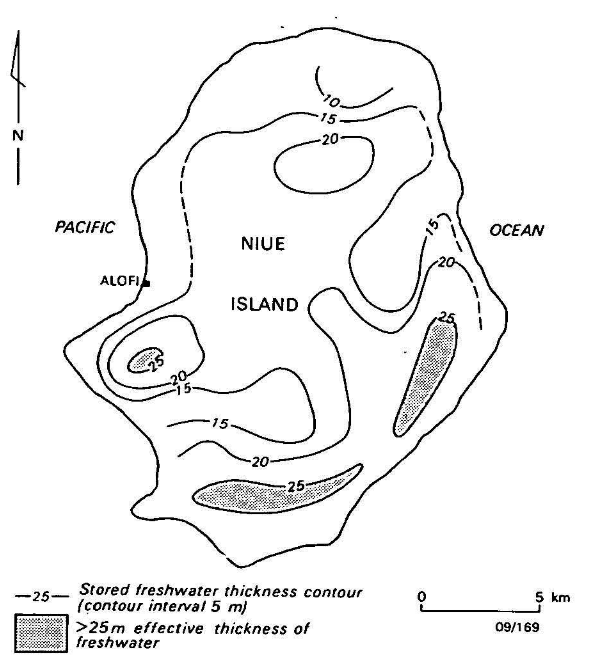

Figure 10. Freshwater storage inferred from resistivity data.

Aquifer productivity

Aquifer productivity was assessed by pumping tests at two sites in the interior of Niue—PB1 in the south and PB2 in the north (Fig. 2).

At the southern site a 24-hour pump test was conducted with a constant discharge of 3.82 l/s. In the pumping bore, drawdown of the water table reached a maximum of 2.10 m. Thus, the specific capacity, or yield to drawdown ratio, of the bore was 1.82 l/s per metre of drawdown. Specific capacity is an index of productivity related in part to permeability and in part to efficient bore construction. It was considered that the bore efficiency could be improved by deepening and redevelopment; this was done, and a subsequent aquifer test by the Niue Public Works Department showed no detectable drawdown in 4 hours pumping.

At the northern site a 12-hour pump test was conducted at a constant discharge of 3.52 l/s. Drawdown of the water table was 0.28 m, indicating a specific capacity of 12.64 l/s per metre of drawdown.

At both sites, observation bores were constructed 3-20 m from the pumping bore, but drawdown of the water table in the observation bores was masked by tidal fluctuations with an amplitude of up to 6 cm.

During the first pump test at the northern site, monitoring of conductivity in an observation bore showed 4 m upwards movement of the freshwater layer after 22 hours pumping (Fig. 6).

The results of the pumping tests, and observations of tidal fluctuations in groundwater throughout the island, indicate a high overall permeability in the aquifer.

Safe yield

The safe yield of the Niue aquifer has been estimated using a method developed for other oceanic islands (Mather, 1975). The depth to the freshwater/saltwater interface of an aquifer is proportional to the square root of the rate of uniform vertical recharge (Henry, 1964). As the removal of groundwater can be considered equivalent to reducing the vertical recharge, the depth to the interface can be calculated for various rates of groundwater extraction. This is illustrated in Figure 11 for a model freshwater layer

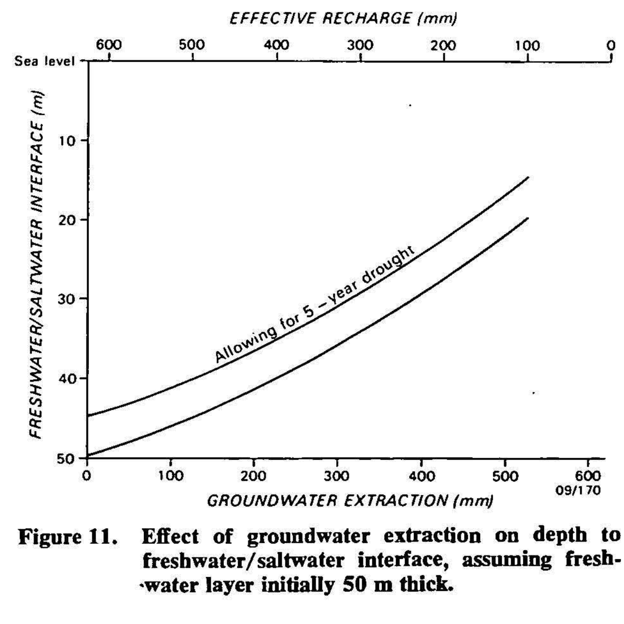

Figure 11. Effect of groundwater extraction on depth to freshwater/saltwater interface, assuming freshwater layer initially 50 m thick.

on Niue with an original depth of 50 m below sea level.

The effects of drought can be assessed by considering the annual rainfall deficit as a loss of effective recharge to the aquifer. During the worst historical drought on Niue, 1940-44, the annual rainfall was 23.6 percent below the mean for the 5-year period (Fig. 5). The effective annual recharge would have been reduced by 23.6 percent, that is, from 624 mm to 476 mm, during this time. The total rainfall deficit would have been $5 \times 148 = 740$ mm over 5 years, and this can be considered equivalent to a reduction in recharge. If a specific yield of 15 percent is assumed for the Niue aquifer, then the rainfall deficit of 740 mm would be stored in approximately 4.9 m of aquifer. Thus 4.9 m must be subtracted from the estimated depths to the interface (Fig. 11) to allow for the drought period.

Allowing for the effects of drought, Figure 11 indicates that the freshwater/saltwater interface could be maintained at 25 m below sea level, that is, at about half the original freshwater layer thickness, with 222 mm of annual rainfall as effective recharge. This would leave the equivalent of 402 mm of rain available for abstraction annually. This is equivalent to a safe yield of about 4 000 m^3 of groundwater per year per hectare or 11 m^3/day/ha.

Assuming that drawing up the lens to half its original thickness is acceptable, then the safe pumping rate can be estimated from specific capacity data. Drawdown must be controlled in order to prevent the upwards coning of saltwater beneath abstraction points. The necessary control could be achieved by operating the pump at a specified level and rate such that drawdown never exceeds one-half of the elevation of the water table above mean sea level.

Measurements in Production Bore 2 at the northern site showed that the elevation of the water table was 1.27 m above sea level. The permissible drawdown would be half of this, that is 0.63 m. The specific capacity of the bore was 12.64 l/s per metre of drawdown. Thus, for a drawdown of 0.63 m, the safe pumping rate would be 7.98 l/s or 690 m^3 per day. Applying the figure previously derived for safe yield of a model aquifer—11 m^3/day/ha—then the area of land required to maintain the discharge of this bore would be 63 ha.

As a first approximation then, groundwater development in the interior of Niue could be by a bore field with one bore to every 63 ha, producing approximately 8 l/s. However, local variations in permeability, and in thickness of the freshwater layer, mean that every individual bore will require testing to ascertain its safe yield. The closer spacing of lower yielding bores would be a suitable option.

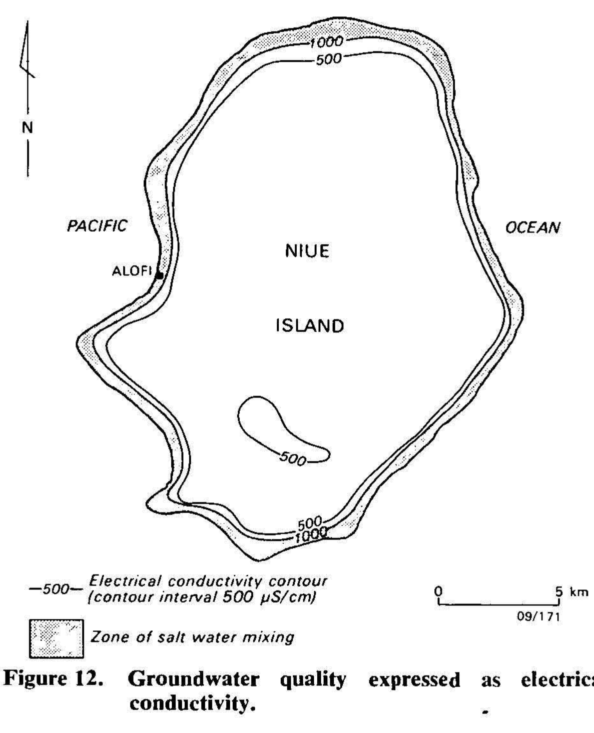

Figure 12. Groundwater quality expressed as electrical conductivity.

Water quality

Results of field conductivity determinations on groundwater samples are shown in Figure 12. Water quality is generally good in the interior of the island and beneath the former atoll rim. However, the coastal strip up to one kilometre wide shows evidence of saltwater mixing, with conductivity above 500 μS/cm.

A typical chemical analysis of fresh groundwater, from the dug well at Fonuakula, which supplies drinking water for Alofi, is:

Calcium	44 mg/l
Magnesium	9 mg/l
Sodium	6 mg/l
Potassium	2 mg/l
Bicarbonate	163 mg/l
Sulphate	4 mg/l
Chloride	10 mg/l
Nitrate	23 mg/l
Total dissolved solids	179 mg/l
Total hardness	149 mg/l
Carbonate hardness	134 mg/l
Non-carbonate hardness	15 mg/l
Total alkalinity	134 mg/l
Electrical conductivity	321 μS/cm
pH	7.7
Radium −226	1.0 picocurie /l

Eleven samples of inland groundwaters were analysed, and found to be in the range 136-261 mg/l total dissolved solids. This is below the World Health Organisation's (1963) maximum acceptable limit for drinking water, which is 500 mg/l. One analysed sample, from a coastal bore near Alofi, had 500 mg/l total dissolved solids.

Figure 13 is a Piper trilinear diagram showing the ionic composition of Niue groundwater. The inland bores have bicarbonate waters with calcium and magnesium the dominant cations. The coastal bore has chloride-bicarbonate water, indicating seawater mixing.

The Niue groundwater is classified as hard to very hard, and softeners could be required for some industrial applications. The water is slightly alkaline with a hydrogen ion concentration, pH, of 7.5-8.0.

According to guidelines for the interpretation of water quality for irrigation (Ayers, 1975), no problems with salinity effects on crop yield are expected with irrigation water having electrical conductivity below 750 μS/cm. Furthermore, the chloride and sodium concentrations in the inland bores are below those which could cause toxicity problems for plants. Nitrogen concentrations are also below the level at which problems with production or quality of crops could occur. Bicarbonate concentrations, however, are above 90 mg/l in all the Niue groundwater; this could lead to white carbonate deposits on fruit or leaves with overhead sprinkler irrigation. The sodium absorption ratio was calculated as 0.2 to 0.4 for the inland

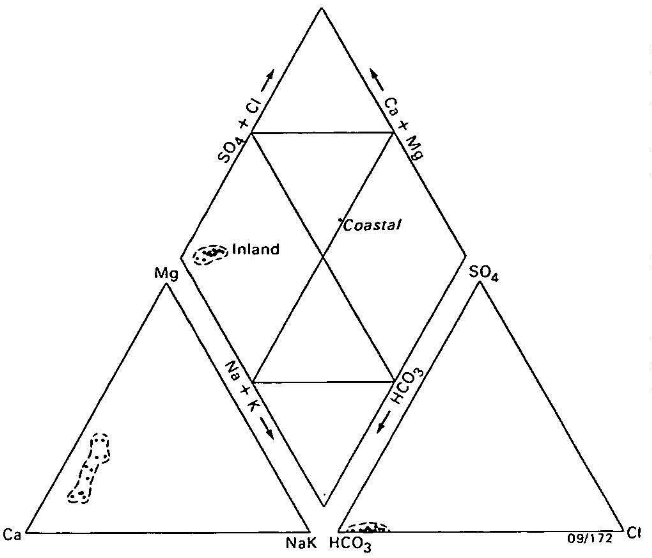

Figure 13. Ionic composition of Niue groundwater, plotted on a Piper trilinear diagram.

bores; this is a low value, indicating that problems connected with the deflocculation of clay will not occur.

Because of the known radioactivity of Niue soils, the possibility of radioactive elements being present in harmful concentrations in the groundwater has been raised (Schofield, 1967). Five samples taken during the present investigation were analysed for radium–226. All had radium–226 concentrations of 1 picocurie/l or less, which is below the maximum limit of 3 picocuries/l specified by the United States Public Health Service (1962).

The groundwater is bacteriologically clean unless some contamination from outside sources occurs. At present water supply bores are carefully monitored by the Niue Health Department and are closed down if contamination does occur. Two bores which were abandoned because of bacteriological contamination at Toi Village and Mutalau are believed to have been polluted by cave lavatories situated several hundred metres away. The aquifer is very susceptible to pollution, because of the fissured and permeable limestone and the lack of soil cover. Waste disposal in the outer 500 m coastal strip is less hazardous, because groundwater flows towards the coast. At present, waste disposal is restricted to this coastal zone, and there are also restrictions on latrines and on livestock close to bores used for drinking water.

The possibility of groundwater being polluted by agricultural development needs consideration. The use of fertilisers would add phosphate and nitrate to the soil. Phosphate would probably become fixed in the soil and the underlying limestone. Nitrate, however, would be leached and would percolate to the water table, which could lead to contamination of the groundwater. Inorganic pesticides would be fixed in the limestone; organic pesticides would not be fixed, but may be biodegradable. The choice of fertilisers and pesticides will need to be made accordingly, and water quality monitoring will be required.

Conclusions

The conclusion from this investigation is that Niue can be assured of a freshwater supply sufficient for its foreseeable requirements. Follow-up measures that are needed include provision of a suitable drilling rig and ancillary equipment, agricultural studies of the effects of irrigation, and formulation of water management and pollution control policies.

The resistivity depth probe technique has proved to be a useful tool for delineating the configuration of the freshwater layer. This technique could be more extensively used for groundwater resource evaluation on other oceanic islands which have water supply problems, and in other coastal areas.

Results of resistivity surveys indicate that the classical Ghyben-Herzberg freshwater lens does not exist on Niue Island, which is a relatively large limestone island with varying permeability. Geological factors rather than head of freshwater seem to determine the configuration of the freshwater layer.

Acknowledgements

The investigation was done for the Australian Development Assistance Bureau. The third man in the investigation team was A. W. Schuett, who was responsible for hydrographic measurements and aquifer testing.

The drilling was done under contract by F. A. Kelly Pty Ltd, Broadmeadow, NSW. Assistance with other aspects of the field work was provided by the Directors and staff of the Niue Department of Works; Department of Agriculture; Department of Justice, Lands and Survey; and Department of Health. Geological and survey information from the investigations of Mr J. Barrie of Avian Mining Pty Ltd, a company which is prospecting for minerals on Niue, was most helpful and was freely provided. Tidal information was obtained from the Hydrographic Office of the New Zealand Navy by courtesy of Mr I. McGregor, the New Zealand Representative on Niue. The help and cooperation of these people and of other Niue residents who helped in many ways, is gratefully acknowledged.

Chemical analyses of water samples were done by the Australian Mineral Development Laboratory in Adelaide. The resistivity inversion program was written by D. L. B. Jupp of Macquarie University. We thank G. M. Bladon for reviewing the manuscript.

The paper is published with the consent of the Niue Government.

References

ARCHIE, G. E., 1942—The electrical resistivity log as an aid in determining some reservoir characteristics. *Transactions of the American Institute of Mining and Metallurgical Engineers* **146**, 54.

AYERS, R. S., 1975—Quality of water for irrigation. *Proceedings of the Irrigation and Drainage Division, Speciality Conference, American Society of Civil Engineers, August 1975, Logan, Utah*, 24-56.

BRODIE, J. W., 1966—Niue Island provisional bathymetry. *New Zealand Oceanographic Institute Chart, 1:200 000 Island Series.*

FIELDES, M., BEALING, G., CLEARIDGE, G. C., WELLS, N., & TAYLOR, N. H., 1960—Mineralogy and radioactivity of Niue Island soils. *New Zealand Journal of Science* **3**, 658-75.

HENRY, H. R., 1964—Interfaces between salt water and fresh water in coastal aquifers. *In* COOPER, H. H., KOHOUT, F. A., HENRY, H. R., & GLOVER, R. E.—Sea water in coastal aquifers. *United States Geological Survey, Water Supply Paper* **1613–C**, 35-70.

HERZBERG, B., 1901—Die Wasserversorgung einiger Nordseebäder. (The water supply on parts of the North Sea Coast). *Journal für Gasbeleuchtung und Beleuchtungsarten, sowie für Wasserversorgung, Munich,* **44**, 815-9, 842-4.

HILL, P. J., in prep.—Gravity and magnetic survey of Niue Island. *Bureau of Mineral Resources, Australia, Record* (unpublished).

JACOBSON, G., & HILL, P. J., 1980—Groundwater resources of Niue Island. *Bureau of Mineral Resources, Australia, Record* **1980/14** (unpublished).

MATHER, J. D., 1975—Development of the groundwater resources of small limestone islands. *Quarterly Journal of Engineering Geology*, **8**, 141-50.

SCHOFIELD, J. C., 1959—The geology and hydrology of Niue Island, South Pacific. *New Zealand Geological Survey, Bulletin* **62**.

SCHOFIELD, J. C., 1967—Origin of radioactivity at Niue Island. *New Zealand Journal of Geology and Geophysics*, **10**, 1362-71.

SCHOFIELD, J. C., 1968—Niue groundwater. *In* Industrial minerals and rocks, 1968. *New Zealand Department of Scientific and Industrial Research, Information Series* **63**, 105-10.

SCHOFIELD, J. C., & NELSON, C. S., 1978—Dolomitisation and Quaternary climate of Niue Island, Pacific Ocean. *Pacific Geology*, **13**, 37-48.

THORNTHWAITE, C. W., 1948—An approach toward a rational classification of climate. *Geographical Review*, **38**, 55-94.

UNITED STATES PUBLIC HEALTH SERVICE, 1962—Drinking water standards. *United States Department of Health, Education and Welfare, Washington, D.C.*

VACHER, H. L., 1978—Hydrogeology of Bermuda—significance of an across-the-island variation in permeability. *Journal of Hydrology*, **39**, 207-26.

WORLD HEALTH ORGANISATION, 1963—International Standards for drinking water. *World Health Organisation, Geneva.*

WRIGHT, A. C. S., & VAN WESTERNDORP, F. J., 1965—Soils and agriculture of Niue Island. *New Zealand Department of Scientific and Industrial Research, Soil Bureau Bulletin* **17**.

BMR Journal of Australian Geology & Geophysics, 5, 1980, 279-288

Geochemistry of Precambrian metapelites from East Antarctica: secular and metamorphic variations

J. W. Sheraton

Early Archaean (>3 b.y. old) metapelites from the Napier Complex of East Antarctica are enriched in MgO and depleted in K_2O and Rb compared with late Archaean and Proterozoic metapelites, probably reflecting a higher proportion of mafic to ultramafic material and sodic (tonalitic to granodioritic) felsic igneous rocks in the source. A number of the more magnesian are strongly depleted in Cr, Ni, Cu, and V, and may have been formed by metamorphism of sediments derived from hydrothermally altered mafic or ultramafic igneous rocks. There is evidence for metamorphic depletion of Rb relative to K in these high-temperature granulite-facies metapelites, many of which have high K/Rb ratios, and for depletion of U relative to Th in granulite-facies metapelites compared with those of amphibolite facies.

The unique occurrence, on a regional scale, of assemblages containing sapphirine + quartz, and osumilite in metapelites of the Napier Complex may be due to their unusual chemical compositions, as well as to exceptionally high temperatures of metamorphism (900-950°C). Such assemblages are found only in the more magnesian rocks (mostly with mg > 0.6) in the Napier Complex, whereas younger metapelites are, with few exceptions, relatively iron-rich. Nevertheless, regional high-grade metamorphism with geothermal gradients sufficiently steep to allow formation of these rare assemblages is likely to have been confined to the Archaean.

Introduction

Geological mapping of part of the East Antarctic Precambrian Shield in the western section of Australian Antarctic Territory over the past ten years has established the presence of a wide variety of mostly high-grade metamorphic rocks ranging in age from early Archaean to Late Proterozoic. The oldest rocks (referred to here as early Archaean) belong to the Napier Complex in Enderby Land (Fig. 1), and consist of granulite-facies metamorphics (Sheraton & others, 1980), preliminary isotopic dating of which indicates an age of at least 3000 m.y. (Black & James, 1979), and possibly as much as 4000 m.y. (Sobotovich & others, 1976). Unusually high temperatures of metamorphism at very low water pressures are indicated

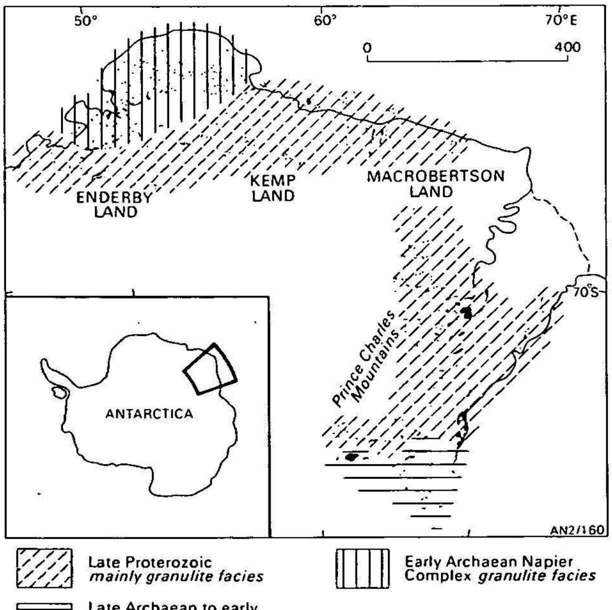

Figure 1. Map showing metamorphic complexes of Enderby, Kemp, and MacRobertson Lands.
Late Proterozoic metamorphics in the northern part of the southern Prince Charles Mountains are greenschist to amphibolite facies. Metamorphic rocks of this age in Enderby Land are classified as Rayner Complex. Outcrops are shown in black.

by the rare associations sapphirine + quartz, orthopyroxene + sillimanite, and osumilite in metapelites (Ellis & others, 1980), and by the abundance of calcic mesoperthite (Sheraton & others, 1980). Granitic basement rocks and a variety of associated metasediments, mostly metamorphosed at amphibolite facies, are present in the southern Prince Charles Mountains, MacRobertson Land; the majority are of late Archaean age, but some may be early Proterozoic (Tingey, in press).

Granulite-facies metamorphism occurred about 1000 m.y. ago in the northern Prince Charles Mountains and MacRobertson Land Coast, although Sr isotope data indicate that at least some of the metamorphic rocks formed during this event were derived from much older sialic crustal material (Tingey, in press). Metamorphic rocks of probable similar age crop out in Kemp Land and the western part of Enderby Land, where they are classified as the Rayner Complex (Sheraton & others, 1980).

The Precambrian rocks of this part of the East Antarctica thus provide an opportunity to investigate possible chemical variations as a function of both age (early Archaean to late Proterozoic) and metamorphic grade (amphibolite to granulite facies). This paper is concerned with the geochemistry of metapelites; the geochemistry of felsic gneisses and mafic rocks will be considered elsewhere.

The chemical characteristics of early Archaean sediments (or metasediments) will provide information on their provenance, and hence, indirectly, on the composition of the earliest crust. The occurrence of rare mineral assemblages only in the early Archaean rocks may be due partly to unusual chemistry, as well as particularly high temperatures of metamorphism. As an additional complication, possible chemical effects of high-grade metamorphism must be considered, and an attempt is made to distinguish between primary and metamorphic chemical features.

Petrography

Early Archaean granulite-facies metapelites of the Napier Complex contain a variety of assemblages of which the following are characteristic:

garnet + sillimanite + K-feldspar + quartz;
garnet + cordierite + orthopyroxene + quartz ±

K-feldspar ± plagioclase ± biotite;
garnet + sillimanite + cordierite + K-feldspar + quartz ± plagioclase;
garnet + spinel + K-feldspar + quartz ± plagioclase.

However, in a large area of the Complex, cordierite-bearing assemblages give way to rare, very high-grade assemblages containing sapphirine + quartz, orthopyroxene + sillimanite, and osmulite:

sapphirine + orthopyroxene + quartz;
sapphirine + garnet + osumilite + quartz ± sillimanite ± orthopyroxene;
osumilite + orthopyroxene + quartz ± phlogopite ± garnet ± K-feldspar ± plagioclase;
osumilite + sillimanite + K-feldspar + quartz;
garnet + sillimanite + orthopyroxene + K-feldspar + quartz;

Osumilite, with a composition near $K_{0.93}Na_{0.13}Mg_{2.04}Fe_{0.21}Al_{4.60}Si_{10.16}O_{30}$, is commonly replaced by a fine-grained symplectite of cordierite and subordinate K-feldspar, quartz, and orthopyroxene. K-feldspar and plagioclase are commonly combined as mesoperthite.

These unusual assemblages are not found amongst the younger metamorphic rocks in the Rayner Complex and further east. Thus, late Proterozoic granulite-facies metapelites of MacRobertson Land are characterised by the assemblage

garnet + sillimanite + cordierite + biotite + K-feldspar + quartz ± plagioclase,

although garnet is absent from some rocks and cordierite from others; spinel is a widespread minor constituent.

Most analysed samples of late Archaean to early Proterozoic metapelites from the southern Prince Charles Mountains are of amphibolite facies, and contain such assemblages as:

kyanite + staurolite + biotite + quartz ± muscovite ± garnet ± plagioclase;
sillimanite + biotite + muscovite + plagioclase + quartz;
garnet + biotite + muscovite + quartz;

although there is evidence that some of these assemblages may have resulted from late Proterozoic metamorphism. The higher grade assemblage

garnet + sillimanite + cordierite + biotite + K-feldspar + plagioclase + quartz

occurs locally. A number of rocks show evidence of retrogression, commonly with development of chlorite, and chloritoid is present in two samples.

More detailed descriptions of the geological relations and petrography of the metapelites and associated rocks are given by Tingey (in press), Sheraton & others (1980), and Ellis & others (1980).

	1		2		3		4		5	
	mean	*s.d.*	*mean*	*s.d.*	*mean*	*s.d.*	*mean*	*s.d.*	*mean*	*s.d.*
SiO_2	64.81	7.96	56.47	7.42	63.50	12.94	71.30	5.89	59.05	13.90
TiO_2	1.04	0.37	0.90	0.17	0.82	0.38	0.65	0.40	0.91	0.35
Al_2O_3	17.19	3.34	21.87	4.06	18.81	7.64	13.25	3.11	21.98	7.70
Fe_2O_3	2.97	1.63	3.22	2.30	1.23	1.31	0.63	0.36	1.58	1.53
FeO	5.03	1.81	6.81	2.51	4.88	2.93	3.19	1.62	5.84	3.12
MnO	0.12	0.07	0.11	0.04	0.07	0.08	0.03	0.02	0.10	0.08
MgO	2.43	1.12	3.08	1.37	6.11	3.73	6.02	3.18	6.17	4.13
CaO	0.71	0.49	0.64	0.68	0.76	1.24	0.41	0.24	0.96	1.53
Na_2O	0.99	0.91	0.77	0.60	1.01	1.17	1.31	0.92	0.84	1.29
K_2O	3.67	1.15	3.58	2.04	1.74	1.30	2.27	1.50	1.44	1.14
P_2O_5	0.10	0.05	0.10	0.05	0.04	0.05	0.05	0.06	0.03	0.04
H_2O	0.62	0.23	2.03	0.99	0.59	0.21	0.56	0.17	0.61	0.19
Total	99.73		99.58		99.56		99.67		99.51	
				Trace elements in parts per million						
V	145	57	193	37	151	113	36	39	204	95
Cr	140	52	511	312	431	563	6	4	674	582
Ni	56	28	180	107	104	170	10	12	157	195
Cu	10	15	28	31	16	24	3	1	24	27
Zn	114	44	125	78	46	50	34	32	53	58
Ga	26	7	28	6	29	13	19	3	33	14
Rb	163	47	195	145	51	32	64	46	44	20
Sr	100	33	84	54	43	40	28	23	51	46
Y	35	17	32	11	35	21	39	15	30	30
Zr	231	69	190	42	294	163	295	181	294	159
Nb	12	4	14	4	19	17	12	7	23	20
Ba	838	467	500	205	423	470	663	602	286	325
La	30	10	22	17	34	32	47	42	26	24
Ce	61	21	60	19	53	52	75	65	41	41
Pb	24	7	14	14	9	11	8	8	9	13
Th	20	9	14	10	11	10	19	12	6	6
U	1.5	1.2	3.0	1.4	1.3	0.9	1.5	1.1	1.1	0.8
mg	0.35	0.40	0.37	0.16	0.65	0.12	0.74	0.10	0.60	0.10
k	0.74	0.12	0.75	0.12	0.53	0.26	0.53	0.22	0.53	0.26
K/Rb	189	37	152	43	283	148	294	123	272	161
Th/U	13	7	5	2	8	9	13	11	5	2

s.d. — standard deviation

Table 1. Average compositions of Precambrian metapelites.

1. 11 late Proterozoic granulite-facies metapelites from the northern Prince Charles Mountains and MacRobertson Land coast.
2. 10 late Archaean to early Proterozoic mostly amphibolite-facies metapelites from the southern Prince Charles Mountains.
3. 22 early Archaean granulite-facies metapelites from the Napier Complex of Enderby Land.
4. 8 Cr-poor metapelites from the Napier Complex.
5. 14 Cr-rich metapelites from the Napier Complex.

All elements analysed by X-ray fluorescence spectrometry in BMR laboratory, except H_2O (gravimetric), FeO (volumetric), and Cr, Ni, Cu, and Zn (atomic absorption spectrophotometry). For details of methods see Sheraton & Labonne (1978).

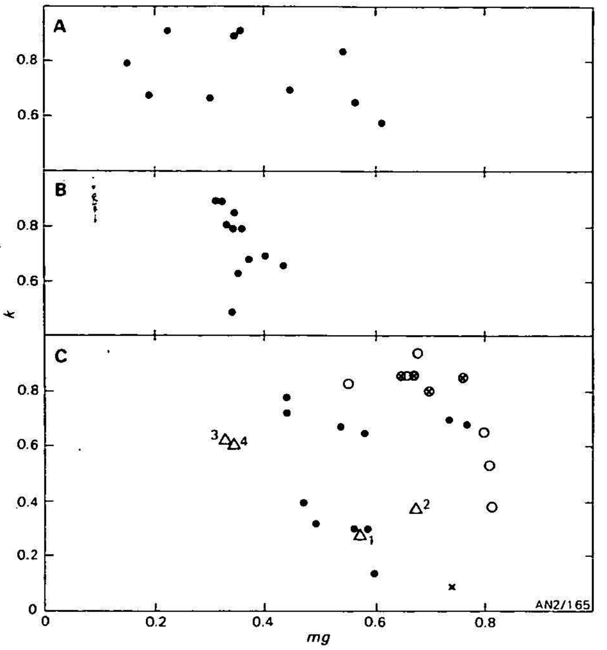

Figure 2. Plots of k (molecular $K_2O/(K_2O + Na_2O)$) against mg (molecular $MgO/(MgO$ + total $FeO)$) for Precambrian metapelites.
A, late Archaean to early Proterozoic amphibolite-facies metapelites from the southern Prince Charles Mountains, MacRobertson Land; **B,** late Proterozoic granulite-facies metapelites from the northern Prince Charles Mountains and MacRobertson Land coast; **C,** early Archaean granulite-facies metapelites from Napier Complex of Enderby Land. Assemblages containing sapphirine + quartz (crosses), osumilite (open circles), or both are indicated. Triangles show average compositions of 3.2-3.5 b.y. (1 and 2) and 2.6-2.8 b.y. (3 and 4) metapelites from India (Naqvi, 1978).

Geochemistry

Forty-three metapelite samples were analysed: means and standard deviations of those from the early Archaean Napier Complex of Enderby Land (granulite facies), the late Archaean to early Proterozoic of the southern Prince Charles Mountains (mostly amphibolite facies), and the late Proterozoic of the northern Prince Charles Mountains-MacRobertson Land Coast (granulite facies) are given in Table 1 (individual analyses are available from the the author). Despite the relatively few analyses and the wide range of compositions, particularly amongst the Napier Complex metapelites, certain systematic chemical differences are apparent. Chemical features which are thought to be primary (i.e. pre-metamorphic) and those which have apparently resulted from high-grade metamorphism are considered separately, although for some elements it is difficult to make such a distinction; indeed, both factors are likely to be of importance. Nevertheless, for reasons given below, the major compositional features of the metapelites are thought essentially to reflect those of the original sediments.

Figure 3. Modified AFM diagrams for Precambrian metapelites.
A-C and symbols as in Figure 2. $A' = Al_2O_3 - (K_2O + Na_2O + CaO)$; F = total Fe as FeO; M = MgO (all as molecular proportions). Approximate mineral compositions are indicated (those in C from Ellis & others, 1980): Bi, biotite; Cd, cordierite; Gt, garnet; Opx, orthopyroxene; Os, osumilite; Sa, sapphirine; Si, sillimanite; Sp, spinel.

Secular chemical trends

The most significant chemical characteristic of the early Archaean Napier Complex metapelites, compared to those of late Archaean and Proterozoic age, is their considerably higher MgO content and mg (molecular $MgO/(MgO$ + total $FeO)$) values; most have mg >

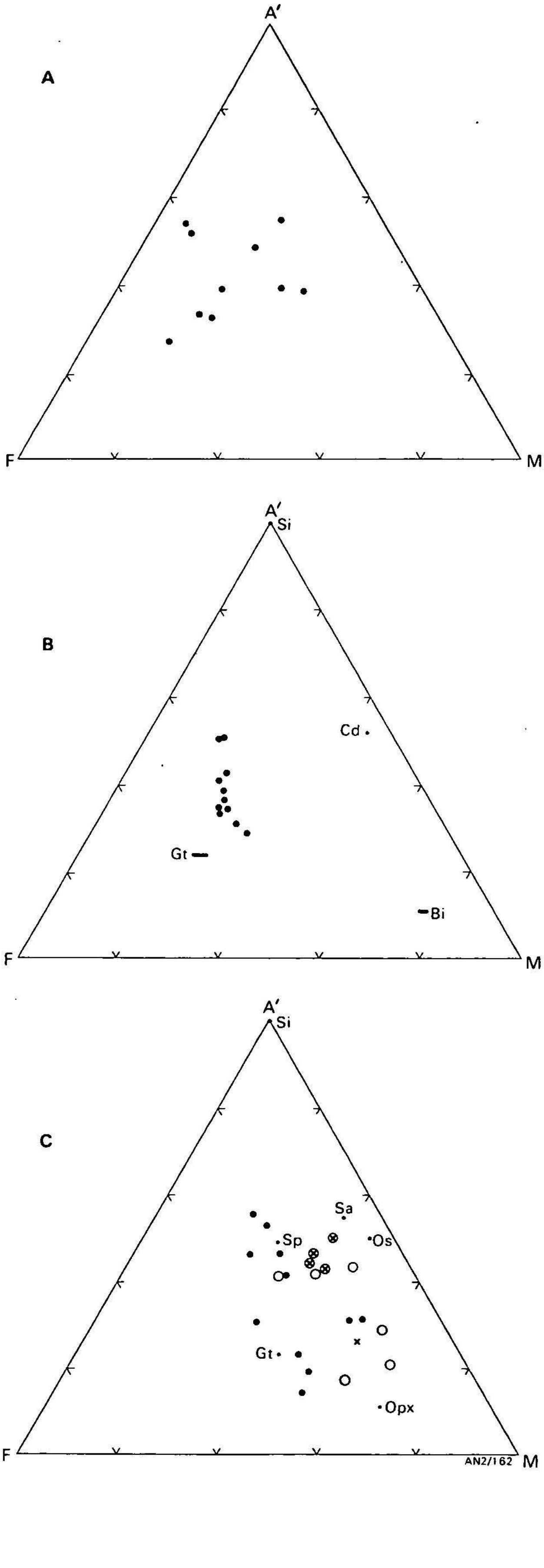

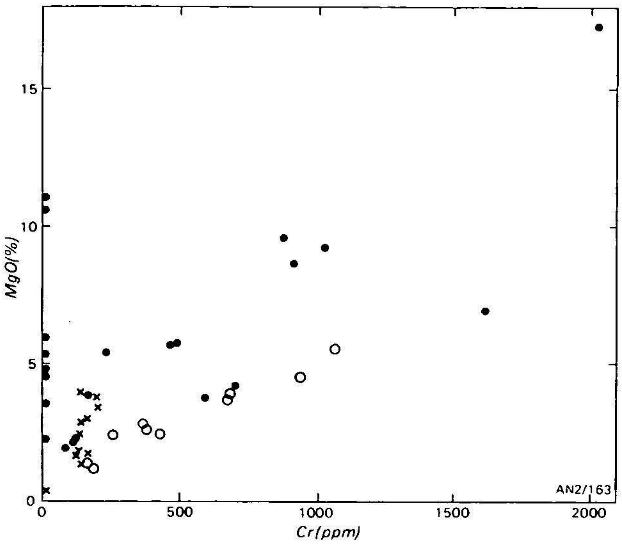

Figure 4. Plot of MgO against Cr for Precambrian metapelites.
Early Archaean Napier complex—solid circles; late Archaean to early Proterozoic—open circles; late Proterozoic—crosses.

0.5 (Figs. 2, 3). Although there may have been some bias towards analysis of metapelites containing sapphirine + quartz, or osumilite, which are restricted to relatively magnesian compositions in the Napier Complex (Ellis & others, 1980), an attempt was made to include samples containing a wide range of other assemblages, and the compositional fields on Figures 2 and 3 are thought to be reasonably representative. Retrograde chloritoid-bearing metapelites of late Archaean to Proterozoic age from the southern Prince Charles Mountains have mg < 0.2, particularly low MgO, and high Al_2O_3. Many of the early Archaean metapelites have relatively low k (molecular K_2O/(K_2O + Na_2O)) values, although some are more potassic and similar in this respect to younger ones (Fig. 2).

There appear to be no systematic differences in k or mg between the late Archaean-early Proterozoic and late Proterozoic metapelites, although the former have a much wider range of mg values. This general similarity may be due in part to the derivation of the late Proterozoic meta-sediments either by direct re-metamorphism of the late Archaean to early Proterozoic rocks which crop out immediately to the south, or possibly by metamorphism of their weathering products. However, isotopic data indicate that not all the late Proterozoic metamorphics were derived from very much older sialic crusal rocks (Tingey, in press).

The considerably higher average MgO content of the early Archaean, compared with younger, Antarctic metapelites (Table 1) presumably reflects differences in source-rock composition, such as a higher proportion of mafic or ultramafic material (Engel & others, 1974; Veizer, 1979); Ronov (1972) has suggested that mafic lavas were the predominant crustal rocks prior to 3.5 b.y. ago. This explanation would also account for the high Cr and Ni contents of many (but not all) samples (compare MacPherson, 1958), although most of the late Archaean-early Proterozoic metapelites are also high in these elements; however, late Proterozoic metapelites have relatively low Cr and Ni contents, close to typical shale values (Shaw, 1956; Frohlich, 1960; Shiraki, 1978). Figure 4 shows that, whereas there is a reasonably good correlation between MgO and Cr for most of the analysed metapelites, a number of the early Archaean rocks are very Cr-poor (average of 8 is 6 ppm), in spite of MgO contents up to 11 percent, and define a quite distinct trend. These rocks, many of which are strictly psammo-pelites, are also significantly lower in Al_2O_3, total FeO, V, Ni, and Cu, but have higher SiO_2 Ba, Th, and mg values than the

	1	2	3	4	5	6	7	8	9	10
SiO_2	59.05	71.30	68.2	58.4	56.1	64.2	53.4	61.54	56.30	60.15
TiO_2	0.91	0.65	0.94	0.65	0.6	1.26	1.0	0.82	0.77	0.76
Al_2O_3	21.98	13.25	13.09	20.50	18.7	13.4	19.0	16.95	17.24	16.45
*FeO	7.26	3.76	6.52	4.45	5.6	3.7	4.7	6.20	9.73	6.54
MnO	0.10	0.03	0.03	0.08	—	0.00	—	—	0.10	—
MgO	6.17	6.02	10.57	11.09	9.3	13.1	19.7	2.52	2.54	2.32
CaO	0.96	0.41	0.06	0.22	1.1	0.1	0.45	1.76	1.00	1.41
Na_2O	0.84	1.31	0.07	1.79	—	1.5	0.05	1.84	1.23	1.01
K_2O	1.44	2.27	0.01	3.01	2.4	0.25	1.5	3.45	3.79	3.60
P_2O_5	0.03	0.05	0.02	0.05	—	0.09	—	—	0.14	0.15
H_2O (tot)	0.61	0.56	0.75	0.28	—	2.5	—	3.47	3.69	4.71
Total	99.37	99.61	100.26	100.52	—	100.10	99.80†	100.22	98.83	100.02
mg	0.60	0.74	0.74	0.81	0.75	0.86	0.88	0.42	0.32	0.39
Cr	674	6	4	12	23	—	—	110	—	—

* Total Fe as FeO. † Calculated water-free.

Table 2. Compositions of Napier Complex metapelites compared to other occurrences of magnesian metapelites and average pelite.

1. 14 Cr-rich metapelites from the Napier Complex.
2. 8 Cr-poor metapelites from the Napier Complex.
3. Sapphirine-orthopyroxene-cordierite-quartz metapelite, Mt Hardy, Enderby Land (BMR sample No. 77284633).
4. Sapphirine-osumilite-orthopyroxene-plagioclase-K-feldspar-quartz metapelite, Mt Bartlett, Enderby Land (78285058).
5. 4 cordierite-anthophyllite-biotite-quartz-chlorite metapelites from the Corrella Formation, Mary Kathleen area, Queensland (Ramsay & Davidson, 1974). Cr value is the average of 11 analyses (G. M. Derrick, personal communication, 1980).
6. 4 whiteschists (kyanite-talc schists) from Zambia (Schreyer, 1977).
7. 2 evaporite mudstones, Sahara Atlas, NW Africa (Schreyer, 1977).
8. Average pelite (Shaw, 1956). Total includes 1.67% CO_2. Cr value is for the average Littleton pelite.
9. Average Precambrian (mostly Proterozoic) lutite (Nanz, 1953). Total includes 0.84% CO_2, 1.18%C, and 0.28% SO_3; original analysis includes 1.98% FeS_2.
10. Average Palaeozoic shale (Nanz, 1953). Total includes 1.46% CO_2, 0.88% C, and 0.58% SO_3.

rest of the early Archaean metapelites (Table 1). Both groups include sapphirine and osumilite-bearing rocks. Whereas the high-Cr group has fairly typical pelite chemistry (albeit rather magnesian), the unusual composition of the low-Cr metapelites requires further explanation and their origin is considered in a later section. Even if the low-Cr samples are excluded from the early Archaean average, the remaining metapelites are still considerably more magnesian than their younger Antarctic analogues (Table 1) and average pelite (Table 2).

Apart from source-rock composition, a further possible explanation of the high mg values of the early Archaean metapelites must be considered, namely, enhanced leaching of Fe during weathering. In a reducing, or at least anoxic atmosphere, such as may have existed during the early Archaean (Kimberley & Dimroth, 1976; Schidlowski, 1976; Walker, 1976), iron could be removed as Fe^{2+} during weathering (Smith, 1979), resulting in a tendency for pelitic sediments to be correspondingly more magnesian (that is, having higher mg values). Ronov (1972) has reported a generally increasing oxidation ratio (Fe_2O_3/FeO) of sediments through Precambrian time, and the early Archaean metapelites from Antarctica tend to have lower oxidation ratios than younger examples, although this may be a metamorphic effect. The iron would presumably be ultimately deposited as banded ironstones or other ferruginous sediments, but, although the metamorphosed equivalents of such rocks (magnetite-quartz-orthopyroxene and magnetite-quartz-garnet granulites) are widespread in the Napier Complex, they are volumetrically minor. Indeed, banded ironstones are considerably more abundant amongst the late Archaean-early Proterozoic metamorphics of the southern Prince Charles Mountains (Tingey, in press), and reach a maximum development world-wide during the early Proterozoic (Ronov, 1972; Goldich, 1973). Hence, taking their abundances into account would actually increase the compositional contrast (in terms of mg values) between Antarctic metasediments of the different age groups, and it seems unlikely, on this admittedly slender evidence, that such a process can account for the unusual compositions of the early Archaean metapelites.

The relatively low k values of many of the early Archaean metapelites may, to a large extent, reflect the predominance of sodium-rich (commonly tonalitic or trondhjemitic) compositions among Archaean felsic igneous rocks (Glikson & Sheraton, 1972; Glikson, 1979). Napier Complex felsic gneisses are mostly of granodioritic or tonalitic composition, whereas those of late Archaean or younger age are mostly granitic (s.s.) (Sheraton, in press, and unpublished data). The increase in Rb, Ba, Pb, and Th contents with time (i.e., decreasing age) may also be related to this trend. Other chemical differences (e.g., P_2O_5, Zn, and Sr) are more difficult to explain, but apparently reflect significant variations in source rock composition (see below).

Naqvi (1978) found 3.2-3.5 b.y. old metapelites from India to be enriched in Al, Ti, Fe, Mg, Cr, and Ni, and depleted in Si, K, Sr, and Rb compared with late Archaean (2.6-2.8 b.y.) metapelites. He attributed these differences to derivation of the early Archaean metapelites from a crust composed of low-K tholeiite (60%), anorthosite (30%), and ultramafics (10%). Similarly, Schwab (1978) found that the average Archaean sediment is higher in Al, Mg, and Na, and lower in Si, Ca, and K than younger sediments. Rogers (1978) presented evidence for a general increase in Si, K, and k, and decrease in Al, Fe, Mg, Ca, Na, and mg in Precambrian crustal rocks with time, and Fahrig & Eade (1968) and Engel & others (1974) pointed out the generally low K/Na ratios of Archaean, compared with Proterozoic, crustal rocks. Although data for the Antarctic metapelites reflect these general trends with respect to Mg, K, Sr, and Rb, and possibly Cr and Ni, they do not indicate any systematic increase in Si or Si/Al with time, perhaps because of the relative immaturity of Archaean pelites (Engel & others, 1974). It is noteworthy that quartzites are considerably more abundant amongst the late Archaean-early Proterozoic metamorphics of the southern Prince Charles Mountains than the early Archaean Napier Complex (Tingey, in press; Sheraton & others, 1980).

Chemical effects of metamorphism

No clear pattern of changes in the major-element composition of pelitic rocks with metamorphic grade has been demonstrated. Shaw (1956) and Sighinolfi & Gorgoni (1978) found little change (apart from partial dehydration) in the composition of such rocks up to amphibolite facies, although pelitic gneisses from Spain tend to be somewhat enriched in granitic components (Si, K, etc.) relative to slates and schists (Aparicio & others, 1979). Sighinolfi & Gorgoni (1978) considered that, apart from the loss of a differentiated low-viscosity silicate melt fraction, rich in water and granitophile elements, even at granulite facies the bulk of the partial melt would not migrate and would recrystallise with the unmelted solids on cooling. The local survival of sedimentary structures in many high-grade terrains supports this conclusion.

In the Napier Complex, even gneiss of granitic composition shows little evidence of remobilisation; the very limited degree of melting is thought to have been due to the very low water pressure during metamorphism (Sheraton & others, 1980). Amphibolite-facies terrains, such as that of the southern Prince Charles Mountains in MacRobertson Land, generally show evidence of rather more extensive melting under relatively hydrous conditions. However, field observations of metapelites in such terrains suggest that the mobilisation was commonly very localised and effectively confined to the development of a more pronounced compositional layering. For this reason, the possibility that the unusual chemistry of the Mg-rich, commonly sapphirine-bearing, metapelites of the Napier Complex may be due to loss of a granitic melt is not considered plausible; furthermore, the chemical variations in Antarctic metapelites of different ages cannot be explained in detail on this basis. Such an explanation has been suggested by some authors for the origin of unusually sapphirine-rich rocks of even more extreme compositions (e.g., Clifford & others, 1975; Lal & others, 1978), but extremely high degrees of melting combined with complete separation of the melt from the restite would be necessary. It is difficult to understand how such rocks, which occur as layers and lenses up to several metres thick and crop out at a few localities in Enderby and MacRobertson Lands (see below) can be restites, when associated gneisses of much less refractory composition do not appear to have been extensively melted. Rather, the chemistry of high-grade metapelites is considered likely to reflect, at least to a first approximation, that of the

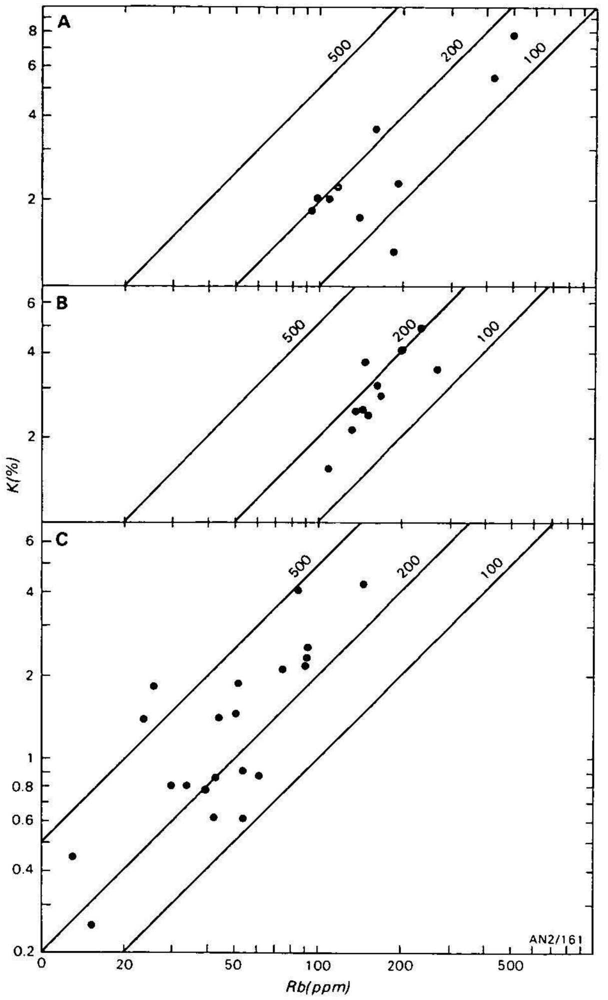

Figure 5. Plots of K against Rb for Precambrian metapelites.
A-C as in Figure 2. Lines of constant K/Rb ratio are shown.

original sediments, although the probability of small-scale metamorphic differentiation and some degree of anatexis must be considered during sampling for analytical purposes.

Although it may be difficult in specific cases to distinguish primary chemical features from those due to metamorphic processes, the common depletion of granulite-facies metamorphics in certain lithophile elements (notably K, Rb, Th, and U) is well established (Lambert & Heier, 1968; Tarney & others, 1972; Sheraton & others, 1973). Tarney (1976) has convincingly demonstrated the significance of lithophile element depletion during high-grade metamorphism, possibly near the base of the lower continental crust in association with mantle degassing, and in this context the chemical characteristics of unusually dry, high-temperature metamorphics of the Napier Complex may be compared with those of more typical granulite and amphibolite-facies metamorphics from Antarctica.

Figure 5 shows that there is little difference between the amphibolite-facies and granulite-facies metapelites of MacRobertson Land in terms of K and Rb contents, whereas many of the Napier Complex metapelites have relatively high K/Rb ratios (200-500). These high ratios may partly reflect those of the source rocks, particularly if significant amounts of mafic to ultramafic composition or K and Rb-poor felsic were involved, but the fact that the more potassic Napier Complex metapelites have relatively high K/Rb ratios—the reverse of the normal trend in crustal rocks—suggests that some depletion of Rb relative to K occurred during metamorphism. Felsic gneisses from the Napier Complex also show evidence of Rb depletion during metamorphism—in general the more potassic (i.e., granitic) compositions have the lowest K/Rb ratios (average 343: Sheraton, unpublished data), but these are still considerably higher than normal values for granitic rocks, including Archaean granites (s.s.) (Glikson, 1979).

U is commonly significantly lower in granulite-facies compared with amphibolite-facies metamorphics, and Th may show a similar depletion (Lambert & Heier, 1968; Kalsbeek, 1976; Tarney & Windley, 1977). Figure 6 shows that U is lower in the MacRobertson Land granulites than the amphibolites, and lowest in those from the Napier Complex, although the latter may be partly a primary feature. For Th the pattern is less clear, although many of the Napier Complex metapelites have very low Th contents. Th/U ratios of the amphibolite-facies rocks are only slightly higher than the crustal average (~3.5: Taylor, 1966) and greywackes of a wide range of ages (Rogers & McKay, 1972), whereas those of metapelites from both granulite-facies terrains range up to high values, consistent with various degrees of depletion in U relative to Th. K/U and K/Th ratios do not show any clear trends. Associated felsic gneisses show more marked differences, with U and, to a lesser extent, Th being more depleted in granulite-facies gneisses, and Th/U being significantly higher (Sheraton, in press, and unpublished data).

Sighinolfi & Gorgoni (1978) have presented evidence for a slight depletion in Pb and Zn during granulite-facies metamorphism. The Antarctic rocks show no systematic change in Pb or K/Pb with metamorphic grade, however; the Archaean and early Proterozoic metapelites (of both amphibolite and granulite facies) have generally lower Pb and higher K/Pb than the late Proterozoic granulite-facies metapelites (Table 1). Zn contents are lowest and Fe/Zn ratios mostly higher in the Napier Complex rocks, but there is no clear difference between those of amphibolite and granulite facies from MacRobertson Land. The available data thus suggest that the differences in Pb and Zn contents are probably primary rather than due to metamorphic processes, although they are insufficient to adequately test this.

Origin of Cr-poor metapelites of the Napier Complex

The unusual composition of the Cr-poor metapelites, in particular their very low Cr, Ni, Cu, and V contents and high mg values compared with typical shales (Shaw, 1956; Wedepohl, 1978), and the quite distinct trend they define on the MgO-Cr plot (Fig. 4) suggest a fundamentally different origin from that of the other early Archaean metapelites, the compositions of which more closely resemble normal shales. Major-element compositions of most of the analysed Napier Complex metapelites are compatible with metamorphism of mixtures of various proportions of, for example, Mg-rich chlorite, clay minerals (illite, kaolinite, smectite), and quartz. Trace-element contents of argillaceous sediments are generally considered to depend largely on those of the source rocks (Mosser, 1979); however, although the systematic differences in trace element

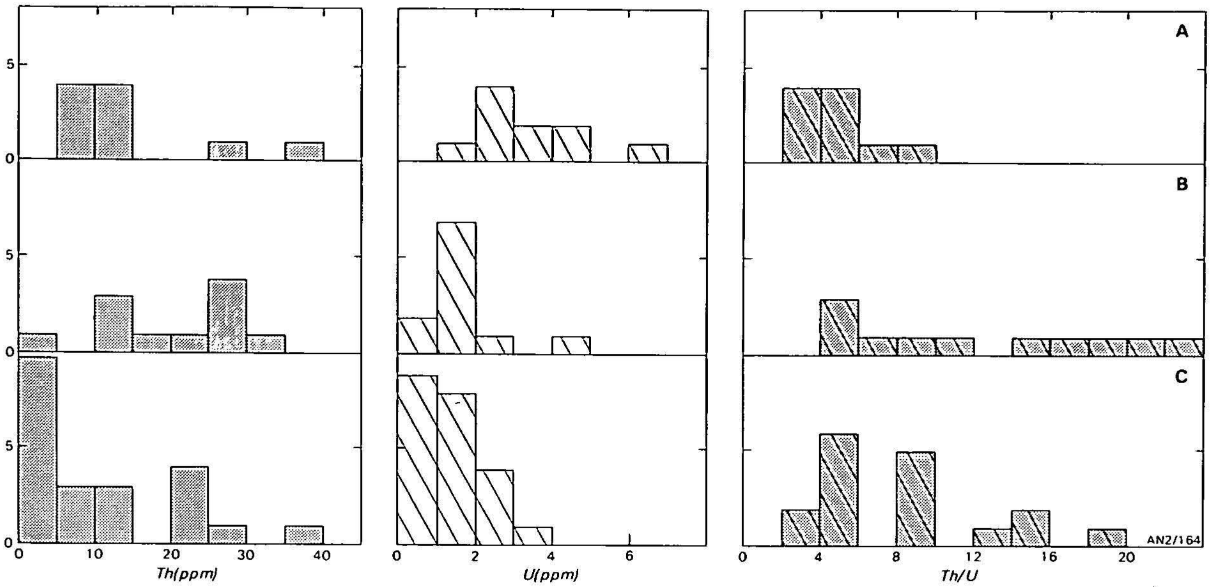

Figure 6. Frequency distributions of Th, U, and Th/U for Precambrian metapelites. A-C as in Figure 2.

contents between the low-Cr and high-Cr groups could be due to a higher proportion of mafic and ultramafic material in the source rocks of the latter, this would not explain the absence of compositions intermediate between the two groups. Cr is particularly resistant to leaching, being effectively fixed in residual weathering products, essentially clays (McLaughlin, 1955; Dennen & Anderson, 1962; Shiraki, 1978; Schmoll & Forstner, 1979), so that the Cr-poor rocks may well represent sediments rich in newly formed, as opposed to detrital, Mg-rich clays or chlorites. In other words, the observed combination of high MgO (relative to FeO) and low Cr may have developed by enrichment of Cr-poor pelitic sediments in Mg from percolating solutions during diagenesis.

The Cr-poor metapelites have some chemical affinities with, but are much less extreme in composition than, the highly aluminous and magnesian, commonly sapphirine-bearing granulites found in a number of high-grade terrains (Segnit, 1957; Wilson, 1971; Clifford & others, 1975; Lal & others, 1978). Sapphirine-enstatite(-spinel-phlogopite) granulites crop out at several places in Enderby Land and are inter-layered with more siliceous, Cr-poor metapelites at one locality. They are similarly characterised by very high MgO and low Cr, and generally have low V, Ni, and Cu (Table 3); mg values are exceptionally high, but SiO_2 relatively low (none contains quartz). Their bulk compositions approximate to that of magnesian chlorite, apart from low water contents.

Two main hypotheses have been proposed for the pre-metamorphic origin of such sapphirine-bearing granulites and chemically similar rock types (for example, cordierite-anthophyllite rocks), if, as is argued above, a restite origin is discounted: (1) low-temperature hydrous alteration of mafic igneous rocks (Vallance, 1967; Wilson, 1971), and (2) derivation from evaporitic mudstone or other magnesian pelites (Segnit, 1957; McKie, 1959; Ramsay & Davidson, 1974; Schreyer, 1977). Neither hypothesis is without problems in the case of the Antarctic metapelites. There is no clear field association with mafic or ultramafic igneous rocks, and the very low Cr and Ni contents of the metapelites are difficult to explain on the basis of a direct derivation from such rocks. However, Archaean low-Cr, sapphirine-bearing granulites are associated with Cr-rich pyroxenites in Western Australia, and are thought to have been formed by metamorphism of the products of low-temperature leaching of basic lavas (Wilson, 1971); they also show depletion in Ni, though not to the same extent as Cr (Table 3, analysis 4). Napier Complex metapelites are interlayered with a variety of gneisses of probable sedimentary origin (Sheraton & others, 1980), but there is no evidence for the presence of sediments indicative of an evaporitic environment. In fact, carbonate

	1	2	3	4
SiO_2	38.8	38.2	36.2	38.1
TiO_2	0.13	0.50	0.12	0.78
Al_2O_3	26.0	31.7	26.7	22.1
*FeO	1.25	0.60	1.73	9.09
MnO	0.04	0.02	0.03	0.07
MgO	32.7	26.7	24.6	25.0
CaO	0.08	0.10	0.06	0.35
Na_2O	0.10	0.12	0.27	0.25
K_2O	0.63	0.66	6.80	2.74
P_2O_5	n.d.	0.03	0.03	0.31
H_2O (tot)	0.28	0.69	1.29	0.67
Total	100.01	99.32	97.83	99.46
V	17	41	32	103
Cr	5	7	4	+
Ni	6	22	45	75
Cu	1	24	4	n.d.
mg	0.98	0.99	0.96	0.83

* Total Fe as FeO. n.d. Not detected.

Table 3. Composition of sapphirine-rich granulites.

1. Average of 2 phlogopite-spinel-sapphirine-enstatite granulites from xenolith in late Proterozoic Mawson Charnockite. Mawson base, MacRobertson Land (sample Nos. 73282051, 52).
2. Average of 2 phlogopite-spinel-sapphirine-enstatite granulites from the Napier Complex. Gage Ridge, Enderby Land (77284338, 43A).
3. Sapphirine-enstatite-phlogopite granulite. Gage Ridge, Enderby Land (77284340).
4. Average of 4 orthopyroxene-mica-sapphirine-spinel (-cordierite-apatite) granulites, South Quairading, Western Australia (from Wilson, 1971). + Cr values are n.d., n.d., 5, and 104 p.p.m.

and scapolite-bearing gneisses are conspicuously absent from the Napier Complex. The very low CaO content of the metapelites effectively precludes the original presence of calcite or dolomite in the sediments; magnesite is a possibility, but would, of course, imply complete removal of carbonate during metamorphism. Moreover, evaporites appear to be rare among Archaean rocks (Ronov, 1972), although their metamorphosed equivalents, commonly characterised by an abundance of scapolite, have been reported from a number of localities (Serdyuchenko, 1975). Nevertheless, the Cr-poor metapelites have some chemical features in common with evaporitic mudstones and their metamorphosed equivalents, namely, high mg values compared with typical pelites, and probably low Cr contents, although trace-element data for comparable evaporitic rocks are sparse (Table 2). Two of the least siliceous Cr-poor metapelites (Table 2, analyses 3 and 4) can be matched fairly closely with rocks considered to have been derived by metamorphism of evaporitic sediments (Table 2, analyses 5 and 6). Others have generally similar chemical features, except for higher SiO_2, implying greater amounts of quartz in the original sediments.

In summary, it is not possible to unequivocally identify the source rocks of the Cr-poor metapelites of the Napier Complex, except that sediments rich in magnesian clays, chlorites, or both, are probable. These could be evaporitic mudstones, hydrothermally altered mafic or ultramafic igneous rocks, or weathering products of the latter. The evaporitic mudstones are the least probable, in view of the complete lack of evidence for any other metamorphosed evaporitic rocks in the Napier Complex, and the weathered hydrothermally altered igneous rocks are the most probable. Mg-rich clays, such as sepiolite, can form both in evaporitic environments and by alteration of ultramafic rocks, although in the presence of significant amounts of Al, chlorite would be formed instead (Wollast & others, 1968; Weaver & Pollard, 1973; Stoessell & Hay, 1978). In any case, whatever the conditions of deposition of the original sediments, much of the Mg in them was probably ultimately derived by leaching or hydrothermal alteration of mafic to ultramafic igneous rocks.

Discussion and Conclusions

The considerably more magnesian character of the early Archaean compared with younger metapelites is thought to reflect, in part, a higher proportion of mafic to ultramafic rocks (presumably lavas) in the source material. Some of these metapelites differ in composition from typical shales not only in their particularly high mg values, but also in their very low Cr, Ni, Cu, and V contents; they probably originated either by direct metamorphism of hydrothermally altered mafic or ultramafic igneous rocks or more likely in view of their relatively siliceous compositions, by metamorphism of sediments derived by weathering of such rocks. The possibility of derivation from evaporitic mudstones cannot be entirely dismissed, but is militated against by the absence of associated rocks of clearly evaporitic origin. The relative abundance of sodic compositions (i.e., low k values) among Napier Complex metapelites may be due to the predominance of tonalitic to granodioritic types among felsic igneous rocks (or their metamorphosed equivalents) during the early Archaean.

Although the compositions of the Antarctic metapelites are considered to be essentially those of the original sediments, there is evidence for metamorphic depletion of Rb relative to K in the Napier Complex metapelites, and for depletion of U (and, of course, H_2O) in granulite-facies metapelites compared with those of amphibolite facies. Associated felsic gneisses show similar depletions (Sheraton, unpublished data). Tarney & Windley (1977) considered that two factors are important in determining lithophile element depletion during granulite-facies metamorphism, viz., the development of assemblages of minerals which do not hold K and Rb, and the presence of fluids capable of removing these elements. The highest grade Antarctic metapelites, from the Napier Complex, contain K-rich phases (K-feldspar and osumilite), so that loss of K during metamorphism was probably not significant; there may have been some separation of a granitic component during anatexis (Sighinolfi & Gorgoni, 1978), but field observations suggest that this is likely to have been minimal. One possibility is that loss of H_2O, Rb, and perhaps some K, accompanied biotite breakdown, as biotite commonly has low K/Rb ratios (Heier & Billings (1970) quote a range of 29-275). Biotite (and in a few cases muscovite) is abundant (20-40%) in the amphibolite-facies metapelites, less common (up to 10%) in the MacRobertson Land granulite-facies rocks, and absent from most of the Napier Complex metapelites. However, there is no apparent negative correlation of biotite content with K/Rb ratio in the MacRobertson Land metapelites, and, although many of those from the Napier Complex have high K/Rb, this does not necessarily imply a causal relationship.

Sapphirine + quartz appears to be restricted to early Archaean Napier Complex metapelites with mg greater than about 0.65 (more Fe-rich compositions contain abundant garnet, with or without spinel), although osumilite occurs in rocks with mg as low as 0.55 (Figs. 2, 3). In contrast, with few exceptions, the late Archaean and Proterozoic metapelites are more Fe-rich than this and would presumably therefore lie outside the stability fields of sapphirine and osumilite. Thus, in addition to the fact that temperaures as high as those recorded in the Napier Complex (900-950° C: Ellis & others, 1980; Sheraton & others, 1980) are apparently rarely reached during regional metamorphism, suitable Mg-rich compositions may also be relatively uncommon, although they are by no means unknown among post-Archaean rocks. The combination of a steep Archaean geothermal gradient with the unusual composition of early Archaean shales may account for the uniqueness (on a regional scale) of these assemblages, although they have been reported in rare cases of restricted extent from younger metamorphic terrains. It should be noted, however, that the presence of ferric iron would stabilise sapphirine + quartz to lower pressures and temperatures than would otherwise be the case. Napier Complex sapphirines are low in ferric iron (Ellis & others, 1980), but some of the other occurrences of coexisting sapphirine and quartz were apparently stabilised in this way (Caporuscio & Morse, 1978). Cr would have a similar effect, but cannot have been a critical factor in the Napier Complex, because some sapphirine-bearing metapelites contain very little Cr ($<$ 10 ppm), whereas others contain up to 1000 ppm (with up to 2.5% Cr_2O_3 in sapphirine: Ellis & others, 1980).

Acknowledgements

I thank B. I. Cruickshank, K. H. Ellingsen, G. R. Ewers, J. L. Fitzsimmonds, C. R. Madden, J. G. Pyke, and T. I. Slezak for chemical analyses, G. Warren for useful discussions, and J. Ferguson, A. Y. Glikson, A. D. Haldane, and R. J. Tingey for critically reading the manuscript. Logistic support in the field was provided by the Antarctic Division, Department of Science and the Environment.

References

APARICIO, A., BRÄNDLE, J. L., & BELLIDO, F., 1979—Chemical evolution in an old crustal area (Sistema Central Espanol). *Physics and Chemistry of the Earth*, **11**, 505-17.

BLACK, L. P., & JAMES, P. R., 1979—Preliminary isotopic ages from Enderby Land, Antarctica (abstract). *Journal of the Geological Society of Australia*, **26**, 266-7.

CAPORUSCIO, F. A., & MORSE, S. A., 1978—Occurrence of sapphirine plus quartz at Peekskill, New York. *American Journal of Science*, **278**, 1334-42.

CLIFFORD, T. N., STUMPFL, E. F., & MCIVER, J. R., 1975—A sapphirine-cordierite-bronzite-phlogopite paragenesis from Namaqualand, South Africa. *Mineralogical Magazine*, **40**, 347-56.

DENNEN, W. H., & ANDERSON, P. J., 1962—Chemical changes in incipient rock weathering. *Geological Society of America Bulletin*, **73**, 375-84.

ELLIS, D. J., SHERATON, J. W., ENGLAND, R. N., & DALLWITZ, W. B., 1980—Osumilite-sapphirine-quartz granulites from Enderby Land, Antarctica—mineral assemblages and reactions. *Contributions to Mineralogy and Petrology*, **72**, 123-43.

ENGEL, A. E. J., ITSON, S. P., ENGEL, C. G., STICKNEY, D. M., & CRAY, E. J., JR, 1974—Crustal evolution and global tectonics: a petrogenic view. *Geological Society of America Bulletin*, **85**, 843-58.

FAHRIG, W. F., & EADE, K. E., 1968—The chemical evolution of the Canadian Shield. *Canadian Journal of Earth Sciences*, **5**, 1247-52.

FROHLICH, F., 1960—Beitrag zur Geochemie des Chroms. *Geochimica et Cosmochimica Acta*, **20**, 215-40.

GLIKSON, A. Y., 1979—Early Precambrian tonalite-trondhjemite sialic nuclei. *Earth-Science Reviews*, **15**, 1-73.

GLIKSON, A. Y., & SHERATON, J. W., 1972—Early Precambrian trondhjemitic suites in Western Australia and northwest Scotland, and the geochemical evolution of shields. *Earth and Planetary Science Letters*, **17**, 227-42.

GOLDICH, S. S., 1973—Ages of Precambrian banded iron formations. *Economic Geology*, **68**, 1126-34.

HEIER, K. S., & BILLINGS, G. K., 1970—Rubidium abundance in rock-forming minerals. *In* WEDEPOHL, K. H. (editor)—HANDBOOK OF GEOCHEMISTRY. *Springer-Verlag, Berlin*, **II/4**, 37-D-1-4.

KALSBEEK, F., 1976—Metamorphism of Archaean rocks of West Greenland. *In* WINDLEY, B. F. (editor)—THE EARLY HISTORY OF THE EARTH. *Wiley, London*, 225-35.

KIMBERLEY, M. M., & DIMROTH, E., 1976—Basic similarity of Archaean to subsequent atmospheric and hydrospheric compositions as evidenced in the distributions of sedimentary carbon, sulphur, uranium and iron. *In* WINDLEY, B. F. (editor)—THE EARLY HISTORY OF THE EARTH. *Wiley, London*, 579-85.

LAL, R. K., ACKERMAN, D. D., SEIFERT, F., & HALDAR, S. K., 1978—Chemographic relationships in sapphirine-bearing rocks from Sonapahar, Assam, India. *Contributions to Mineralogy and Petrology*, **67**, 169-87.

LAMBERT, I. B., & HEIR, K. S., 1968—Geochemical investigations of deep-seated rocks in the Australian Shield. *Lithos*, **1**, 30-53.

MCKIE, D., 1959—Yoderite, a new hydrous magnesium iron alumino-silicate from Mautia Hill, Tanganyika. *Mineralogical Magazine*, **32**, 282-307.

MCLAUGHLIN, R. J. W., 1955—Geochemical changes due to weathering under varying climatic conditions. *Geochimica et Cosmochimica Acta*, **8**, 109-30.

MACPHERSON, H. G., 1958—A chemical and petrographic study of Pre-Cambrian sediments. *Geochimica et Cosmochimica Acta*, **14**, 73-92.

MOSSER, C., 1979—Eléments traces dans quelques argiles des altérations et des sediments. *Physics and Chemistry of the Earth*, **11**, 315-29.

NANZ, R. H. JR, 1953—Chemical composition of Pre-Cambrian slates, with notes on the geochemical evolution of lutites. *Journal of Geology*, **61**, 51-64.

NAQVI, S. M., 1978—Geochemistry of Archaean metasediments: evidence for prominent anorthosite-norite-troctolite (ANT) in the Archaean basaltic primordial crust. *In* WINDLEY, B. F., & NAQVI, S. M. (editors)—ARCHAEAN GEOCHEMISTRY. *Elsevier, Amsterdam*, 340-60.

RAMSAY, C. R., & DAVIDSON, L. R., 1974—Cordierite-anthophyllite rocks formed by isochemical regional metamorphism at Mary Kathleen, northwestern Queensland, Australia. *Proceedings of the Royal Society of Queensland*, **85**, 43-55.

ROGERS, J. J. W., 1978—Inferred composition of early Archaean crust and variation in crustal composition through time. *In* WINDLEY, B. F., & NAQVI, S. M. (editors)—ARCHAEAN GEOCHEMISTRY. *Elsevier, Amsterdam*, 25-39.

ROGERS, J. J. W., & MCKAY, S. M., 1972—Chemical evolution of geosynclinal material. *In* DOE, B. R., & SMITH, D. K. (editors)—STUDIES IN MINERALOGY AND PRECAMBRIAN GEOLOGY. *Geological Society of America Memoir* **135**, 3-28.

RONOV, A. B., 1972—Evolution of rock composition and geochemical processes in the sedimentary shell of the Earth. *Sedimentology*, **19**, 157-72.

SCHIDLOWSKI, M., 1976—Archaean atmosphere and evolution of the terrestrial oxygen budget. *In* WINDLEY, B. F. (editor)—THE EARLY HISTORY OF THE EARTH. *Wiley, London*, 525-35.

SCHMOLL, G., & FÖRSTNER, U., 1979—Chemical association of heavy metals in lacustrine sediments. I. Calcareous lake sediments from different climatic zones. *Neues Jahrbuch für Mineralogie Abhandlungen*, **135**, 190-208.

SCHREYER, W., 1977—Whiteschists: their compositions and pressure-temperature regimes based on experimental, field, and petrographic evidence. *Tectonophysics*, **43**, 127-44.

SCHWAB, F. L., 1978—Secular trends in the composition of sedimentary rock assemblages—Archaean through Phanerozoic time. *Geology*, **6**, 532-6.

SEGNIT, E. R., 1957—Sapphirine-bearing rocks from MacRobertson Land, Antarctica. *Mineralogical Magazine*, **31**, 690-7.

SERDYUCHENKO, D. P., 1975—Some Precambrian scapolite-bearing rocks evolved from evaporites. *Lithos*, **8**, 1-7.

SHAW, D. M., 1956—Geochemistry of pelitic rocks. Part III: major elements and general geochemistry. *Geological Society of America Bulletin*, **67**, 919-34.

SHERATON, J. W., in press—Origin of charnockitic rocks of MacRobertson Land. *In* CRADDOCK, C. (editor)—ANTARCTIC GEOSCIENCE. *University of Wisconson Press.*

SHERATON, J. W., & LABONNE, B., 1978—Petrology and geochemistry of acid igneous rocks of northeast Queensland. *Bureau of Mineral Resources, Australia, Bulletin* **169**.

SHERATON, J. W., OFFE, L. A., TINGEY, R. J., & ELLIS, D. J., 1980—Enderby Land, Antarctica—an unusual Precambrian high-grade metamorphic terrain. *Journal of the Geological Society of Australia*, **27**, 1-18.

SHERATON, J. W., SKINNER, A. C., & TARNEY, J., 1973—The geochemistry of the Scourian gneisses of the Assynt district. *In* PARK, R. G., & TARNEY, J. (editors)—THE EARLY PRECAMBRIAN OF SCOTLAND AND RELATED ROCKS OF GREENLAND. *University of Keele*, 13-30.

SHIRAKI, K., 1978—Chromium abundance in common sediments and sedimentary rock types. *In* WEDEPOHL, K. H. (editor)—HANDBOOK OF GEOCHEMISTRY. *Springer-Verlag, Berlin*, **II/3**, 24-K-1-7.

SIGHINOLFI, G. P., & GORGONI, C., 1978—Chemical evolution of high-grade metamorphic rocks—anatexis and remotion of material from granulite terrains. *Chemical Geology*, **22**, 157-76.

SMITH, J. V., 1979—Mineralogy of the planets: a voyage in space and time. *Mineralogical Magazine*, **43**, 1-89.

SOBOTOVICH, E. V., KAMENEV, E. N., KOMARISTYY, A. A., & RUDNIK, V. A., 1976—The oldest rocks of Antarctica (Enderby Land). *International Geology Review*, **18**, 371-88.

STOESSELL, R. K., & HAY, R. L., 1978—The geochemical origin of sepiolite and kerolite at Amboseli, Kenya. *Contributions to Mineralogy and Petrology*, **65**, 255-67.

TARNEY, J., 1976—Geochemistry of Archaean high-grade gneisses, with implications as to the origin and evolution of the Precambrian crust. *In* WINDLEY, B. F. (editor)—THE EARLY HISTORY OF THE EARTH. *Wiley, London*, 405-17.

TARNEY, J., SKINNER, A. C., & SHERATON, J. W., 1972—A geochemical comparison of major Archaean gneiss units from northwest Scotland and East Greenland. *24th International Geological Congress, Section* **1**, 162-74.

TARNEY, J., & WINDLEY, B. F., 1977—Chemistry, thermal gradients and evolution of the lower continental crust. *Journal of the Geological Society of London*, **134**, 153-72.

TAYLOR, S. R., 1966—The application of trace element data to problems in petrology. *Physics and Chemistry of the Earth*, **6**, 133-213.

TINGEY, R. J., in press—The geological evolution of the Prince Charles Mountains—an Antarctic Archaean cratonic block. *In* CRADDOCK, C. (editor)—ANTARCTIC GEOSCIENCE. *University of Wisconsin Press*.

VALLANCE, T. G., 1967—Mafic rock alteration and isochemical development of some cordierite-anthophyllite rocks. *Journal of Petrology*, **8**, 84-96.

VEIZER, J., 1979—Secular variations in chemical composition of sediments: a review. *Physics and Chemistry of the Earth*, **11**, 269-78.

WALKER, J. C. G., 1976—Implications for atmospheric evolution of the inhomogeneous accretion model of the origin of the Earth. *In* WINDLEY, B. F. (editor)—THE EARLY HISTORY OF THE EARTH. *Wiley, London*, 537-46.

WEAVER, C. E., & POLLARD, L. D., 1973—THE CHEMISTRY OF CLAY MINERALS. *Elsevier, Amsterdam*.

WEDEPOHL, K. H., 1978—HANDBOOK OF GEOCHEMISTRY, **II/1-3**. *Springer-Verlag, Berlin*.

WILSON, A. F., 1971—Some geochemical aspects of the sapphirine-bearing pyroxenites and related highly metamorphosed rocks from the Archaean ultramafic belt of south Quairading, Western Australia. *Geological Society of Australia Special Publication* **3**, 401-11.

WOLLAST, R., MACKENZIE, F. T., & BRICKER, O. P., 1968—Experimental precipitation and genesis of sepiolite at earth-surface conditions. *American Mineralogist*, **53**, 1645-62.

BMR Journal of Australian Geology & Geophysics, 5, 1980, 289-300

A regional review of the geological sources of magnetic and gravity anomaly fields in the Lachlan Fold Belt of NSW

B. W. Wyatt, A. N. Yeates, & D. H. Tucker[1]

Regional airborne magnetic and gravity data and field observations have been used to define four geophysical domains in the Lachlan Fold Belt of New South Wales. Each has a different pattern of anomaly trend and amplitude. Three domains correspond with provinces containing rocks of similar lithology and age; the other corresponds with the Darling Basin. The magnetic data highlight minor variation in magnetite abundance, chiefly in igneous rocks, and, across the region, reflect slight differences in magma composition, structural trends, and possibly also style of volcanism and sedimentation. The gravity data also delineate the same structural trends and some major lithological variations. The boundary of the Darling Basin is gradational. The other domain boundaries are sharp, but with no evidence of major faulting.

Within the geophysical domains a classification of magnetic anomalies by length, width, and amplitude appears capable of distinguishing between the various sources, thereby providing a useful mapping tool in regions with surficial cover. Circular anomalies of largest extent occur over granitoids, the smallest over small pipes and veins, and the intermediate size over basic and ultrabasic stocks. Elliptical anomalies are associated with magnetic granitoids and some basic and ultrabasic bodies. Sources of narrow anomalies include basic dykes, steeply tilted Palaeozoic lavas, ignimbrites, and serpentinites. Sources of complex zones include Tertiary basalt flows, piles of basic and intermediate lavas surrounding small intrusions, and some inhomogeneous granitoids.

The regional gravity data reflect features with very large dimensions or large density contrasts. A major north-northeast trending Bouguer anomaly low corresponds with the Eastern Highlands, a region of high relief, thick crust, and extensive granitoids. A narrower low corresponds to another belt of granitoids trending north-northwest from Holbrook to Cobar. Small-scale gravity features include the Coolac Serpentinite and its associated basic rocks, the Mid-Silurian to Mid-Devonian Hill End Trough, and numerous regions of Late Devonian quartzose sedimentary rocks.

Introduction

The Lachlan Fold Belt (Scheibner, 1974, 1976) in central and southeastern New South Wales (Fig. 1) is a region of Early and Middle Palaeozoic sedimentary and volcanic rocks, gently to mainly steeply dipping, and intruded by many granitoids (Brown & others, 1968; Packham, 1969).

A study of regional magnetic and gravity data was begun in March 1979. The data include total magnetic intensity contours from surveys flown mostly at 150 m above ground along east-west lines 1500 m apart (Gerula, 1979) and gravity measurements on a square grid with 11-km spacing (Anfiloff & others, 1976). Magnetic susceptibility and four-channel gamma-ray spectrometer measurements have been made at about 1000 representative localities throughout the region, from which rock samples were collected for laboratory measurement of magnetic properties, density, and porosity, and petrological studies.

The study has characterised the observed geophysical responses and attempted to relate these to the underlying rocks. It is hoped that a better understanding of the use of geophysical data in geological mapping and mineral exploration will be achieved as the project progresses.

Geology

The regional geology of the Lachlan Fold Belt has been reviewed by Brown & others (1968), Packham (1969), and Markham & Basden (1974). Accounts of the Devonian and Ordovician rocks of the region include those of Webby (1973 and 1976, respectively). Kemežys (1978) gave an account of the Ordovician and Silurian palaeogeography of the region.

Geological histories of some small regions in the Fold Belt include those of Owen & others (1976), Crook & others (1973), and Crook & Powell (1976) for the southeast of the region; Stanton (1955) and Cas (1978) for areas in the northeast; and Rayner (1969) for the Cobar region. Some granitoids in the region have been described by Chappell & White (1976), and Evans (1977) has described the Darling Basin.

Four major rock groups are present (Fig. 1): Ordovician marine sedimentary rocks, basaltic lavas, and tuffs; Silurian to Early Devonian mainly felsic tuffs, lavas, and mainly marine sedimentary rocks; Mid to Late Devonian non-marine and marine sedimentary rocks with less common lavas and tuffs; and granitoids. In some places the major stratigraphic divisions are conformable (e.g. Stanton, 1955), but more commonly they are unconformable (e.g. Crook & others, 1973; Rayner, 1969; Paterson, 1976). Powell & Edgecombe (1978) and Powell (pers. comm., 1979) have shown that orogeny and sedimentation in the northern Lachlan Fold Belt may be synchronous, at least in its later history, and that some of the observed unconformities are of local extent and due mainly to marginal tilting and faulting of nearby, intra Fold Belt, positive regions. The unconformities are, therefore, a result of the growth of volcanic rises throughout the region's 150 m.y. history.

Minor rock types in the Fold Belt include serpentinites, and other basic and ultrabasic rocks, as subcircular stocks, plutons, dykes, and pipes. Erosional outliers of sedimentary rocks belonging to younger geological provinces and basins surrounding the Fold

1. Present address: CRA Exploration, P.O. Box 444, Broken Hill, NSW.

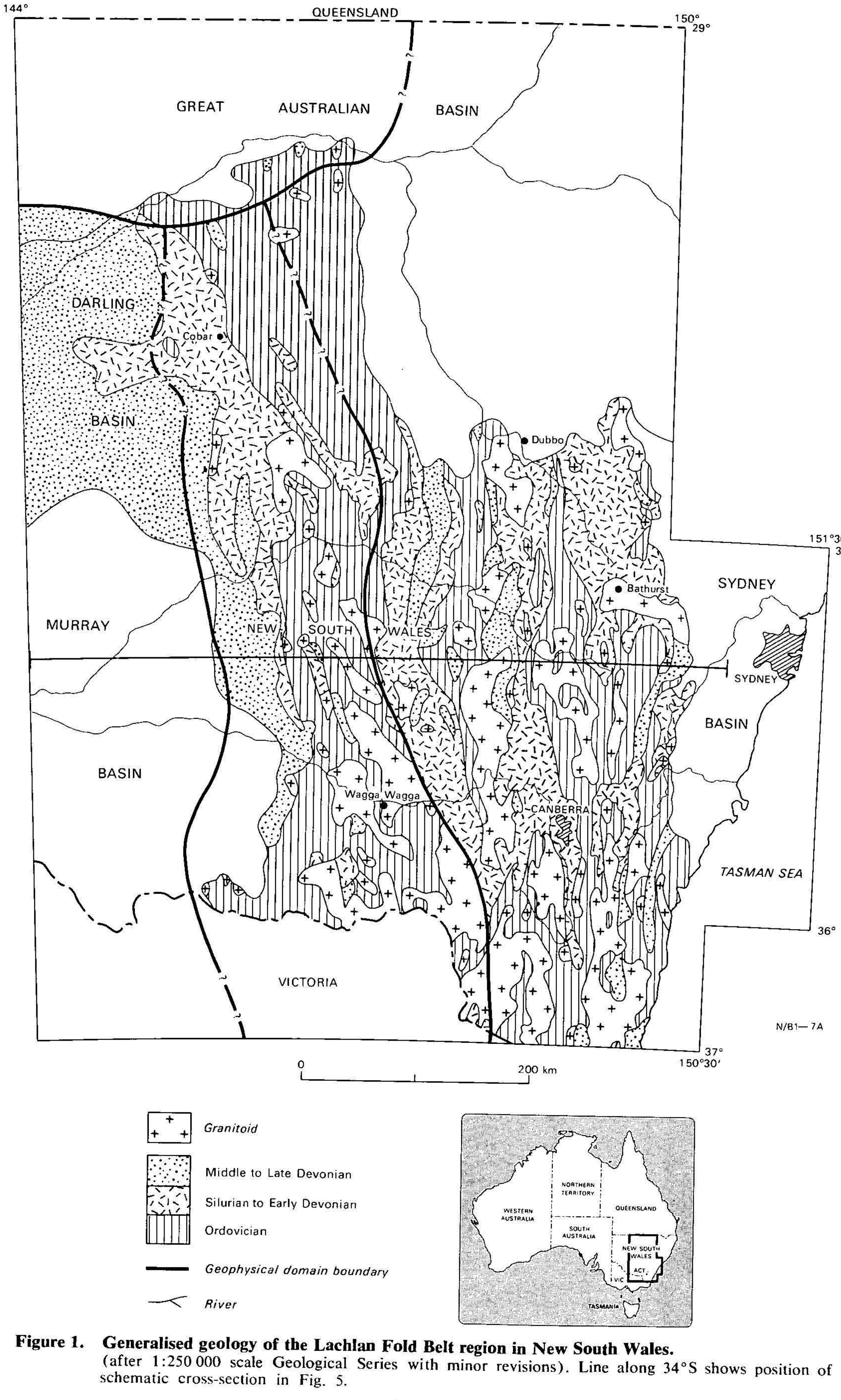

Figure 1. Generalised geology of the Lachlan Fold Belt region in New South Wales.
(after 1:250 000 scale Geological Series with minor revisions). Line along 34°S shows position of schematic cross-section in Fig. 5.

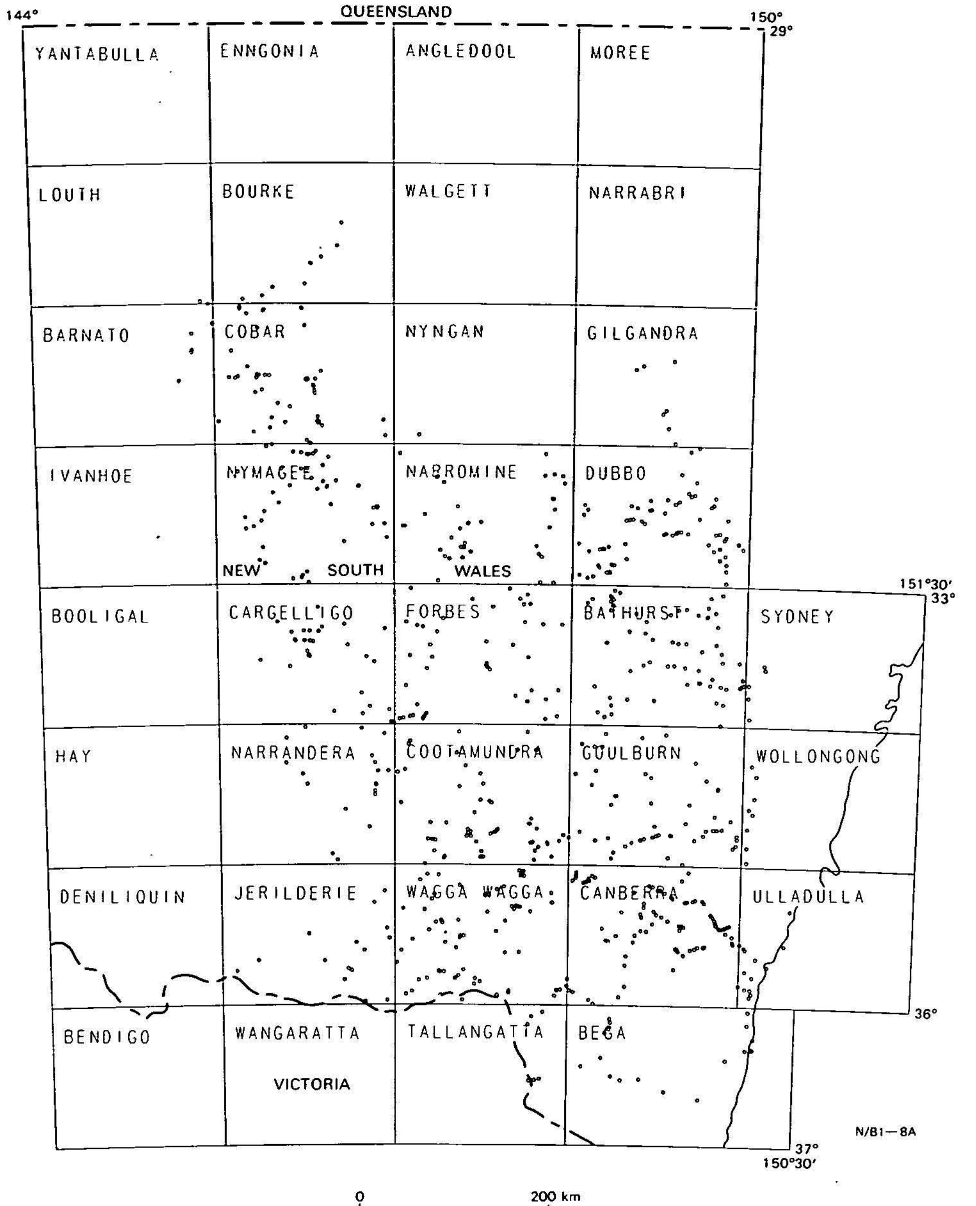

Figure 2. Locality map with sample locations. Reference to the 1:250 000 Sheet areas in the text appears in capital lettering.

Belt are also present, as are Permian and Mesozoic plutons, thin Cainozoic basalt flows, and their associated intrusions. Soil and thin surficial sediments cover much of the area, particularly in the west.

Magnetic zones and trends (Fig. 3)

A regional view of the magnetic field of the Lachlan Fold Belt has been compiled from BMR maps of total magnetic intensity. The quality of the data is variable, and differences in its appearance are the result of different instrument sensitivities, altitude, and flight line spacing for the various surveys. BMR surveys at 150 m ground clearance along lines 1.5 km apart have provided the most useful data.

In the east of the area as far north as 32°S, high-amplitude (200-500 nT) short-wavelength anomalies are common. Prominent trends of narrow and elliptical anomalies range from north-northwest to north-northeast. In the far northeast of the region, anomaly amplitudes and trends are largely obscured by the combined effects of survey and contouring parameters, the thick cover rocks of the Eromanga and Surat Basins, and the magnetic response of overlying Tertiary lavas.

Previous workers (Smith & others, 1974; Emerson, 1976) have analysed the trend directions of 850 magnetic anomalies, totalling 5690 km in length, from part of the Fold Belt. Their results indicate that trends are mostly distributed between 325° and 25°, with 41% of the total trend length distributed between 325° and 355° and 25% between 355° and 25°.

In the magnetic pattern, there is a major and abrupt change in anomaly amplitude across a roughly north-northwest line from southeast WAGGA WAGGA* to central BOURKE (Figs. 2 & 3). To the west, most short-wavelength anomalies are of low amplitude (50-100 nT) and the field appears fairly flat with the main disturbances being scattered 'bull's-eyes', and narrow anomalies with northwest to north-northwest trend.

*** Capitalised names refer to standard 1:250 000 map sheet areas.**

In the far west of the area the data quality is poor, but it appears that the only anomalies present are very broad, of amplitude 50-200 nT, and of north-northeast trend. These are probably due to sources at a depth of several hundred metres or more.

In the far northwest of the region the magnetic pattern is dominated by an arcuate southeast to north-east trending belt of narrow and complex anomalies of up to 500 nT amplitude.

Gravity zones and trends (Fig. 4)

The Bouguer anomaly field (Anfiloff & others, 1976) has been calculated using a reduction density of 2.67 t/m^3 and has been contoured at 50 μm/s^2. Bouguer anomaly amplitude ranges from -900 to $+700$ μm/s^2; individual features have widths between 20 and 180 km, and lengths between 80 and 1500 km.

The regional gravity field of Australia has been described in terms of gravity provinces and their subdivisions. These are characterised by uniformity of contour trend, gravity level, or degree of contour disturbance (Fraser, 1976; Fraser & others, 1977).

The gravity pattern in the eastern half of the area is dominated by very broad, regional north-northeast trends. The narrow gravity high along the coast, which reaches 650 μm/s^2 (Fig. 4), is attributed to the eastern edge of the Australia continent. G. D. Karner (personal communication) suggests that an Airy model with a depth of compensation of 32 km and a narrow continental margin lacking thick sediments can account

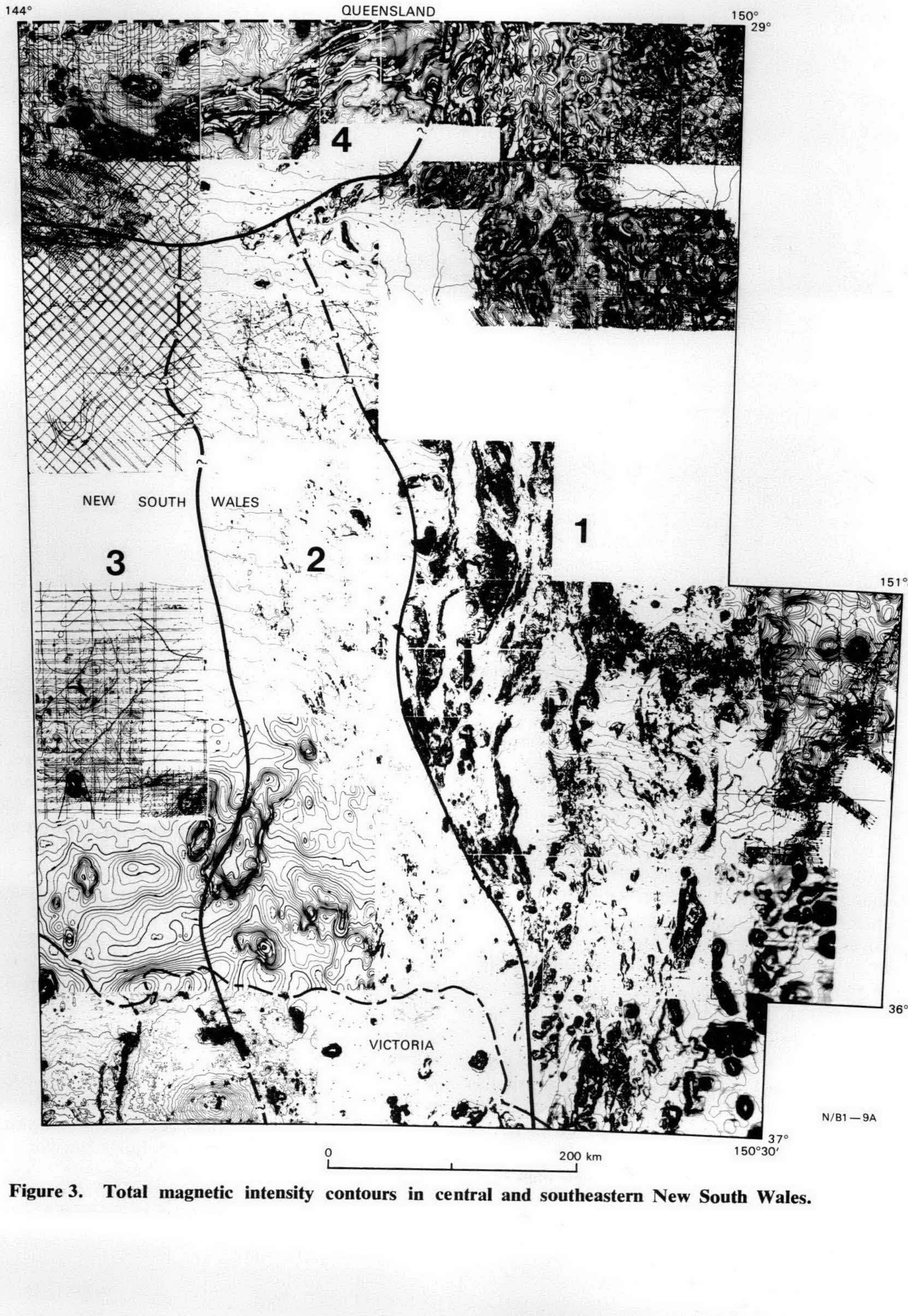

Figure 3. Total magnetic intensity contours in central and southeastern New South Wales.

for the feature. The major elliptical area of negative Bouguer anomaly which falls to -800 $\mu m/s^2$ corresponds to the Eastern Highlands, a region containing extensive granitoid plutons and with the crust thickening to about 50 km (Finlayson & others, 1979). This broad low is discordant with the provinces and subdivisions identified by Fraser & others (1977). Superimposed on the broad low and continuing across the centre of the area are strong north to northwest trending zones of high and low Bouguer anomalies, which parallel the strike of rock units, volcanic rises, major synclines, and graben. These zones constitute the Lachlan Regional Gravity Province of Fraser (1976). The most prominent, the Hume Gravity Trough falls to -550 $\mu m/s^2$ and coincides with the north-northwest trending belt of granitoids between Wagga Wagga and Cobar.

In the far west, and extending beyond the study area into the Murray and Darling Basins, the dominant trend direction is northeast. In the Darling Basin the

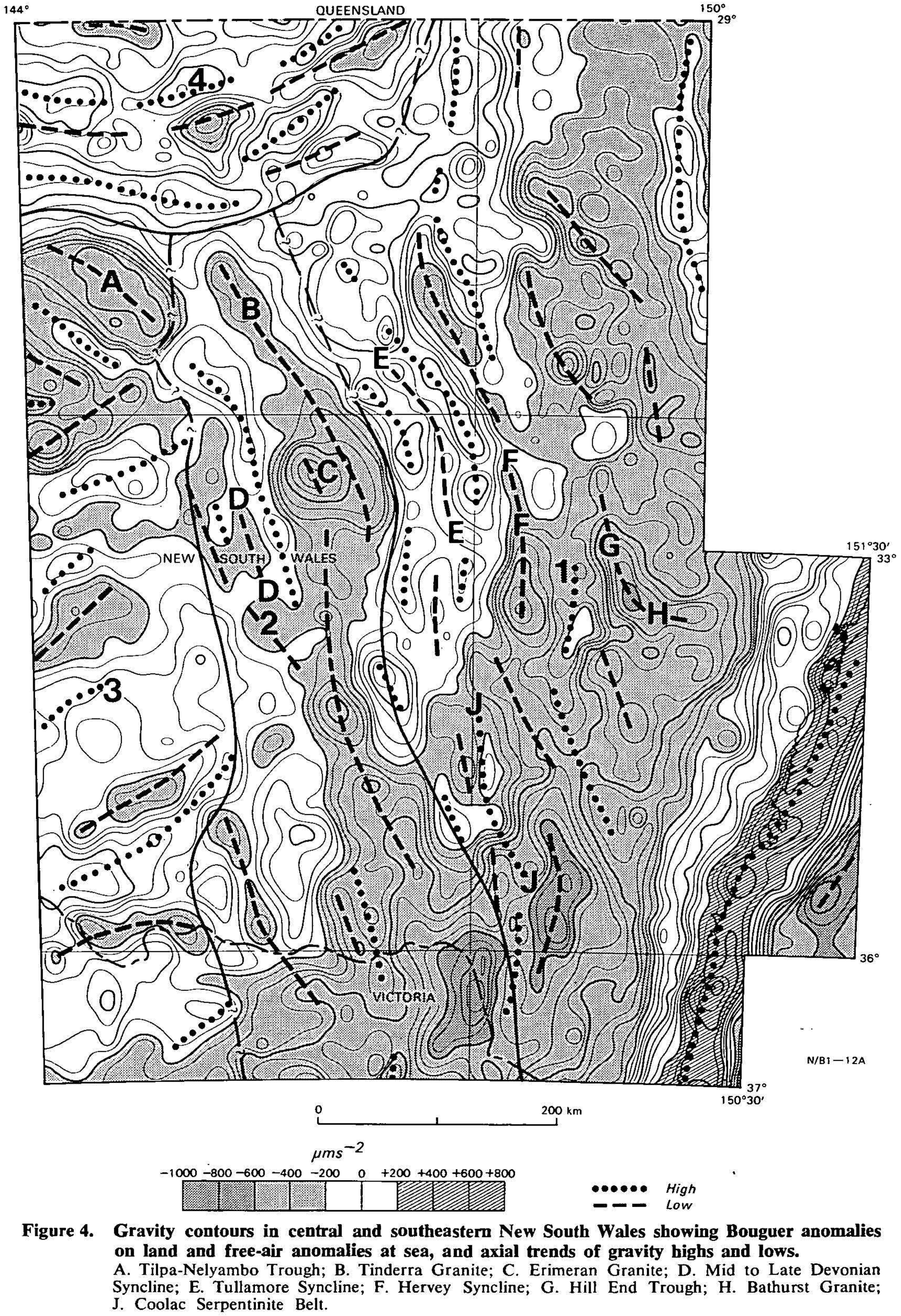

Figure 4. Gravity contours in central and southeastern New South Wales showing Bouguer anomalies on land and free-air anomalies at sea, and axial trends of gravity highs and lows.
A. Tilpa-Nelyambo Trough; B. Tinderra Granite; C. Erimeran Granite; D. Mid to Late Devonian Syncline; E. Tullamore Syncline; F. Hervey Syncline; G. Hill End Trough; H. Bathurst Granite; J. Coolac Serpentinite Belt.

Bouguer anomaly lows reflect the positions of Devonian graben containing several kilometres of sediments. More local northwest trends reflect boundaries of the Tilpa-Nelyambo Trough, Mount Jack High, and Lake Poopelloe Trough Complex, which Evans (1977, fig. 4) has designated.

In the far northwest of the area the Bourke Regional Gravity High (Fraser, 1976) is a province of broad arcuate highs and lows, which trend between east and northeast, and which truncate the north-northwest trends associated with the outcropping Lachlan Fold Belt rocks.

Geophysical domains

The magnetic and gravity data indicate four distinct geophysical domains with boundaries shown in Figures 1, 3 & 4. Between Domains 1 and 2 the boundary is sharp and best defined by an abrupt change in magnetic anomaly amplitude, although there is little change in gravity. The Domain 2/3 boundary is less well defined and mainly corresponds to the western limit of north to north-northwest trends in the gravity pattern of Domain 2 (Fig. 4). Further west, in Domain 3, the trends become northeast. The Domain 4 boundary is sharp and is defined by the change in trend directions in both magnetic and gravity fields.

Domain 1 is characterised by high amplitude (200-500 nT) magnetic anomalies; narrow and elliptical anomalies trend north-northwest to north-northeast. The gravity field shows a series of essentially parallel north to north-northwesterly anomalies, superimposed on the broad regional, north to northeast trends.

Domain 2 is characterised by isolated, low amplitude (50-100 nT) 'bull's-eye' and narrow magnetic anomalies trending northwest to north-northwest. The Bouguer anomaly pattern shows an essentially north-northwest trend, parallel to smaller anomalies in Domain 1.

The magnetic field in Domain 3 contains only a few broad anomalies of amplitude 50-200 nT. The gravity trend directions appear to be mainly northeast in contrast to the west-of-north trends in adjacent Domain 2.

Domain 4 is characterised by arcuate, east-west to northeast-trending high amplitude (200-500 nT) narrow, magnetic anomalies. This trend is also shown by 250 $\mu m/s^2$ gravity anomalies.

Nature of domain boundaries

In the Wagga Wagga region, the Domain 1/2 boundary coincides with the western edge of a Silurian to Early Devonian graben, the Tumut Trough and its northern continuation. North of about 33°S, the boundary does not coincide with the Trough, and the margins of numerous other graben to the east are not major geophysical boundaries. Equivalent time-stratigraphic sequences are present either side of the Domain 1/2 boundary, but cannot be matched in detail. The granites of each Domain differ, as well as the overall magnetic response and regional strike trends (Fig. 8). Whilst a near-vertical fault is present in the Wagga Wagga region, it was active for only part of the Fold Belt's history. The lack of detailed stratigraphic, magnetic and granitoid similarity, different regional strikes, and absence of major vertical faulting along the entire length of the boundary, imply a disjunction separating two distinct but adjacent rock provinces.

The eastern edge of Scheibner's (1976) 'Girilambone-Wagga Anticlinorial Zone' corresponds to the southern half of the Domain 1/2 boundary, but departs from it north of about 33°S. It is the only one of his 'anticlinorial zones' to have any correspondence to the geophysical domain boundaries recognised in this paper.

North of about 34°S, the Domain 2/3 boundary approximates the effective eastern edge of the Darling Basin, and the western limit of Silurian to Early Devonian volcanic and volcaniclastic rocks that are present in Domain 2.

The boundary of Domain 4 with Domains 1, 2 and 3 is not sufficiently exposed to describe with certainty. However, as the regional strike of units in Domains 1 and 2 is parallel to the trends of their respective elliptical and narrow magnetic anomalies, it is inferred the same situation could apply to the more easterly-trending magnetic anomalies in Domain 4. If so, then the southern boundary of Domain 4 would also be a disjunction against Domains 1 and 2, and therefore may be similar to the Domain 1/2 boundary.

Magnetic properties of rocks are often not related to factors used to classify rock types (Mutton & Shaw, 1979) or separate rock provinces from each other. This perhaps accounts for the imperfect correlation between the domain boundaries and previously designated structural boundaries.

Geological significance of domains

Most magnetic anomalies in Domains 1 and 2 coincide with igneous rocks (granitoid, ignimbrite, andesite, basalt, dolerite, gabbro, and ultrabasic rocks). The substantial difference in amplitude and density of anomalies between the two domains is evident in Figures 3 and 5. This difference is due to variation in magnetic susceptibility of granitoid plutons and variation in abundance of other igneous rocks.

Magnetic susceptibilities have been measured for most granitoid plutons in the area. The mean susceptibility from 133 outcrops in Domain 1 is 7600 $\times 10^{-6}$ SI units, whereas 61 outcrops in Domain 2 give a mean of only 170 $\times 10^{-6}$ SI units. The granitoids of Domain 2 are relatively leucocratic, lack hornblende and often contain muscovite. In contrast, those of Domain 1 vary from leucocratic to melanocratic, and many have conspicuous hornblende. The different magnetic characteristics could be due to differences in parent and residual magma types and crystallisation conditions.

The greater abundance of ignimbrite, andesite, and basalt in Domain 1 is related to the greater number and more complete development of volcanic rises formed during the evolution of the Lachlan Fold Belt in that region, and the tendency for shallowest marine and/or terrestrial volcanism to occur around the axis of greatest uplift (the Domain 1 region). However, in Domain 2 these rock types are far less frequent, and some of the rises here are flanked by great thicknesses of micaceous marine sedimentary rocks and comparatively uncommon volcanic rocks (e.g. Wagga Wagga and Cobar regions). It follows that the depth of water above the rises in these regions might have been too great in many places, to allow eruptions of the kind resulting in felsic tuffs and lavas to take place. The equivalent rocks in Domain 2 are the largely chloritic and aluminous metasedimentary rocks and chemical siliceous sediments of the Wagga Wagga and Cobar regions.

In Domain 3 the gravity and magnetic profiles are less disturbed than those over Domains 1 and 2 (e.g. Fig. 5). The flat gravity profile along this section coincides with an inferred, relatively uniform thickness of known Early to Late Devonian sedimentary rocks

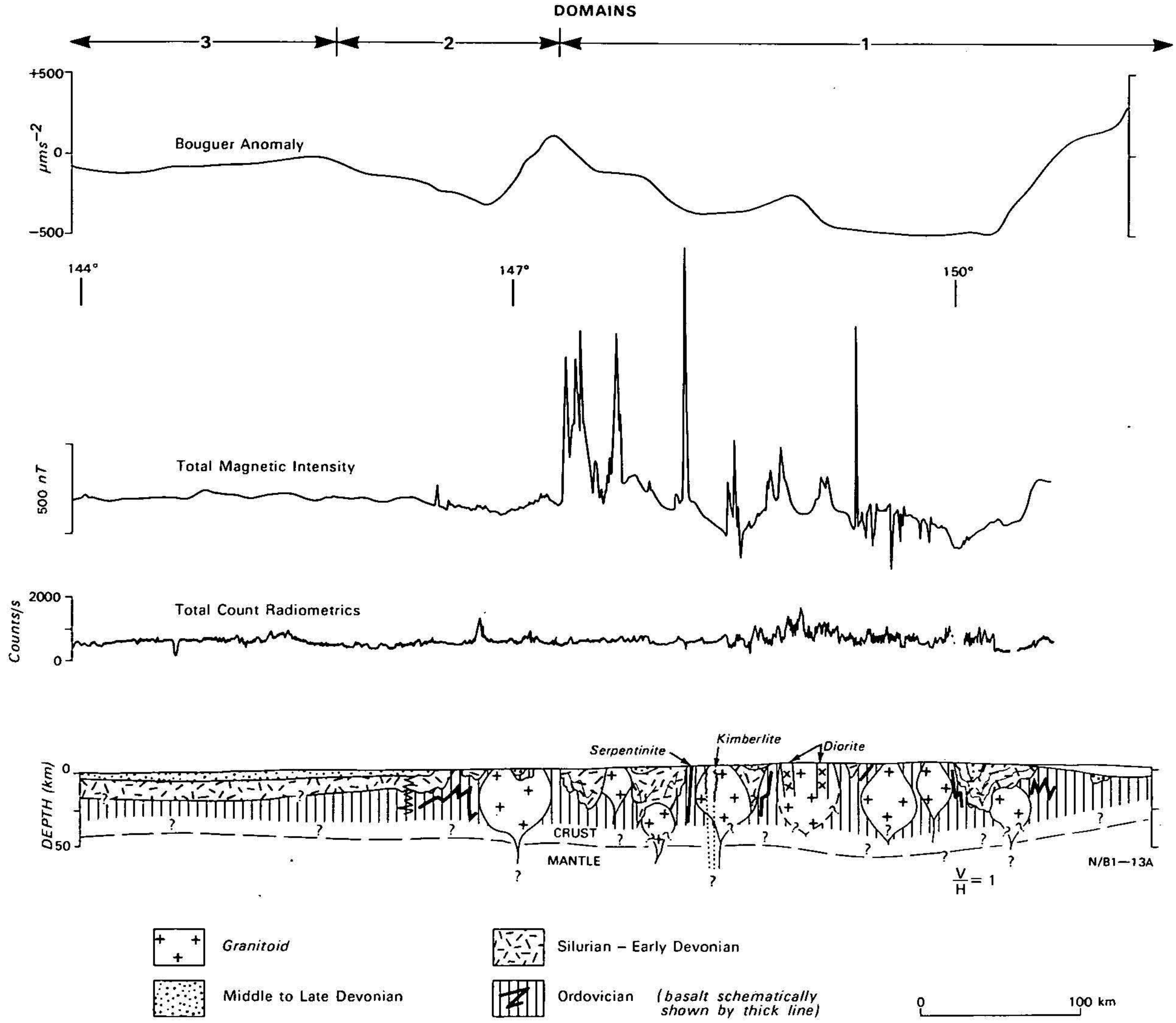

Figure 5. Schematic geological cross section and geophysical profiles across the Lachlan Fold Belt region in New South Wales.

of the Darling Basin, and in places, a much thinner cover of Tertiary sedimentary rocks of the Murray Basin (Fig. 1). Evans (1977) has noted that a thick sedimentary section is present beneath known Devonian rocks in Domain 3, north of about 34°S and west of the study region. This section is inferred here to include possible Silurian and Ordovician rocks (Fig. 5) which may have been deposited in a subsiding region between the emergent, stable, Broken Hill-Tibooburra regions in far west New South Wales, and positive areas in Domain 2.

Cropping out Early Devonian rocks in Domain 3 are non-volcanic marine shales, which grade laterally eastward into volcaniclastic sediments (Brunker, 1973, fig. 2) and volcanic rocks of Domain 2. This gradation is exposed in northwest NYMAGEE and southwest COBAR where rocks characteristic of each domain are interbedded, and where nearby outcrops of them have the same strike and dip. North of about 34°S, the flat magnetic and gravity profiles (e.g. Fig. 5) provide no evidence for volcanic rises west of Domain 2. We therefore infer that any Silurian and Ordovician rocks in this part of the Domain 3 region may also grade laterally into their Domain 2 equivalents in the same way as the Early Devonian rocks do.

West of the study region, northeast-trending grabens with several kilometre thicknesses of Devonian sedimentary rocks are present. They directly coincide with similar-trending gravity and magnetic lows (Bembrick, 1974; Thornton, 1976; Evans, 1977). A northwest trending gravity low in southern LOUTH and northern BARNATO coincides exactly with outcrops of low density Devonian quartzose sedimentary rocks mapped in the compilations of Loudon & others (1965) and Rose (1965) within a sub-basin of the Darling Basin known as the Tilpa-Nelyambo Trough (Evans, 1977).

Granodiorite has been intersected 400 m below the surface beneath Tertiary sediments of the Murray Basin in Bundy No. 1 well (central north DENILIQUIN), a considerable distance to the south (Shiels, 1962). This well, which was also sited on a gravity low, indicates that the Darling Basin does not continue into Victoria beneath the Murray Basin, in the study region. Instead, the rocks beneath the Basin south of about 34°S in Domain 3 may be subsurface extensions northwards of Early to Mid Palaeozoic sedimentary and volcanic rocks and granitoids which crop out south of the study region, in central Victoria.

Most of the Domain 4 Palaeozoic rocks are concealed beneath younger subhorizontal sedimentary rocks of the Eromanga and Surat Basins. The few scattered outcrops of granitoids and slate at its southern edge, together with drill hole data described by Offenberg (1968) in ANGLEDOOL, Graham (1972) in DIRRANBANDI (Queensland), and Murdoch (1969, 1970), as well as subsurface data shown in the compilation of Johnson & Menzies (1965) all in southern ENNGONIA, suggest the geophysical responses are caused by Early to Mid Palaeozoic rocks. The magnetic responses in Domain 4 most likely arise from volcanic piles, and clusters of moderately-sized plutons. The gravity lows may coincide with weakly magnetic to non-magnetic granitoids.

Geological associations with geophysical data

Magnetic data

The amplitude and ratio of length to width (both at half-amplitude points) of magnetic anomalies at 150 metres above ground level provide a simple means of classifying the anomalies of the region into groups which correlate broadly with lithology. Those anomalies with a length to width ratio between one and two are described as circular, between two and five as elliptical, and greater than five as narrow. Areas where one or more of these anomaly classes occur together are described as complex. Examples of anomalies belonging to various classes are shown in Figure 6. Lithological association, amplitude, and geometric character of selected anomalies from Domains 1 and 2 are compared in Figure 7. The location, lithology, and susceptibility of the sources of the anomalies shown in

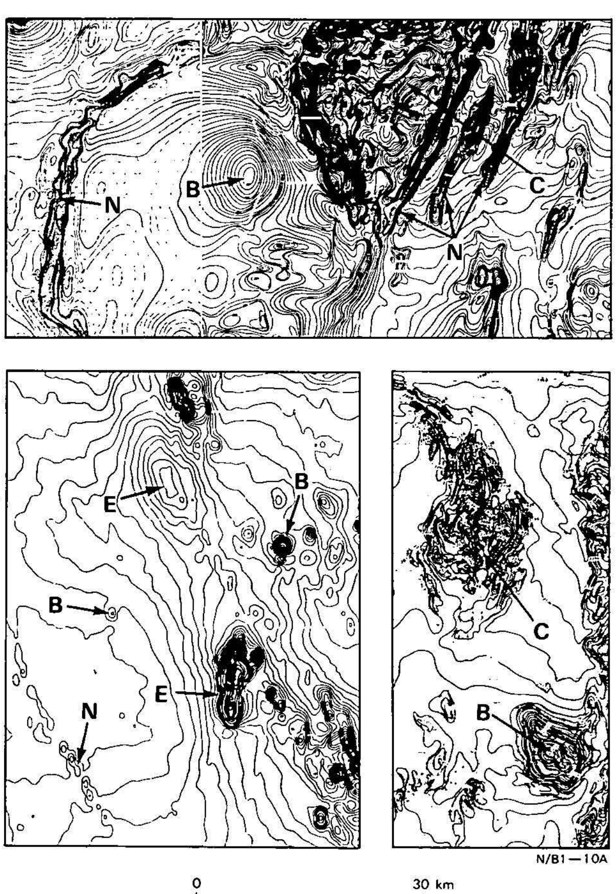

Figure 6. Examples of magnetic anomaly classifications by shape: B = 'Bull'seye' or Circular, E = Elliptical, N = Narrow, and C = Complex.

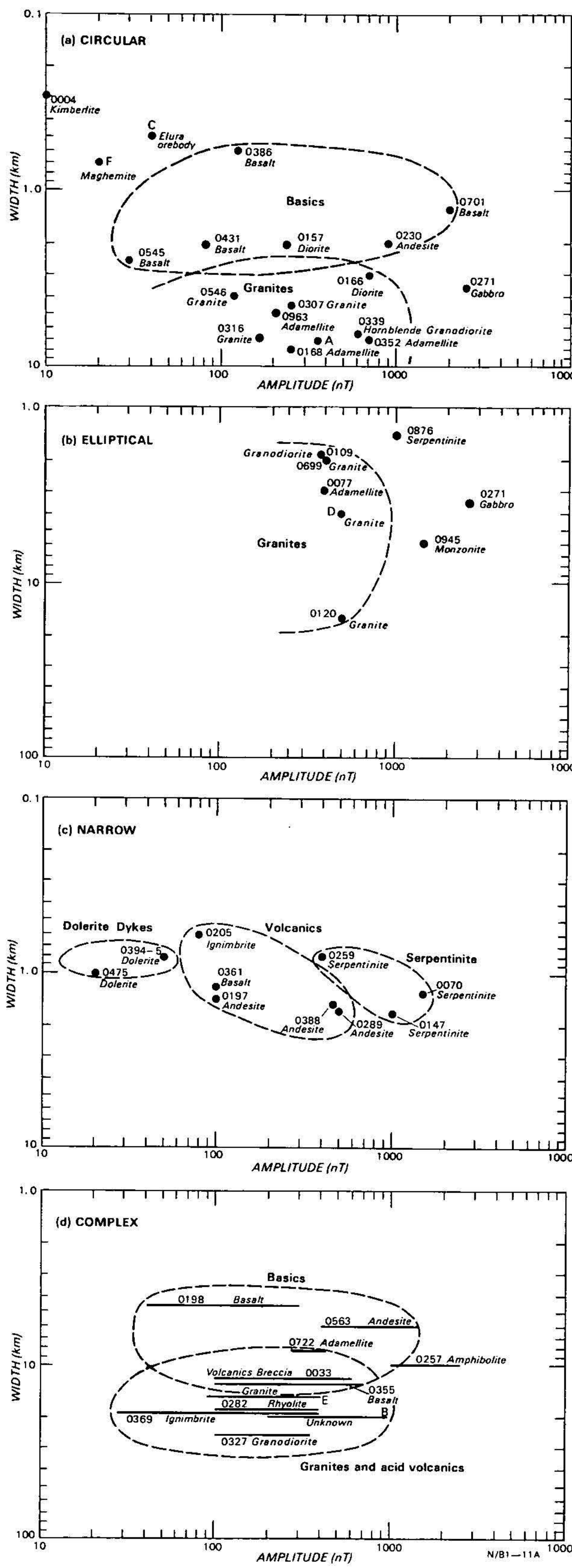

Figure 7. Amplitude and width characteristics of selected (a) circular, (b) elliptical, (c) narrow, and (d) complex magnetic anomalies, measured at 150 metres above ground level.

Dashed lines indicate broad lithological groupings. The location and measured susceptibilities of these sources is given in Table 1.

Figure 7 are tabulated in Table 1. Although some overlap occurs in the lithology fields of Figure 7, there is obvious correlation between broad lithology and magnetic anomaly characteristics for magnetic rocks. Hence, this classification may be broadly used to indicate the lithology of the non-outcropping sources of magnetic anomalies. Because of steep tilting, folding and erosion, the upper surfaces of most magnetic sources are covered only by a relatively thin veneer of sediments. However, both anomaly amplitude and length-to-width ratio will decrease with increasing depth below plane of observations.

Circular anomalies (Fig. 7a) range in size from the minimum width (250 m) expected for shallow essentially point sources, up to 20 km. Such anomalies appear to result from two distinct source models. The first can be approximated as a shallow vertical cylinder and produces anomalies where the body's horizontal extent is delineated by the narrow subcircular region of steep gradient. Anomalies of this type with amplitudes between 100 and 1000 nT and from 3 to 10 km across are mostly associated with granitoid plutons, while those with amplitudes between 30 and 2000 nT, and from 0.4 to 3 km wide, are generally associated with some Palaeozoic basic volcanic centres, and isolated Cainozoic basalt plugs. The source of the second type of circular anomaly can be approximated by the pole or dipole model which produces a characteristic 'bull's-eye' pattern with equispaced contours. Very small 'bull's-eye' anomalies with amplitudes in the range 10 to 100 nT and widths commonly less than 500 m, are detected only if a flight line passes close to the source. The regional data have insufficient resolution to enable interpretation of the geometry of their sources, or distinction between possible sources, which include kimberlite pipes, magnetite veins, maghemite concentrations, and pyrrhotite-bearing orebodies. Slightly larger 'bull's-eye' anomalies are associated with individual basic and ultrabasic stocks with widths of a few kilometres, such as those in central-west NARROMINE. 'Bull's-eye' anomalies of 5 to 20 km width may be due to similarly shaped basic and ultrabasic bodies at several kilometres depth or to granitoids with hemispherical upper surfaces at relatively shallow depth (Fig. 6 top).

Elliptical anomalies (Fig. 7b) are frequently caused by magnetic granitoids and have amplitudes in the range 200 to 600 nT and widths of 2 to 5 km; an

Locality or Anomaly	*Latitude*	*Longitude*	*In situ magnetic susceptibility (SI × 10^{-6})* *Mean*	*No.*	*Range*	*S.D.*	*Domain*	*Lithology*
79620004	34.839	148.310	21854	15	3116-60569	15894	1	Kimberlite
0033	35.077	148.083	28668	11	21362-37573	4350	1	Volcanic breccia
0070	34.837	148.188	33381	14	15456-81681	17941	1	Serpentinite
0077	35.077	148.563	40322	4	35814-49008	6119	1	Granite
0109	34.870	149.947	12597	6	7539-17404	3697	1	Granodiorite
0120	35.405	149.785	41749	13	36442-48443	3923	1	Granite
0147	34.052	148.135	34567	5	29028-38201	3380	1	Serpentinite
0157	34.628	147.686	6770	8	5026- 8293	1319	1	Diorite
0166	34.351	147.735	805	14	502- 1193	220	1	Diorite
0168	34.202	147.528	289	10	0- 1130	406	1	Adamellite
0197	33.316	146.917	9424	1			2	Andesite
0198	33.517	146.758	13899	9	9550-16776	2355	2	(Tertiary) basalt
0205	32.432	146.469	1822	1			2	Ignimbrite
0230	30.883	145.995	42449	15	14451-86896	18679	2	Andesite
0257	31.831	146.909	15945	9	9676-28023	5788	1	Amphibolite
0259	31.939	146.926	23951	15	11309-45490	10740	2	Serpentinite
0271	32.756	147.382	58974	13	44736-95881	12399	1	Gabbro
0282	32.985	148.343	4754	15	3141- 7414	1232	1	Rhyolite
0289	33.141	148.092	40258	15	29907-45176	4597	1	Andesite
0307	33.169	149.413	6769	15	4838-11058	1544	1	Biotite adamellite
0316	33.397	149.365	6668	15	5654- 7791	562	1	Granite
0327	33.463	149.619	14803	15	12252-16776	1279	1	Porphyritic granodiorite
0339	33.726	149.830	23578	15	19603-29342	2492	1	Hornblende granodiorite
0352	34.672	149.898	27356	15	23184-29091	1724	1	Adamellite
0355	34.442	149.784	10325	15	4523-15456	2981	1	(Tertiary) olivine basalt
0361	34.369	149.205	5642	145	3832- 8922	1384	1	(Tertiary) basalt
0369	34.324	148.729	5244	15	565-27394	7448	1	Ignimbrite
0386	34.827	148.416	627	13	0- 2199	720	1	(Tertiary) basalt
0388	34.741	148.223	4569	15	188-13006	4871	1	Andesite
0395	34.951	147.420	14451	6	6911-23750	5843	2	Dolerite
0431	35.623	148.074	28936	14	25283-35499	3109	2	(Tertiary) basalt
0475	33.402	146.161	9477	15	1130-22971	6018	2	Dolerite
0545	30.710	146.306	14880	15	5026-35964	8373	2	(Tertiary) leucitite
0546	30.667	146.398	726	15	0- 691	204	1	Granite
0563	33.565	147.781	20977	15	7791-36191	9077	1	Andesite
0699	32.623	149.291	9173	15	2010-15582	4449	1	Granite
0701	32.810	149.751	5497	12	1633-11812	2947	1	(Tertiary) basalt
0722	32.457	149.150	15934	15	12189-18975	1667	1	Adamellite
0876	35.892	148.407	90402	15	37196-129810	27112	1	Serpentinite
0945	36.309	150.076	45074	13	10807-57805	15509	1	Monzonite
0963	36.197	148.838	11686	15	7665-15707	2083	1	Adamellite
A	33.21	147.80						Unknown lithology
B	33.75	147.40						Not exposed
C*	31.135	145.673	25000		up to 43000			Massive sulphide (Elura)
D	35.925	149.25						Granite
E	35.60	148.65						Granite
F*	Area A from Wilkes (1979)				10000-50000			Maghemite

* data from Wilkes (1979).

Table 1. Locality, lithology and magnetic susceptibility of samples used in Figure 8.

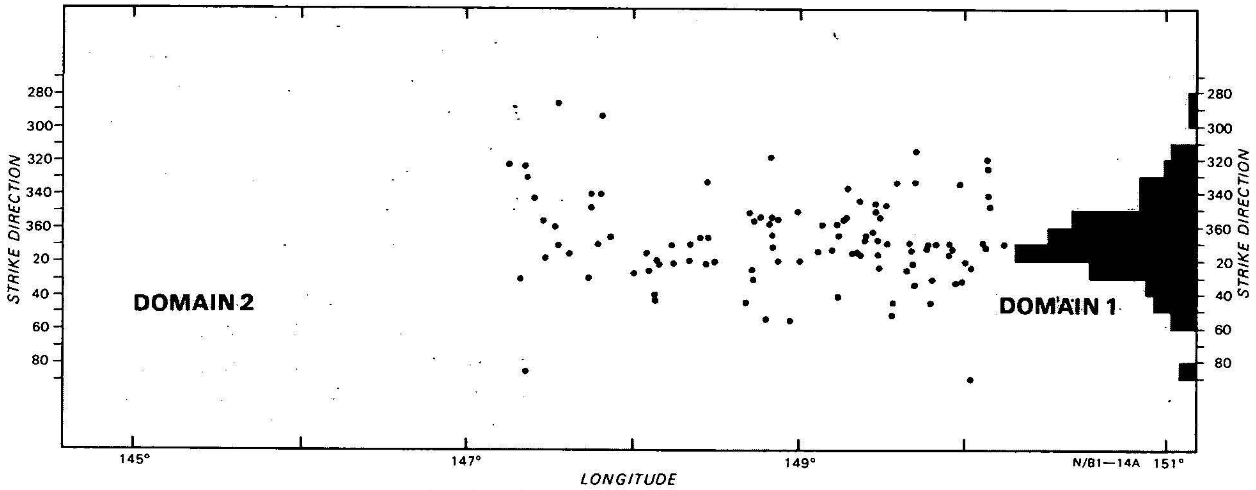

Figure 8. Variation in measured strike directions in Domains 1 and 2.

exception is the anomaly associated with the Braidwood Granodiorite, which is 16 km wide.

Narrow anomalies (Fig. 7c) are all less than 2 km wide and their amplitudes are generally indicative of their sources. The amplitude differences are the result of the basic dykes being generally thinner than the mainly steeply tilted volcanic units of the stratigraphy (though having a similar magnetic susceptibility) and to the serpentinites having a much greater susceptibility than the volcanic rocks (Table 1).

Complex anomalies (Fig. 7d) can arise from a single magnetic source of complex shape, an inhomogeneously magnetised single source, or a number of discrete magnetic sources close together. An example of the first kind is observed over Tertiary basalt flows, where the shape is partly the result of pre-existing topography and subsequent erosion (e.g. eastern GOULBURN). The large inhomogeneous Bathurst Granite (eastern BATHURST), which may be a cluster of adjacent plutons, is an example of the second type. The third kind commonly comprises both linear and circular anomalies of various amplitudes. Many of these could be resolved into separate anomalies (and their associated model sources) by the acquisition of more data at low altitude and with closer line spacing. Examples are the magnetic lavas surrounding small intrusive plutons in northeast FORBES, and the steeply tilted andesitic lava pile flanking a former andesite cone intruded by small dolerite dykes in central FORBES. It is inferred that similar lithologies may be the cause of the southward continuation of this pattern beneath soil, and also of the large complex anomaly in central-southwest FORBES, for which outcrop is sparse.

Gravity data

For a body to be adequately defined by the regional gravity map it must have sufficient thickness (several hundred metres) and density contrast with the adjacent rock units, and be of sufficient extent to be adequately sampled by the 11 km grid.

The Hume Gravity Trough of Fraser (1976) and the major Bouguer anomaly low over the Eastern Highlands both correspond to areas of extensive granitoid plutons. However, correlation between individual plutons and local gravity lows does not exist except for the Erimeran (eastern NYMAGEE), Tinderra (COBAR), and Bathurst Granites. The source of the major areas of Bouguer anomaly low must be attributed to increased crustal thickness and possibly to regional, lateral density variations within the crust.

Anomalies due to smaller scale features of high density contrast include an elliptical positive anomaly which reaches 17 $\mu m/s^2$ and coincides with the Coolac Serpentinite and its nearby basic igneous rocks in COOTAMUNDRA and northeast WAGGA WAGGA. Other small anomalies coincide with thick sequences of Late Devonian quartzose sandstone present in synclines and graben. They have associated negative anomalies, some of which fall to -400 $\mu m/s^2$. Examples are: the Tullamore Syncline, central NARROMINE continuing south into FORBES; the Hervey Syncline, southeastern NARROMINE; an unnamed syncline in southwest NYMAGEE; and the Tilpa-Nelyambo Trough in south LOUTH and north BARNATO. The Siluro-Devonian Hill End Trough in south DUBBO also has an associated broad negative anomaly (Fig. 4).

Conclusions

Magnetic anomalies in the area can be classified according to their dimensions into 'bull's-eye' and circular, elliptical, narrow, and complex types. 'Bull's-eye' and circular magnetic anomalies of largest extent are associated with granitoids; the smallest may be associated with kimberlites, magnetite veins, and magnetic sulphide deposits and the intermediate size with basic and ultrabasic stocks. Elliptical anomalies are associated with magnetic granitoids and some ultrabasic bodies. Sources of narrow anomalies include basic dykes, steeply tilted Palaeozoic lavas and ignimbrites, and serpentinites. Sources of complex zones include Tertiary basalt flows, piles of basic lavas surrounding small intrusions, and some inhomogenous granitoids.

The regional gravity data (Fig. 4) reflect features with very large dimensions or large density contrasts. The narrow positive anomaly along the coast is attributed to the eastern edge of the Australian continent. A major elliptical, north-northeast trending, negative anomaly corresponds with the Eastern Highlands, a region containing extensive granitoid plutons. A narrow negative anomaly in the west corresponds to another belt of granites trending north-northwest from the Holbrook to the Cobar areas. Small-scale gravity features include: the Coolac Serpentinite and its associated basic rocks; the Hill End Trough; and numerous regions and graben of Mid to Late Devonian quartzose sedimentary rocks.

The magnetic and gravity pattern and trends in the region indicate four distinct geophysical domains.

Between Domains 1 and 2 the boundary is sharp and defined by an abrupt change in magnetic anomaly abundance and amplitude. The Domain 2/3 boundary is less well defined and mainly corresponds to the western limit of north to north-northwest trends in the gravity pattern. North of about 34°S it coincides with the effective eastern edge of the Darling Basin. South of here it may separate Domain 2 from possible extensions of Early to Mid-Palaeozoic rocks cropping out in central Victoria, and which are possibly concealed beneath Tertiary sedimentary rocks of the Murray Basin in the study region. The Domain 4 boundary is sharp and defined by a change in the trend directions of both the magnetic and gravity fields. However, the rocks producing anomalies in Domain 4 are mainly concealed beneath the Great Australian Basin.

Most magnetic anomalies are directly attributable to magnetite in granitoids, ignimbrites, andesites, basalts, dolerites, gabbros and ultrabasic rocks. The regional strike in Domain 1 is northerly. Similar rock types are present in Domain 2, but they are less frequent, and the acid rocks are only weakly magnetic, if at all. The regional strike in Domain 2 is northwesterly. Thus the stratigraphy and granitoids of Domains 1 and 2 differ in detail. Small differences in lithology and trends of each are the result of minor variations in their geological histories. However, minor variations in magnetite content result in considerable changes in the magnetic response, and thus often highlight some geological processes or provinces more obviously than conventional, regional, time-stratigraphic geological mapping does.

The Lachlan Fold Belt in NSW should not be regarded as a single province or geosyncline, but as a cluster of three rock provinces and an adjoining Basin containing similar rock systems. The differences between them are the result of minor variations in the geological histories of each domain. Apart from the Domain 2/3 boundary, which is gradational, the other boundaries are sharp, but not faults along which great displacements have occurred.

Acknowledgements

The manuscript has benefitted from the constructive comments of D. C. Stuart, G. E. Wilford, G. M. Brown, M. Owen, J. F. Truswell, and R. S. Abell and from discussions with M. Owen, C. McA. Powell, K. A. W. Crook, R. McLeod, D. Wyborn, and J. I. McIntyre.

References

ANFILOFF, W., BARLOW, B. C., MURRAY, A., DENHAM, D., & SANDFORD, R., 1976—Compilation and production of the 1976 1:5 000 000 Gravity Map of Australia. *BMR Journal of Australian Geology & Geophysics* **1**(4), 273-6.

BEMBRICK, C. S., 1974—Murray Basin. *In* MARKHAM, N. L., & BASDEN, H. (editors) 1974—THE MINERAL DEPOSITS OF NEW SOUTH WALES. *Geological Survey of New South Wales, Sydney*, 557-68.

BROWN, D. A., CAMPBELL, K. S. W., & CROOK, K. A. W., 1968—The Geological Evolution of Australia and New Zealand. *Pergamon Press, Oxford.*

BRUNKER, R. L., 1973—Nymagee, NSW—1:250 000 Geological Series. *Geological Survey of New South Wales, Explanatory Notes* **SI55-2**.

CAS, R. A. F., 1978—Basin characteristics of the Early Devonian part of the Hill End Trough, New South Wales, based on a stratigraphic analysis of the Merrions Tuff. *Journal of the Geological Society of Australia*, **24**(7), 381-401.

CHAPPELL, B. W., & WHITE, A. J. R., 1976—Plutonic rocks of the Lachlan Mobile Zone. *25th International Geological Congress. Excursion Guide* **13C**.

CROOK, K. A. W., BEIN, J., HUGHES, R. J., & SCOTT, P. A., 1973—Ordovician and Silurian history of the southeastern part of the Lachlan Geosyncline. *Journal of the Geological Society of Australia*, **20**(2), 113-43.

CROOK, K. A. W., & POWELL, C., MCA., 1976—The evotion of the southeastern part of the Tasman Geosyncline. *25th International Geological Congress, Excursion Guide* **17A**.

EMERSON, D. W., 1976—Magnetic anomaly trends in the Yilgarn Block, Western Australia. *Australian Society of Exploration Geophysicists Bulletin*, **7**(3), 96-102.

EVANS, P. R., 1977—Petroleum geology of western New South Wales. *The APEA Journal*, **17**(1), 42-9.

FINLAYSON, D. M., PRODEHL, C., & COLLINS, C. D. N., 1979—Explosion seismic profiles, and implications for crustal evolution, in southeastern Australia. *BMR Journal of Australian Geology & Geophysics* **4**(3), 243-52.

FRASER, A. R., 1976—Gravity provinces and their nomenclature. *BMR Journal of Australian Geology & Geophysics*, **1**(4), 350-2.

FRASER, A. R., DARBY, F., & VALE, K. R., 1977—The reconnaissance gravity survey of Australia: a qualitative analysis of results. *Bureau of Mineral Resources, Australia, Report* **198**; *BMR Microform* **MF15**.

GERULA, W. J. (compiler) 1979—Catalogue of airborne magnetic and radiometric surveys up to December 1977. *Bureau of Mineral Resources, Australia, Report* **204**; *BMR Microform* **MF78**.

GRAHAM, B., 1972—Dirranbandi, Queensland—1:250 000 Geological Series. *Bureau of Mineral Resources, Australia, Explanatory Notes* **SH/55-3**.

JOHNSON, I. R., & MENZIES, I. A., 1965—Enngonia, NSW—1:250 000 Geological Series Sheet SH55-6. *Geological Survey of New South Wales, Sydney.*

KEMEŽYS, K. J., 1978—Ordovician and Silurian lithofacies and base-metal deposits of the Lachlan Fold Belt. *Journal of the Geological Socoiety of Australia* **25**(2), 97-107.

LOUDON, A. G., MENZIES, I. A., & WALLIS, G. R., 1965—Louth, NSW—1:250 000 Geological Sheet SH55-9. *Geological Survey of New South Wales, Sydney.*

MARKHAM, N. L., & BASDEN, H. (editors) 1974—THE MINERAL DEPOSITS OF NEW SOUTH WALES. *Geological Survey of New South Wales, Sydney.*

MURDOCH, R., 1969—Bourke reconnaissance magnetic survey. *Analytical Exploration of Australia Pty Ltd., Sydney, Report* **30**. *Geological Survey of New South Wales File Number* **GS69/583**.

MURDOCH, R., 1970—Bourke E. L. A. Field Survey No. 1. *Analytical Exploration of Australia Pty Ltd. Geological Survey of New South Wales File Number* **69/583**.

MUTTON, A. J., & SHAW, R. D., 1979—Physical property measurements as an aid to magnetic interpretation in basement terrains. *Australian Society of Exploration Geophysicists Bulletin* **10**(1), 79-91.

OFFENBERG, A. C., 1968—Angledool, NSW—1:250 000 Geological Series. *Geological Survey of New South Wales, Explanatory Notes* **SH55-7**.

OWEN, M., GARDNER, D. E., WYBORN, D., SALTET, J., & SHACKLETON, M. S., 1976—Geology of the Tantangara and Brindabella 1:100 000 Sheet areas. *Bureau of Mineral Resources, Australia, Record* **1974/176** (unpublished).

PACKHAM, G. H., 1969 (editor)—The Geology of New South Wales. *Journal of the Geological Society of Australia* **16**(1), 73-226.

PATERSON, R., 1976—Ardlethan Tin Mine *in* GILLIGAN, L. B., MARKHAM, N. L., & SUPPEL, D. W. (editors), 1976—Ore deposits of the Lachlan Fold Belt New South Wales. *25th International Geological Congress, Excursion Guide* **15C**, 36-45.

POWELL, C. MCA., & EDGECOMBE, D. R., 1978—Mid-Devonian movements in the northeastern Lachlan Fold Belt. *Journal of the Geological Society of Australia* **25**(3), 165-84.

RAYNER, E. O., 1969—The copper ores of the Cobar region, New South Wales. *Geological Survey of New South Wales Memoir* **10**.

ROSE, G., 1965—Barnato, NSW—1:250 000 Geological Series Sheet SH55-13. *Geological Survey of New South Wales, Sydney*.

SCHEIBNER, E., 1974—Definition and review of structural elements. *In* MARKHAM, N. L., & BASDEN, H. (editors)—THE MINERAL DEPOSITS OF NEW SOUTH WALES. *Geological Survey of New South Wales, Sydney*, 108-113.

SCHEIBNER, E., 1976—Explanatory Notes on the Tectonic Map of New South Wales, 1:1 000 000 scale. *Geological Survey of New South Wales, Sydney*, 103-9.

SHIELS, O. G., 1962—Completion Report Bundy No. 1 Well. *Report for Woodside (Lake Entrance) Oil Company N.L.* (unpublished).

SMITH, M. J., EMERSON, D. W., & MCSHARRY, P. J., 1974—A regional aeromagnetic analysis of part of the Lachlan Geosyncline, New South Wales. *Geoexploration* **12** (2/3), 196.

STANTON, R. L., 1955—Lower Palaeozoic mineralisation near Bathurst, New South Wales. *Economic Geology* **50**(7), 681-714.

THORNTON, R. C. N., 1976—Murray Basin and associated infrabasins. *In* LESLIE, R. B., EVANS, H. J., & KNIGHT, C. L. (editors)—ECONOMIC GEOLOGY OF AUSTRALIA AND PAPUA NEW GUINEA. 3. PETROLEUM. *Australasian Institute of Mining and Metallurgy, Monograph* **7**, 91-4.

WEBBY, B. D., 1973—Devonian geological history of the Lachlan Geosyncline. *Journal of the Geological Society of Australia*, **19**(1), 99-123.

WEBBY, B. D., 1976—The Ordovician system in southeastern Australia. *In* BASSETT, M. G. (editor)—THE ORDOVICIAN SYSTEM. *University of Wales Press and National Museum of Wales, Cardiff*, 417-46.

WILKES, P. G., 1979—Characteristics of magnetic sources and guidelines for exploration in the Cobar Area NSW. *Australian Society of Exploration Geophysicists Bulletin*, **10**(1), 34-41.

BMR Journal of Australian Geology & Geophysics, 5, 1980, 301-304

Precambrian hydrocarbons in the McArthur Basin, NT

M. D. Muir[1], K. J. Armstrong, & M. J. Jackson

An oily liquid and several types of bitumen were found in the silicified porous carbonate-rich Looking Glass Formation, in a BMR stratigraphic hole drilled in the Proterozoic McArthur Basin in 1979. The bitumen is accompanied by sulphides (including pyrite, chalcopyrite, and marcasite), and has been trapped beneath a thin claystone which is present at the unconformity at the base of the Balbirini Dolomite. It is thought to be a residue from oil generated lower in the McArthur Group or in the Tawallah Group and then trapped in the Beetle Spring Anticline. Proterozoic strata as old as the McArthur Group (ca. 1600 m.y.) should not be overlooked in the search for hydrocarbons in Australia.

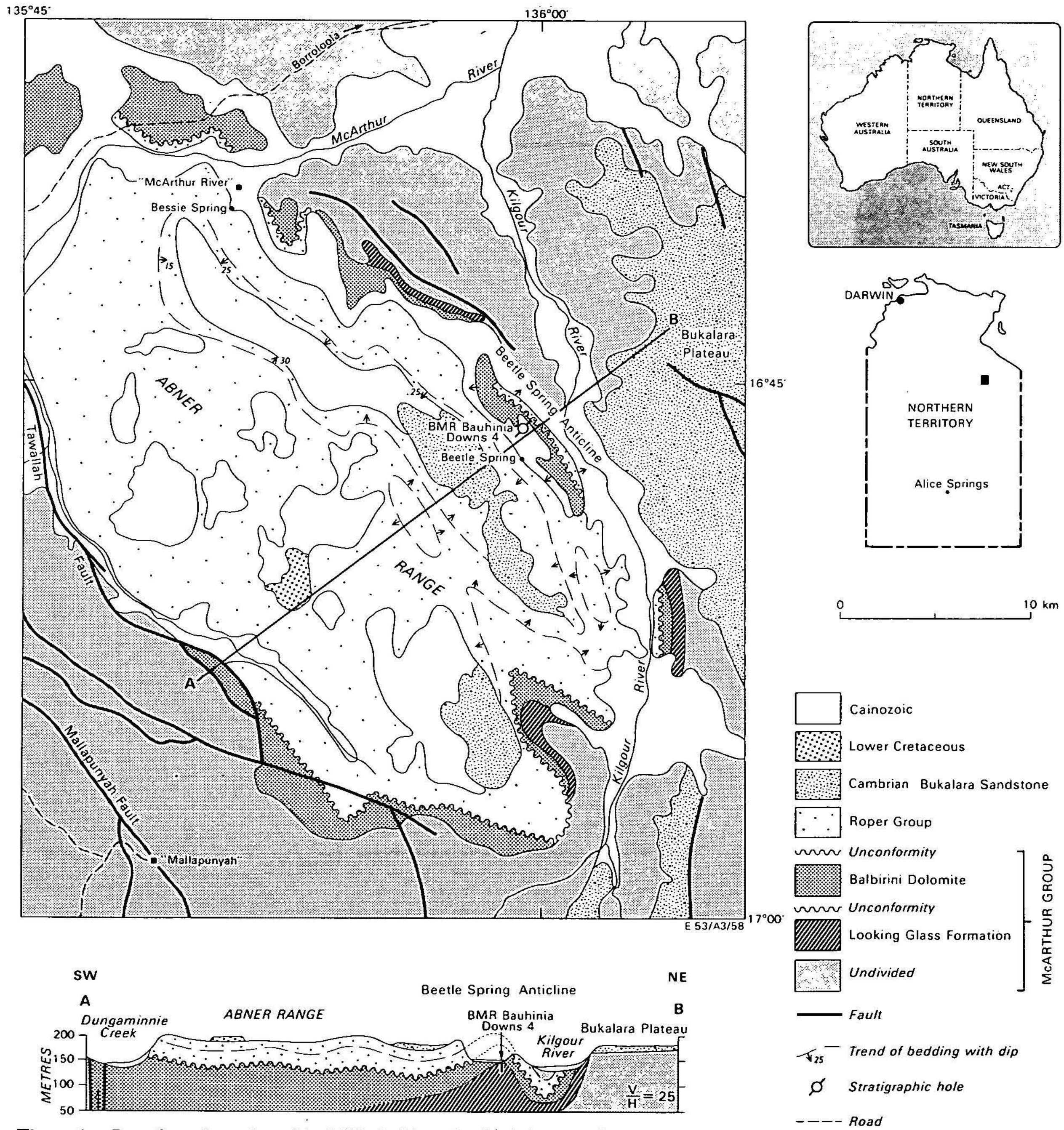

Figure 1. Location of stratigraphic drillhole BMR Bauhinia Downs 4.

1. **Present address: C.R.A. Exploration Pty Ltd, P.O. Box 656, Fyshwick, A.C.T. 2609.**

Introduction

BMR Bauhinia Downs 4 stratigraphic hole, drilled north of Beetle Springs in the southern part of the McArthur Basin (Fig. 1) in 1979, was designed to test the nature of the unconformity between the Balbirini Dolomite and the underlying Looking Glass Formation (Fig. 2), and to provide lithological information on the two units, as they are generally very poorly exposed.

Lithology

In the area of the drillsite the lower sandy beds of the Balbirini Dolomite (equivalent to the Smythe Sandstone and Mount Birch Sandstone in areas to the north and west) are exposed, but the Looking Glass Formation is not. In outcrop to the north the Looking Glass Formation is invariably strongly silicified and commonly vuggy and porous.

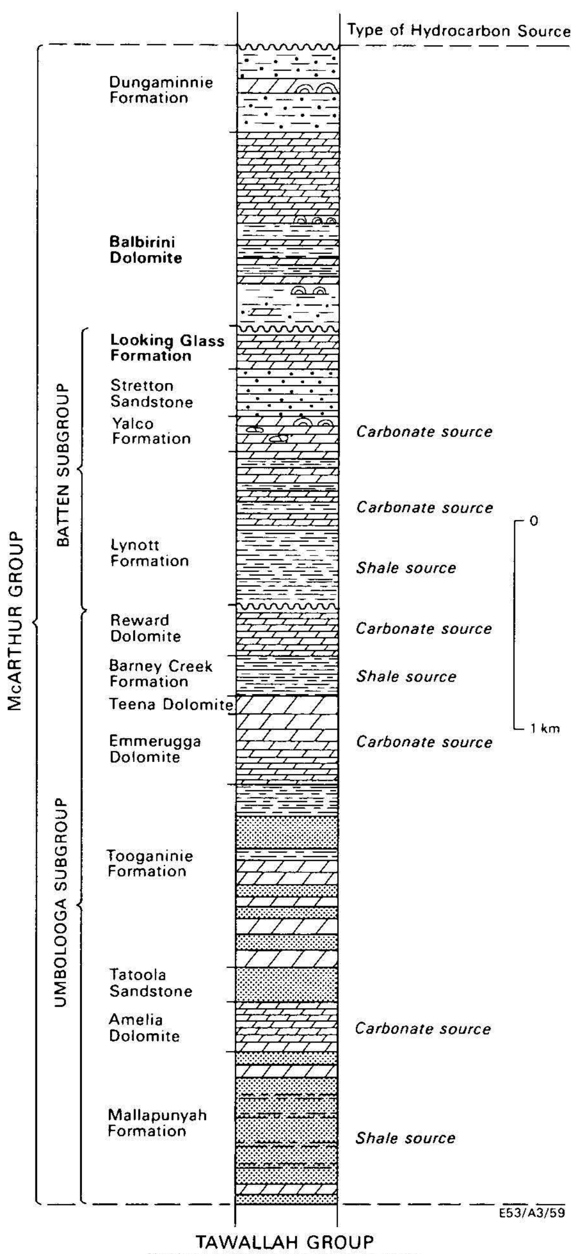

Figure 2. Stratigraphy of the McArthur Group.

In Bauhinia Downs 4 (Fig. 3), the contact between the two formations is placed at a depth of 12.83 m, where the change from mainly sandy Balbirini Dolomite to underlying carbonates of the Looking Glass Formation is marked by 35 cm of claystone. The claystone could represent a soil below the unconformity or a basal unit of the Balbirini Dolomite.

Most of the Looking Glass Formation is a very porous and vuggy siliceous rock that has been extensively stylolitised and brecciated. Prior to silicification, the sediments were obviously carbonate, and stromatolites and intraclast conglomerates are common. Fine-grained, laminated rocks, showing signs of early lithification, in situ brecciation, and the formation of teepee structures, are also present. Various amounts of quartz sand are present in some beds, and slightly phosphatic, non-silicified carbonate occurs near the bottom of the hole.

The vuggy porosity post-dates the primary sedimentary structures, and is similar to the secondary porosity formed in limestones in the vadose zone (Friedman, 1975). Some crusts in void spaces resemble those formed by capillary water movement in a calcrete (Read, 1976) and, on some breccia fragments, snow-on-roof texture* indicates deposition in open space. The degree of silicification decreases with depth, suggesting a genetic relationship to the unconformity at the top of the formation.

The most significant feature of the drillhole, however, is the occurrence throughout the Looking Glass Formation of sulphides, bitumen, and oily liquid.

Occurrence of oily material

The core below the unconformity contains sulphides (mainly pyrite and chalcopyrite) and oily material, both solid (bitumen) and liquid, evenly distributed throughout. Under fluorescence testing, the complete section through the Looking Glass Formation fluoresced; the overlying Balbirini Dolomite did not. Several different forms of oily material have been distinguished on the basis of their mode of occurrence.

Bitumen 1. The most obviously oily matter (but not most abundant) occurs as bitumen globules up to 4 mm in diameter in vugs (Fig. 4a). These are shiny and black on the outside, but are dark brown and crumbly when freshly broken. Similar material is abundant in microfaults and stylolites, and it also coats joint and fracture surfaces. This bitumen appears to be intimately related to the sulphide minerals. In some occurrences a layer of pyrite coats the bitumen and separates it from the substrate (vug wall, microfault, or stylolite). In other occurrences, fine-grained pyrite is disseminated through the bitumen.

Bitumen 2. The most common form of bitumen, volumetrically, is present as an intergranular pore filling. Under the binocular microscope it resembles the globular bitumen, but, owing to its mode of occurrence, little can be deduced without detailed study.

Bitumen 3. A few vugs contain a form of bitumen which is black, hard, and shiny, and breaks with a conchoidal fracture. Although grossly similar to 1 and 2, this bitumen is soluble in trichloroethylene, whereas the others are not.

*** Snow-on-roof texture results from precipitation, from descending solutions, of minerals on the upper surfaces of rock fragments in open spaces.**

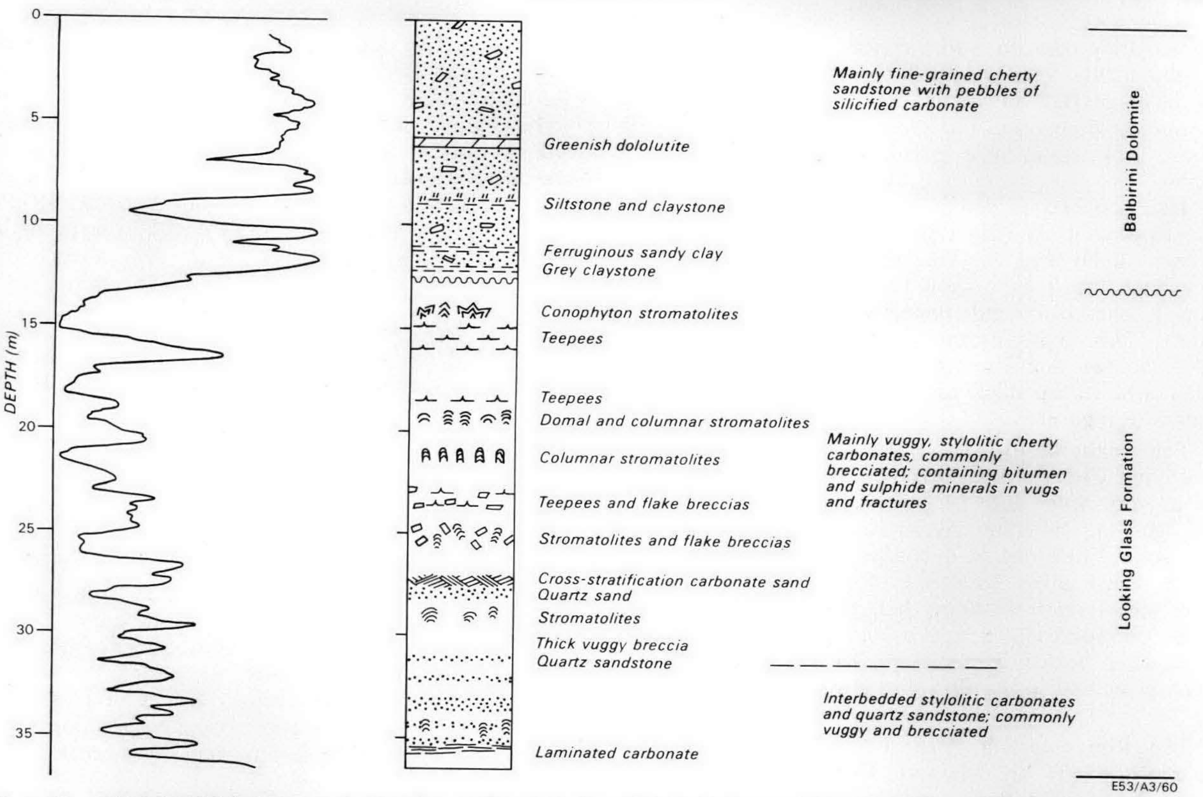

Figure 3. BMR Bauhinia Downs 4, showing radiometric log, lithologic log, and interpreted pre-silicification lithology.

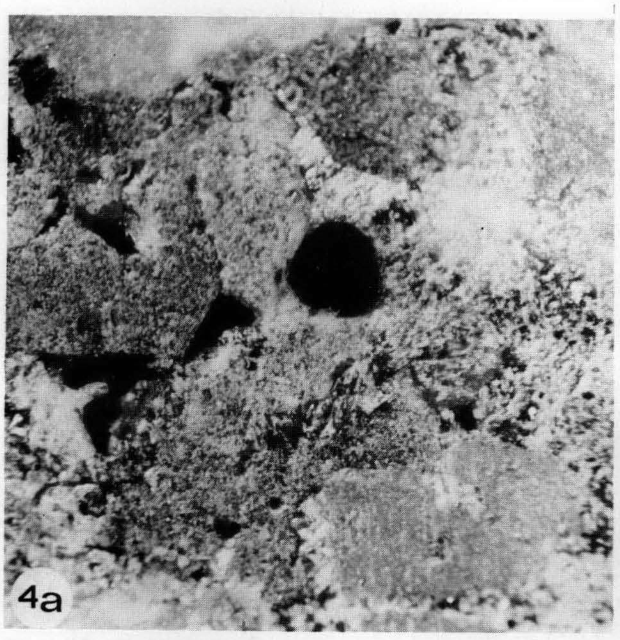

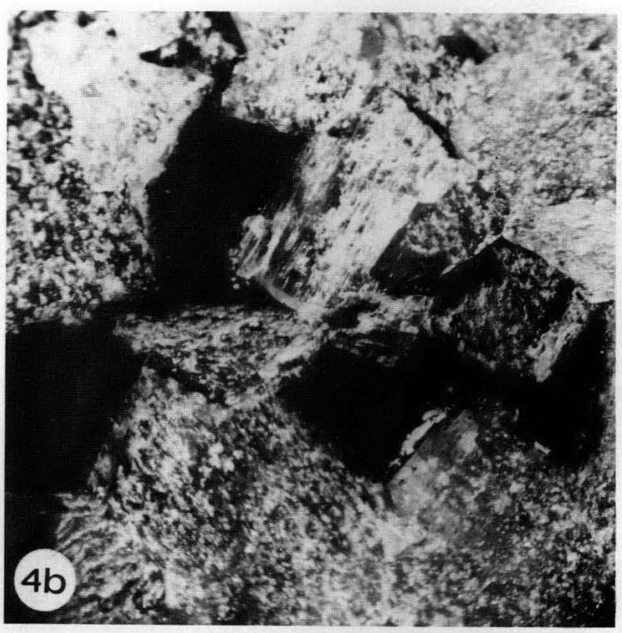

Figure 4. A—Bitumen 1.
Globule about 1 mm diameter in vug within silicified carbonate.

B—Liquid hydrocarbon.
Dark brown viscous liquid (black areas) filling cavities up to about 0.6 mm across, probably after dolomite crystals.

Bitumen 4. A fourth type became obvious five months after the drilling, when bitumen seeped out of the vugs in which it occurred and stained the surrounding rock, thus indicating the presence of some volatile component.

In addition to the bitumen above, some pores and vugs contain a dark brown viscous liquid which is soluble in trichloroethylene (Fig. 4b).

Small samples of bitumen 1 and the liquid failed to provide gas chromatograph patterns characteristic of *normal* oils, when tested in the BMR Petroleum Technology Laboratory. However, the bitumen sample liberated hydrocarbons during pyrolysis. Although the results of this initial geochemistry are disappointing, the general appearance, mode of occurrence and geological setting of this oily material suggest to us that, although it is now largely pyrobitumen, it was originally a liquid hydrocarbon.

Geological setting and origin of the oil

The oily material in Bauhinia Downs 4 occurs in the porous and permeable Looking Glass Formation, immediately beneath a thin claystone unit on the flank of the Beetle Spring Anticline. The claystone appears to have played an important role in confining the formation waters and the hydrocarbons to the Looking Glass Formation, and possibly to other formations below.

The anticline is one of several folds which affect the Roper Group (ca. 1000 m thick) in the adjacent Abner Range (Fig. 1). Thus the Looking Glass Formation there must have been buried to at least 1500 m (i.e. Roper Group plus upper McArthur Group thickness). This depth of burial may have been greater, as Cambrian and Cretaceous strata totalling no more than 400 m in thickness are also preserved in the Abner Range area.

The origin of the oily material is not known. The overlying Cretaceous clearly could not be a source, as it is very thin and has never been buried deeply enough to generate hydrocarbons. The Cambrian Bukalara Sandstone is a coarse-grained arkosic sandstone, which might have been a good reservoir in suitable structural conditions, but it is too organic-poor to be considered as a source, and it also has probably never been buried deep enough. Thus the oil must have been generated in the Proterozoic rocks (ca. 1600 m.y. old).

The Roper Group (Fig. 1) has several potential source horizons (the Mainoru, Corcoran, and McMinn Formations), but it is also unlikely that any of these formations have been buried deeply enough in the Abner Range area for petroleum to have been generated. Further north (200 km) near Roper Bar, the McMinn Formation has excellent source rock potential and shows signs of some migration of hydrocarbons (Peat & others, 1978), but is submature, presumably because it was never buried deeply enough. Little is known about the Mainoru Formation, but the Corcoran Formation in drill core contains abundant organic matter and is as good a potential source rock as the McMinn Formation. Apart from the question of maturity, the Roper Group formations all overlie the Looking Glass Formation and an unlikely structural juxtaposition of the sequences would have to be envisaged for these younger Proterozoic rocks to be the source.

The oily material in the Beetle Spring Anticline is, therefore, most likely to come from the Looking Glass Formation or units below it. Stromatolitic carbonate units, containing abundant organic matter (based on chemical analyses and petrography), include the Amelia, Emmerugga, and Reward Dolomites, and the upper Lynott and Yalco Formations (Fig. 2). Black carbonaceous pyritic shales are abundant in the Lynott, Barney Creek, and Wollogorang Formations. Dolomitic shales from the Mallapunyah Formation in CEC drillhole Apollo 1 contain pale brown organic matter and weak oil staining. The Karns Dolomite (McArthur Group) in the Calvert Hills area (100 km east) contains the solid hydrocarbon impsonite (Dixon, 1957).

The organic matter in both the shale and carbonate sections of the McArthur Group is dark yellow to light brown, indicating these rocks are within the oil generation maturation zone potential (Correia, 1971), and thus any of these formations could have been the source rocks.

Conclusions

- Vadose alteration and silicification beneath a pre-Balbirini Dolomite land surface enhanced the porosity of the Looking Glass Formation.
- Deposition of a claystone at the unconformity sealed the surface of the Looking Glass Formation making it an excellent hydrocarbon trap.
- Burial of the sequence permitted the generation of hydrocarbons from source rocks lower in the sequence.
- After folding, these fluids migrated upwards to accumulate in the Beetle Spring Anticline.
- Gradual escape of lighter hydrocarbons has left behind a residue of bitumen.
- The presence of hydrocarbon residues in 1600 m.y. old rocks indicates that Proterozoic basins should not be ignored in the search for hydrocarbons in Australia.

Acknowledgements

The organic geochemical analyses were done by Zoltan Horvath and Keith Jackson. Ian Crick and Ken Heighway provided helpful criticism and assistance. An early draft of the manuscript was improved following helpful comments from G. E. Wilford and K. A. Plumb.

References

CORREIA, M., 1971—Diagenesis of sporopollenin and other comparable organic substances; application to hydracarbon research. *In* BROOKS, J., GRANT, P. R., MUIR, M. D., SHAW, G., & VAN GIJZEL, P., SPOROPOLLENIN. *Academic Press, London* 569-620.

DIXON, L. H., 1957—Geological studies on Calvert Hills Station. *Frome Broken Hill Pty Co. Ltd., Report* **5100G–3** (unpublished).

FRIEDMAN, G. M., 1975—The making and unmaking of limestones, or the downs and ups of porosity. *Journal of Sedimentary Petrology*, **45**, 379-98.

PEAT, C. J., MUIR, M. D., PLUMB, K. A., MCKIRDY, D. M., & NORVICK, M. S., 1978—Proterozoic microfossils from the Roper Group, Northern Territory, Australia. *BMR Journal of Australian Geology & Geophysics*, **3**, 1-17.

READ, J. F., 1976—Calcretes and their distinction from stromatolites. *In* WALTER, M. R. (editor)—STROMATOLITES, *Elsevier, Amsterdam*, 55-72.

BMR Journal of Australian Geology & Geophysics, 5, 1980, 305-309

Intracrustal seismic reflections from the Lachlan Fold Belt near Canberra

John Pinchin

A deep crustal seismic reflection survey, conducted at Gundary Plains near Canberra, to test a digital seismic recording system, produced additional data for interpretation of seismic refraction profiles in the Lachlan Fold Belt. Good reflections were recorded down to the probable Moho, at an estimated depth of 41 km. The intracrustal reflections are characterised by bands of seismic energy, which probably represent velocity transition zones within the crust. Now that the technique has proved successful, longer seismic reflection traverses are needed to explore the major deep geological features of the Lachlan Fold Belt.

Introduction

During April 1978 and April 1979, BMR conducted a deep crustal seismic reflection survey at Gundary Plains, 70 km northwest of Canberra. The main purpose was to test a digital seismic recording system, but the location was chosen because it lies on a long range seismic refraction profile recorded to study the crustal structure of the Lachlan Fold Belt (Finlayson & others, 1979), and is over a sequence of relatively undisturbed sedimentary rocks expected to be favourable for transmission of seismic energy.

BMR previously conducted deep crustal reflection surveys in the Lachlan Fold Belt at Tidbinbilla and Braidwood in 1969 (Taylor & others, 1972). This paper describes the Gundary Plains survey and compares its results with those from the earlier surveys.

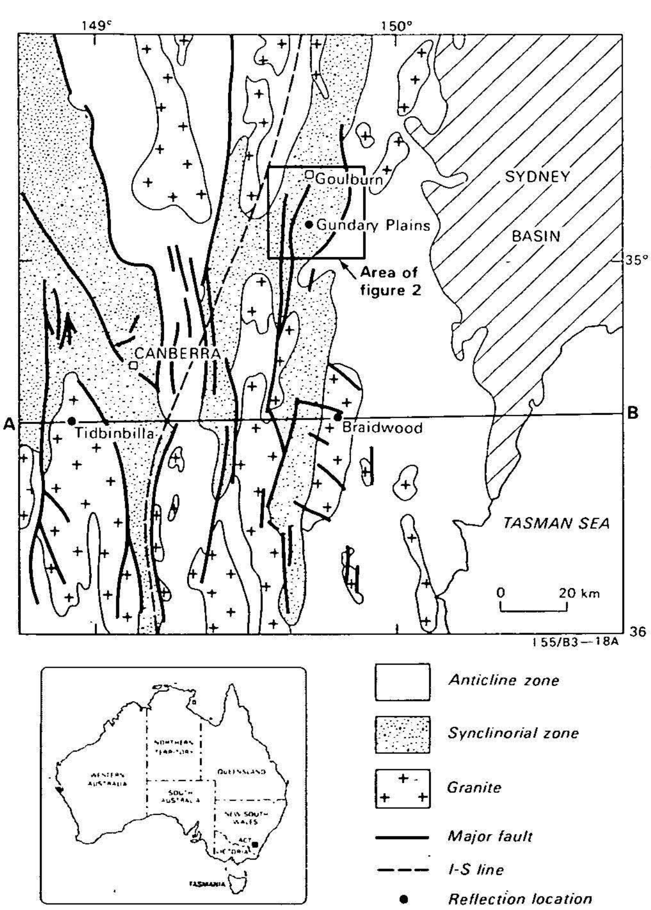

Figure 1. Tectonic setting of the three crustal seismic reflection probes, showing the northerly trending geological structure and granite batholiths.
AB is the line of the cross-section in Figure 5. (Geology from Tectonic Map of New South Wales—Scheibner, 1976.)

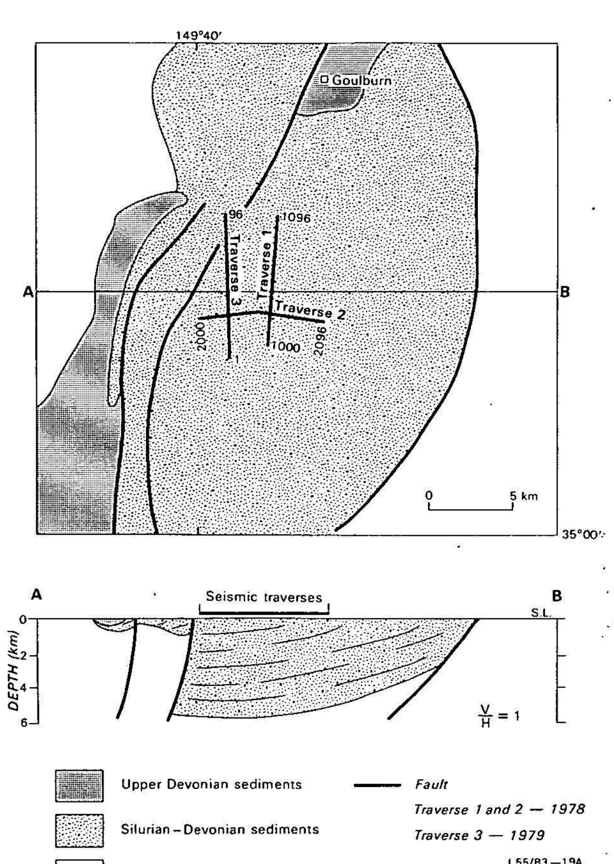

Figure 2. Layout of seismic reflection traverses at Gundary Plains in relation to local geology.

Geological setting

Tidbinbilla, Braidwood and Gundary Plains are situated close to Canberra in the eastern part of the Lachlan Fold Belt. The area is composed of several north-trending anticlinoria and synclinoria of Ordovician to Devonian age (Fig. 1), intruded by a set of north-south elongated granite batholiths with ages ranging from Silurian to Carboniferous (Scheibner, 1976). The Lachlan Fold Belt forms part of the Tasman Fold Belt or Tasman Geosyncline of eastern Australia, which, according to Crook & Powell (1976), was once a com-

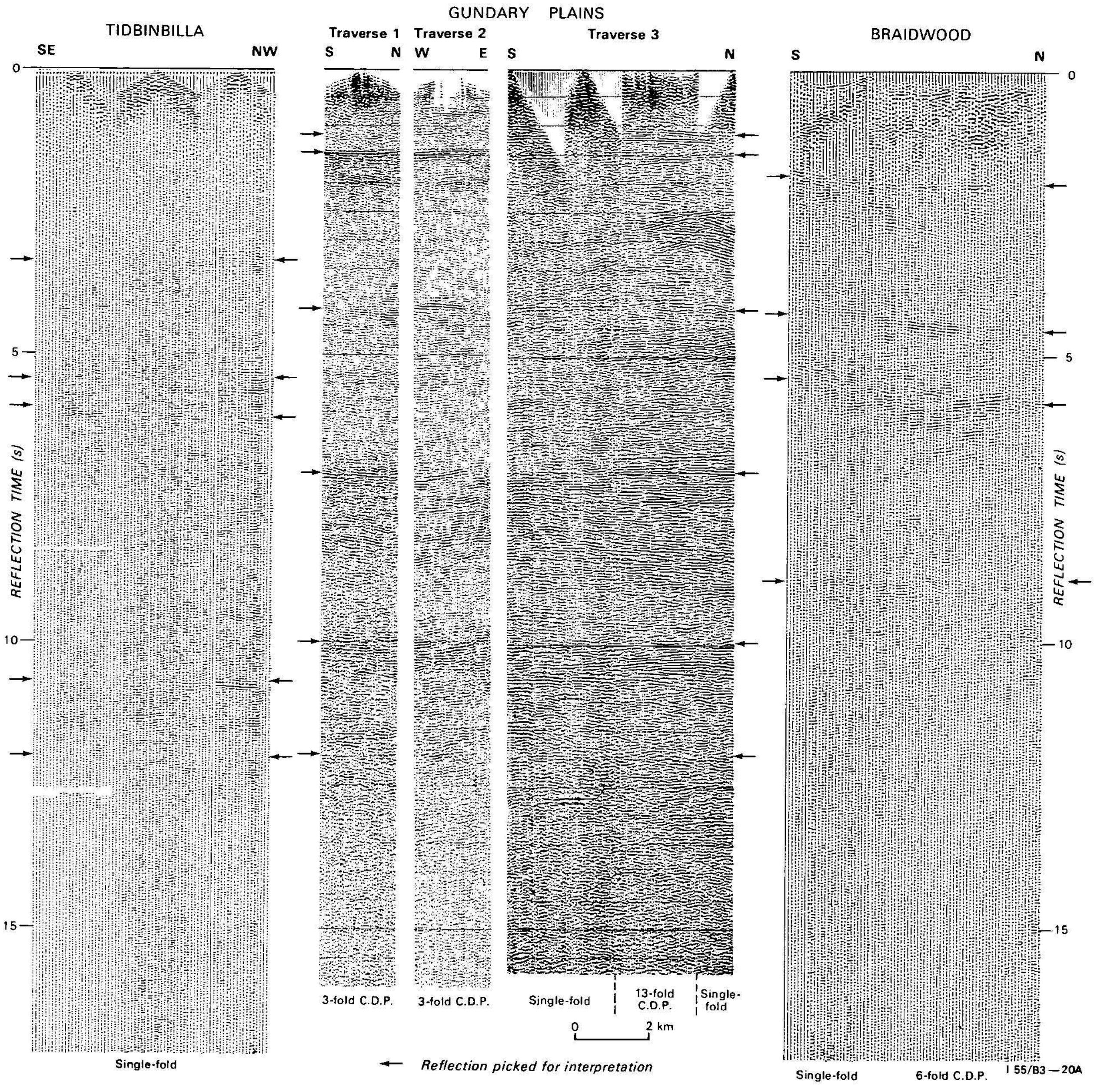

Figure 3. Seismic reflection sections.

plex array of island arcs, inter-arc basins, micro-continents and deep-ocean trenches. The shallow-water sediments, flysch wedges, acid volcanics and ophiolites were metamorphosed, intruded by granites, and accreted onto continental Australia in the process of cratonisation.

These ideas imply that the deepest crust below southeast Australia consists of Ordovician oceanic crustal rocks, but the geochemistry of granitoids in the area indicates otherwise. The granitoids of the Lachlan Fold Belt have been classified by Chappell & White (1974), into I-types and S-types, which they interpret as being derived by partial melting of igneous and sedimentary source rocks, respectively. A north-south-trending line, as shown in Figure 1, delineates the eastern limit of the S-type. Further geochemical study of the S-type granitoids (Wyborn & Chappell, 1979) indicates that they are not derived from the widespread Ordovician sedimentary rocks, and a Cambrian or Precambrian source is suggested.

The local geological setting is different at each of the three seismic survey locations. Tidbinbilla is at the northern end of the Murrumbidgee Batholith, which is an S-type granite, while the Braidwood granite is I-type. Gundary Plains is situated within a syncline containing Silurian to Devonian shales, siltstones and volcanics—The Towrang Beds (Fig. 2). The syncline is north-trending, fault-bounded on its western side, and underlain by mildly metamorphosed and tightly folded Ordovician sediments and volcanics.

Seismic reflection technique

At all three locations, Tidbinbilla, Braidwood, and Gundary Plains, large charges were used in multiple shot-holes. At Gundary Plains, in 1978, six shots were fired, three on each traverse of a cross-spread; the average charge was 370 kg in a 20-hole pattern; each of the cross-traverses was processed separately to give a 3-fold CDP stack. In 1979, thirteen shots were fired along a 6-km traverse to give a 13-fold CDP stack, and

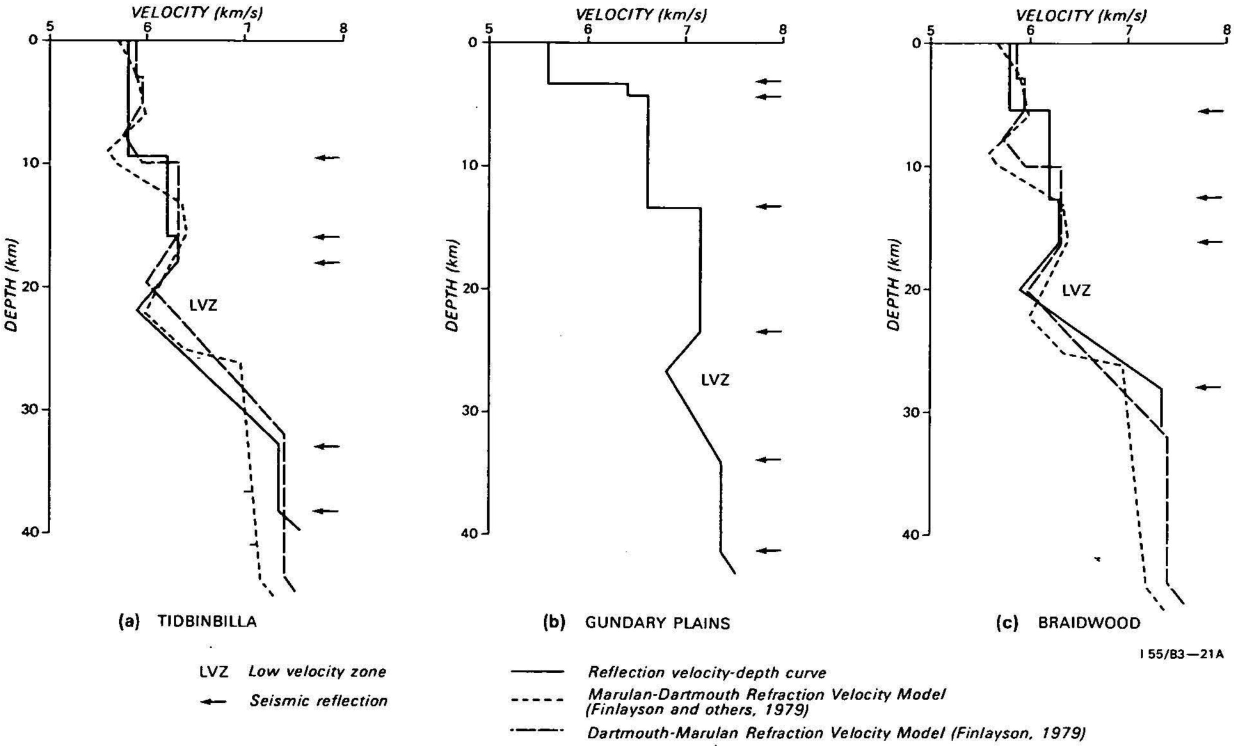

Figure 4. Velocity-depth graphs.

Reflection time (s)	Depth (km)	Dip and dip direction (°)	Average velocity (km/s)	Interval velocity (km/s)
TIDBINBILLA				
3.3	9.6		5.80	5.80
5.35	15.9		5.96	6.20
6.00	18.0		6.00	6.30
*	22.0		6.01	6.10
10.7	33.2		6.21	6.63
12.0	38.0		6.33	7.35
BRAIDWOOD				
1.9	5.5		5.80	5.80
4.2	12.6		6.02	6.20
5.35	16.3		6.08	6.30
*	20.0		6.08	6.10
9.0	28.0		6.23	6.63
GUNDARY PLAINS				
1.2	3.4	03/225	5.60	5.60
1.5	4.3	04/232	5.77	6.40
4.2	13.3	12/047	6.33	6.62
7.0	23.4	20/291	6.67	7.15
*	27.0	—	6.75	6.98
10.0	34.1	16/289	6.82	7.08
12.0	41.4	16/290	6.91	7.35

* Assumed inflection point of low velocity zone used for calculation of interval velocities, no reflection at this point.

Table 1. Reflection times and depths.

the average charge was 100 kg in patterns of 4 holes. The 13 records were digitally processed to obtain statistically more accurate stacking velocities. In addition, two smaller weathering shots of 10 kg gave such good reflections that they were used to extend the subsurface coverage at each end of the main traverse. The location and layout of the traverses at Gundary Plains are shown in Figure 2.

Reflection recordings

The processed seismic record sections are shown in Figure 3. The sections for Tidbinbilla and Braidwood were processed by the BMR analogue seismic processing system; those for Gundary Plains were digitally processed under contract by Geophysical Service International, Sydney.

The data quality at Gundary Plains is very good, with a strong signal to noise ratio; even the small shots of 10 kg produced reflections down to 12 seconds. There are fewer reflections from the shots at Tidbinbilla and Braidwood, possibly due to the sites being located over granite batholiths, whereas Gundary Plains traverses were over gently dipping sediments. The near-surface conditions and geology appear to have a large effect on reflection quality, possibly because the deeply weathered granite scatters returning seismic signals.

The deeper reflections, especially at Gundary Plains, are characterised by bands or multiple legs, rather than single events, even after deconvolution was used to shorten the signal length and remove any near-surface reverberations. In Figure 3, the reflections picked for subsequent interpretation are indicated by arrows.

Interpretation

At Gundary Plains, vertical interval velocities were derived from the digital processing of the reflection data down to a reflection time of 7 s, corresponding to a depth of 23 km. However, the possible error in computing interval velocities increases with depth and at 4 s, or 13 km, is of the order of ten percent. Below 23 km, the interval velocities used were the same as those at Braidwood and Tidbinbilla (Fig. 4, Table 1).

Accurate reflection velocity information was not available at Braidwood or Tidbinbilla, and the interval velocities there were derived from the refraction models of Finlayson (1979) and Finlayson & others (1979).

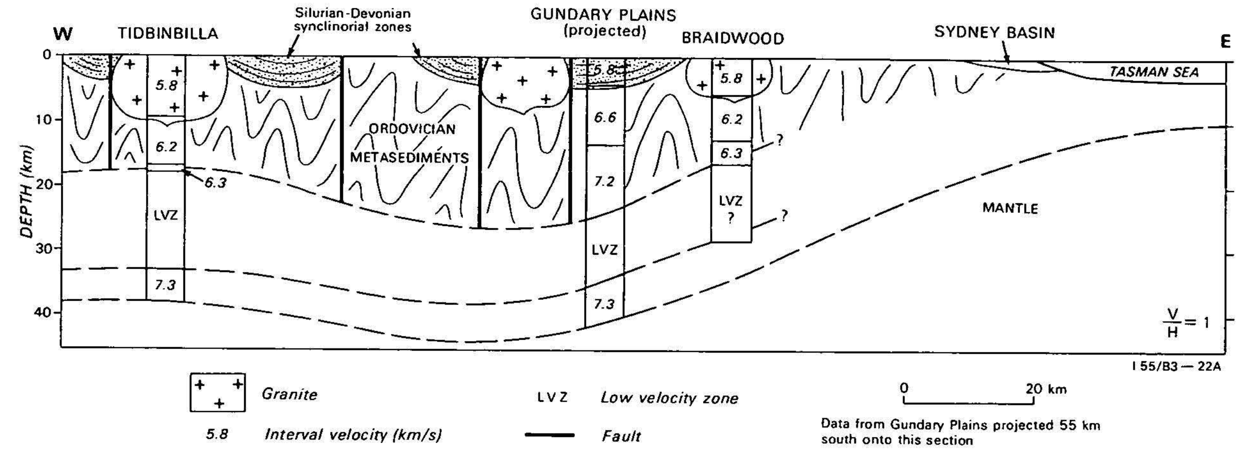

Figure 5. Schematic cross-section through Tidbinbilla and Braidwood.

The two refraction velocity-depth models between Dartmouth and Marulan were averaged to give constant interval velocities between seismic reflections, which were assumed to correspond to the knee points on the graphs (Fig. 4a, 4c). This method has the advantage that reflection times and depths can be compared from place to place using constant interval velocities; but it is realised that, for correct conversion of reflection time to depth, the actual velocity function for each particular location should be determined. The shallow reflection velocities measured at Gundary Plains are much higher than the shallow refraction velocities bebtween Dartmouth and Marulan. This has yet to be explained, but could possibly be due to a local area of high velocity. The values used in preparing Figure 4 are tabulated in Table 1. The cross-traverses at Gundary Plains enable the true dip of the reflectors to be calculated; this is also included in Table 1.

At Gundary Plains, the reflector at 3.4 km lies within the Silurian-Devonian Towrang Beds, while that at 4.3 km marks the base of these beds and top of the Ordovician rocks. This compares with the estimate of 6 km based on geological mapping (Offenberg, 1974). The reflector at 13.3 km dips in exactly the opposite direction to the shallower one, and possibly lies in the opposite limb of an inclined fold in the Ordovician rocks. The reflectors deeper than 23 km dip in the same direction (Table 1), suggesting that they were originally horizontal and have all been tilted by the same sequence of tectonic forces.

The fact that the deep reflections appear as bands agrees with the observation of other workers, such as Meissner (1973), who suggested that the Moho is a laminated transition zone, with the laminae caused by selective remelting or recrystallisation. The bands here are up to 3 km thick. Bamford & Prodehl (1977) suggested that a gradational Moho is characteristic of orogenic belts, and recent reflection results from USA (Schilt & others, 1979) confirm the transition zone nature and lateral inhomogeneity of the crust-mantle boundary.

A possible quasi-geological interpretation of the reflections from the three surveys is shown in Figure 5. It is assumed that the shallowest reflections at Tidbinbilla and Braidwood come from the base of the granite batholiths. Other assumptions are that the reflectors are represented by knees in the velocity-depth model as shown in Figure 4, and that the same set of interval velocities and the low velocity zone are present at each location.

The gravity effect of this suggested interpretation bears a broad correspondence with the observed gravity field; both show crustal thinning towards the coast. However, there are insufficient data on the density variations within the crust to enable quantitative gravity modelling to be carried out.

The depths to the Moho suggested here are similar to those interpreted by Cleary (1973) from refraction data. He showed a two-layer crust, with the Moho deepening from a depth of 30 km near the east coast to 40-42 km below the Snowy Mountains. This schematic cross-section bears some resemblance to that shown by Finlayson (1979) between Dartmouth and Marulan. Finlayson's short, disconnected refractor segments coincide fairly well with the crustal layers shown here in simplified form, as continuous. Finlayson also shows a deeper Moho, 44 km beneath Tidbinbilla and Braidwood, deepening to 50 km towards Dartmouth in the southeast.

A comparison of the seismic reflection sections from Braidwood and Tidbinbilla shows a difference in character that may be due to the difference between the I-type and S-type granites. If this interpretation is correct, then the I-type granite is shallower than the S-type; however many more reflection probes over several different batholiths would be needed before any general conclusion could be drawn regarding their seismic structure.

Conclusions

The interpretation presented here is probably a simplification of the true picture, but the Gundary Plains survey has shown that good quality deep reflection data should be obtainable from tectonically complex areas. Reflections down to 40 km depth were recorded from charges as small as 50 kg. The intra-crustal boundaries shown here as lines are more likely to be transition zones; the lower crust, from seismic refraction, reflection, and geochemical evidence, is likely to be just as complex as the upper crust. Seismic reflection techniques can provide information on intra-crustal boundaries, but long continuous traverses of the type done by COCORP project in the USA (Oliver, 1978), rather than isolated short profiles, are needed to establish the deep structure of a complex area like the Lachlan Fold Belt.

Acknowledgements

I thank F. J. Moss, S. P. Mathur and D. M. Finlayson for their assistance and advice on the interpretation.

References

BAMFORD, D., & PRODEHL, C., 1977—Explosion seismology and the continental crust-mantle boundary. *Journal of the Geological Society, London*, **134**, 139-51.

CHAPPELL, B. W., & WHITE, A. J. R., 1974—Two contrasting granite types. *Pacific Geology*, **8**, 173-4.

CLEARY, J., 1973—Australian crustal structure. *In* MUELLER, S. (editor)—The structure of the Earth based on seismic data. *Tectonophysics*, **20**, 241-8.

CROOK, K. A. W., & POWELL, C. MCA, 1976—The evolution of the southeastern part of the Tasman Geosyncline. *25th International Geological Congress, Excursion Guide* **17A**.

FINLAYSON, D. M., 1979—Seismic structure of southeastern Australia and constraints on crustal evolution. *In* DENHAM, D. (compiler)—Crust and upper mantle of southeast Australia. *Bureau of Mineral Resources, Australia, Record* **1979/2** (unpublished).

FINLAYSON, D. M., PRODEHL, C., & COLLINS, C. D. N., 1979—Explosion seismic profiles, and implications for crustal evolution, in southeastern Australia. *BMR Journal of Australia Geology & Geophysics*, **4**, 243-52.

MEISSNER, R., 1973—The 'Moho' as a transition zone. *Geophysical Surveys*, **1**, 195-216.

OFFENBERG, A. C., 1974—Goulburn, NSW, 1:250 000 Series Explanatory Notes. *Geological Survey of New South Wales, Sydney*.

OLIVER, J., 1978—Exploration of the continental basement by seismic reflection profiling. *Nature*, **275**, 485-9.

SCHEIBNER, E., 1976—Explanatory notes on the Tectonic Map of New South Wales. *Geological Survey of New South Wales, Sydney*.

SCHILT, S., OLIVER, J., BROWN, L., KAUFMAN, S., ALBAUGH, D., BREWER, J., COOK, F., JENSEN, L., KRUMHANSL, P., LONG, G., & STEINER, D., 1979—The heterogeneity of the continental crust: results from deep crustal seismic reflection profiling using the vibroseis technique. *Reviews of Geophysics and Space Physics*, **17**, 354-68.

TAYLOR, F. J., MOSS, F. J., & BRANSON, J. C., 1972—Deep crustal reflection seismic test survey, Tidbinbilla, A.C.T., and Braidwood, N.S.W., 1969. *Bureau of Mineral Resources, Australia, Record* **1972/126** (unpublished).

WYBORN, L. A. I., & CHAPPELL, B., W., 1979—Geochemical evidence for the existence of a pre-Ordovician sedimentary layer in south-eastern Australia. *In* D. DENHAM (compiler)—Crust and upper mantle of southeast Australia. *Bureau of Mineral Resources, Australia, Record* **1979/2** (unpublished).

BMR Journal of Australian Geology & Geophysics
Author index, Volumes 1-5

Numbers refer to volume and number

BMR JOURNAL
of Australian Geology & Geophysics

VOLUME 5

1980

CONTENTS

Number 1, March 1980

Number 2, June 1980

Number 3, September 1980

Number 4, December 1980

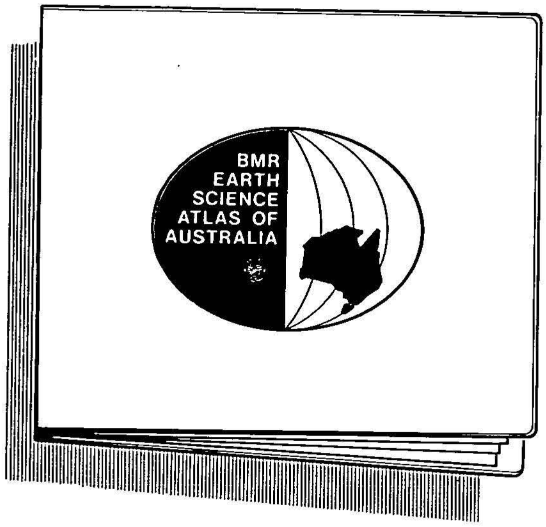

BMR EARTH SCIENCE ATLAS OF AUSTRALIA

The Bureau of Mineral Resources has produced a loose-leaf Earth science atlas of Australia.

The maps are intended to provide a valuable first reference to the geology and geophysics of Australia for use in schools, private companies and governmental organisations. They will also be useful to overseas visitors, and individuals in Australia requiring an introduction to the Earth science characteristics of this continent.

Each map is accompanied by a commentary which aims to provide the reader with additional information and lead to a fuller appreciation of what each map portrays.

The maps and commentary sheets are 57 cm x 43.5 cm in size; most of the maps will be at a scale of 1:10 000 000.

Maps available now are listed below. Maps in preparation include Solid geology, Main rock types, and Surface drainage; more are being planned.

Each map and commentary costs $4.00 (Australian), postage included. A special vinyl atlas cover has also been produced: this costs $5.00 (Australian) plus postage (surface mail) of $3.00 within Australia, $3.50 overseas.

Name/Company ______________________

____

Delivery Address ______________________

____

____

______________ Postcode __________

Date ______________________

Order No. ______________________

QTY	TITLE	PRICE	
	Geology		
	Plate tectonics		
	Major structural elements		
	Earthquakes		
	Bouguer gravity anomalies		
	Free-air gravity anomalies		
	Cover and postage, Australia		
	Cover and postage, Overseas		

Please forward your order together with payment to:

Publication Sales,
Bureau of Mineral Resources,
P.O. Box 378,
Canberra City,
A.C.T. 2601

Payment made by cheque ☐ money order ☐ postal order ☐ or, for account holders only, debit account ☐

Cheques should be made payable to the Receiver of Public Monies

For BMR use

Date Received .... Receipt/Invoice No .... Checked ....

SIV No. .... Date .... Further details required ☐

File ....

CONTENTS

R79/444(4) Cat. No. 80 1132 4

FOR SALE